

Description of *Tanytrachelos ahynis* and its implications for the phylogeny
of Protorosauria

Amy C. Smith

Dissertation submitted to the faculty of the
Virginia Polytechnic Institute and State University
in partial fulfillment of the requirements for the degree of

Doctor of Philosophy
in
Geosciences

Michał Kowalewski, Chair
Nicholas Fraser, Co-chair
Alton Dooley
Kenneth Eriksson
Shuhai Xiao

April 11, 2011, Blacksburg, Virginia

Keywords: Protorosaurs, Archosauromorphs, Cladistics, Quantitative
Morphometrics

Description of *Tanytrachelos ahynis* and its implications for the phylogeny of Protorosauria

Amy C. Smith

ABSTRACT

Tanytrachelos ahynis, a small (21 cm long) aquatic protorosaur from the Upper Triassic sediments in the Cow Branch Formation of the Newark Supergroup, has been briefly described in 1979 by P. E. Olsen. A growing addition of nearly 200 specimens and the availability of CT imaging allow for an extensively detailed redescription. This redescription fills in missing data in cladistic analyses of Protorosauria, allowing for protorosaur monophyly to be retested with a more robust data set.

Two hundred and ninety specimens and two CT scans of specimens were examined, with seventy linear measurements, four angular measurements, and five derived variables comprising the quantitative observations. These qualitative and quantitative observations then provided data for *Tanytrachelos* in two cladistic analyses of Protorosauria. The first analysis included the outgroup *Petrolacosaurus*, twenty-one protorosaurs, and nine other archosauromorphs. The second analysis included the twenty taxa within this sample that had a data completeness of 50% or higher.

Diagnostic qualities of *Tanytrachelos* include large orbits (11% - 13% the lateral area of the skull), a fused axis and atlas, a tail that spans half the vertebral length, and paired curved heterotopic bones in some specimens (a sign of sexual dimorphism). The disparity of size between the hind and fore limbs, as well as traces of soft tissue, suggest that *Tanytrachelos* propelled through the water with its back legs. This taxon is similar to *Gwyneddosaurus*, found in the Locketong Formation (Newark Supergroup) in Montgomery County, PA, but should maintain its generic name due to lack of diagnostic qualities for *Gwyneddosaurus*.

With the new observations of *Tanytrachelos* included, each of the two cladistic analyses yielded a single most parsimonious tree presenting a paraphyletic Protorosauria. Both results placed *Prolacerta* within the confines of Protorosauria, in contrast with the previous suggestion by three publications that *Prolacerta* was not a true protorosaur. The analysis of all taxa presented *Boreopricea* as the most basal protorosaur, while the analysis of the twenty most complete taxa presented *Protorosaurus* as most primitive. Neither tree fully agrees with any previously published data, partly due to differences in taxa sampling between studies.

Dedicated to my loving husband, whose unfaltering support helped me succeed in the face of hardship at Virginia Tech.

ACKNOWLEDGEMENTS

The author would like to thank M. Kowalewski of the Virginia Polytechnic Institute and State University (Blacksburg) for help with morphometric methods, assistance with SAS, and project and academic guidance, A. Dooley of the Virginia Museum of Natural History (Martinsville) and N. Fraser of the National Museum of Scotland (Edinburgh) for access to specimen collections and for project guidance, and S. Xiao and K. Eriksson of the Virginia Polytechnic Institute and State University for project and academic guidance. The author is also grateful for the help from J. Barringer and Y. Tulu of Michigan State University (East Lansing), and S. Godfrey of the Calvert Marine Museum (Solomons, MD), who provided the author with invaluable feedback and support. The author thanks M. Lemon of the Virginia Polytechnic Institute and State University for assistance with printing the poster resulting from this study. This project was funded by the Tillman Geosciences Graduate Research Award (2008, Virginia Tech) and the D.R. Wones Research Award (2009, Virginia Tech).

TABLE OF CONTENTS

LIST OF FIGURES.....	vii
LIST OF TABLES.....	ix
INTRODUCTION.....	1
A morphological and morphometric redescription of <i>Tanytrachelos ahynis</i>	2
ABSTRACT.....	2
INTRODUCTION.....	3
The Newark Supergroup and the Dan River Basin.....	3
The Cow Branch Formation of the Dan River Group.....	4
<i>Tanytrachelos</i> Locality within the Dan River Basin.....	4
Previous Work on <i>Tanytrachelos</i>	6
MATERIALS AND METHODS.....	8
Specimens Studied.....	8
Photograph Acquisition.....	8
Contrast Enhancement in Photographs.....	8
Gathering Qualitative Data.....	10
Gathering Quantitative Data.....	10
RESULTS.....	13
Skull.....	14
Vertebral Column and Ribs.....	17
Pectoral Girdle and Anterior Limbs.....	26
Pelvic Girdle and Posterior Limbs.....	30
Gastralia and Heterotopic Bones.....	34
Soft Tissue Traces.....	37
Specimens with Noticeably Wide Bodies.....	39
Juvenile Specimens of <i>Tantrachelos</i>	39
Quantitative Results.....	41
DISCUSSION.....	47
Diagnostic Qualities of <i>Tanytrachelos</i>	47
Possible Function of Paired Heterotopic Bones.....	47
The Relationship of <i>Gwyneddosaurus</i> to <i>Tanytrachelos</i>	48
Locomotion of <i>Tanytrachelos</i>	51
The Possibility of Neoteny in <i>Tanytrachelos</i>	52
Comparison and Contrast between <i>Tanytrachelos</i> and its proposed sister taxon <i>Tanytropheus</i>	53
Potential Sources of Error in Morphometric Measurements.....	54

LITERATURE CITED.....	55
A reanalysis of protorosaur cladistics and its impact on archosauromorph evolutionary relationships.....	57
ABSTRACT.....	57
INTRODUCTION.....	58
Previous Studies of Protorosaur Phylogeny.....	58
MATERIALS AND METHODS.....	63
Taxa Selection and Character Compilation.....	63
Cladistic Analysis of Protorosauria.....	63
RESULTS.....	65
Results of the Analysis Including All Taxa.....	65
Results of the Analysis Including Only Taxa with 50% or Higher Data Completeness.....	66
DISCUSSION.....	67
Consistencies and Inconsistencies between Both Analyses.....	67
Comparison of Results to Previous Studies.....	68
Possibilities for Future Work.....	69
LITERATURE CITED.....	70
SYNOPSIS.....	75
APPENDICES.....	77
Appendix A: List of <i>Tanytrachelos ahynis</i> Specimens Studied.....	77
Appendix B: Morphometric Measurements of <i>Tanytrachelos</i> Specimen Elements.....	78
Appendix C: Characters Used in the Cladistic Analysis.....	94
Appendix D: Matrix of Character States used in the Cladistic Analyses.....	100

LIST OF FIGURES

FIGURE 1. Locations of the southernmost basins of the Newark Supergroup.....	3
FIGURE 2. The Solite Quarry.....	4
FIGURE 3. Diagrams of the Van Houten Cycles of the Solite Quarry.....	5
FIGURE 4. Photograph of YPM7496A demonstrating the Image>Calculations function as well as the Apply Image function.....	9
FIGURE 5. Photograph of VMNH120016 demonstrating the Apply Image>Multiply>Red channel adjustment.....	10
FIGURE 6. Linear and angle measurements taken from individual elements of <i>Tanytrachelos</i>	11
FIGURE 7. The type specimen of <i>Tanytrachelos ahynis</i> , YPM7496.....	13
FIGURE 8. Skulls of <i>Tanytrachelos</i>	16
FIGURE 9. Comparison of the area of the orbit to the lateral area of the skull.....	17
FIGURE 10. Sequences of cervical vertebrae of <i>Tanytrachelos</i>	18
FIGURE 11. Articulated and disarticulated dorsal vertebrae of <i>Tanytrachelos</i>	20
FIGURE 12. Articulated and disarticulated ribs of <i>Tanytrachelos</i>	22
FIGURE 13. The sacral vertebrae of <i>Tanytrachelos</i>	23
FIGURE 14. Caudal vertebrae of <i>Tanytrachelos</i>	26
FIGURE 15. Scapulae and coracoids of <i>Tanytrachelos</i>	27
FIGURE 16. The anterior limb of <i>Tanytrachelos</i>	29
FIGURE 17. The right manus of <i>Tanytrachelos</i>	30
FIGURE 18. The pelvic girdle of <i>Tanytrachelos</i> in various states of articulation.....	31
FIGURE 19. The right hindlimb and partial left hindlimb of <i>Tanytrachelos</i>	32
FIGURE 20. Illustrations and photographs of the pes of <i>Tanytrachelos</i>	34
FIGURE 21. Sets of gastralialia found in <i>Tanytrachelos</i>	35

FIGURE 22. Heterotopic bones found in <i>Tanytrachelos</i>	36
FIGURE 23. Traces of soft tissue in specimens of <i>Tanytrachelos</i>	38
FIGURE 24. Specimens of <i>Tanytrachelos</i> that have wider ribcages than average specimens.....	39
FIGURE 25. The two smallest juvenile specimens of <i>Tanytrachelos</i> found to date.....	40
FIGURE 26. VMNH3668, the specimen of <i>Gwyneddichnium</i> found in the Solite Quarry.....	51
FIGURE 27. The cladistic analysis of Protorosauria as presented by Benton and Allen (1997).....	59
FIGURE 28. The cladistic analysis of Protorosauria and members of Archosauromorpha as presented by Jalil (1997).....	59
FIGURE 29. The cladistic analysis of Protorosauria and members of Archosauromorpha as presented by Dilkes (1998).....	60
FIGURE 30. The cladistic analysis of Protorosauria as presented by Rieppel et al. (2003).....	61
FIGURE 31. The cladistic analysis of Archosauromorpha as presented by Modesto and Sues (2004).....	61
FIGURE 32. The cladistic analysis of Archosauromorpha as presented by Hone and Benton (2008).....	62
FIGURE 33. Single most parsimonious tree of all thirty-two taxa in the study.....	65
FIGURE 34. Single most parsimonious tree of the twenty taxa in the study with 50% or higher data completeness.....	66

LIST OF TABLES

TABLE 1. Skull morphometrics of four measured specimens.....	17
TABLE 2. Data used in the nonparametric test comparing the presence of heterotopic bones to body size through femur length.....	37
TABLE 3. Measurements of elements from the two smallest specimens of <i>Tanytrachelos</i> yet found.....	41
TABLE 4. Summary statistics of morphometric measurements of the skull and cervical vertebrae.....	42
TABLE 5. Summary statistics of morphometric measurements of the dorsal and sacral vertebrae.....	43
TABLE 6. Summary statistics of morphometric measurements of the forelimb elements.....	44
TABLE 7. Summary statistics of morphometric measurements of the caudal vertebrae and heterotopic bones.....	45
TABLE 8. Summary statistics of morphometric measurements of the hindlimb elements.....	46
TABLE 9. Comparisons of the average lengths of <i>Gwyneddichnium</i> digits to the lengths of <i>Tanytrachelos</i> digits.....	50
TABLE 10. Lengths of total manus digits of the <i>Gwyneddichnium</i> specimen found in the Solite Quarry.....	51
TABLE 11. Ratios of element lengths of the two smallest juvenile specimens of <i>Tanytrachelos</i> found and four distinctly larger (presumably adult) specimens.....	52
TABLE 12. Data completeness for taxa used in study.....	64
TABLE 13. Linear measurements of the skull, orbit, and dentary.....	78
TABLE 14. Length measurements of cervical vertebrae.....	78
TABLE 15. Averaged width measurements of cervical ribs.....	79
TABLE 16. Averaged length measurements of cervical ribs.....	79
TABLE 17. Length measurements of dorsal vertebra.....	80

TABLE 18. Linear measurements of sacral vertebrae and individual hip bones.....	81
TABLE 19. Length measurements of caudal vertebrae 1 through 17.....	82
TABLE 20. Length measurements of caudal vertebrae 18 through 31.....	82
TABLE 21. Averaged length measurements of the caudal transverse processes.....	83
TABLE 22. Linear measurements and aspect ratio of the forelimb long bones.....	84
TABLE 23. Length measurements of individual metacarpals.....	84
TABLE 24. Length measurements of individual phalanges of manus digits I through III.....	85
TABLE 25. Length measurements of individual phalanges of manus digits IV and V.....	85
TABLE 26. Linear measurements and aspect ratio of the hind limb long bones.....	85
TABLE 27. Length measurements of individual metatarsals.....	86
TABLE 28. Length measurements of individual phalanges of pes digits I through III....	87
TABLE 29. Length measurements of individual phalanges of pes digits IV and V.....	87
TABLE 30. Length and angle measurements of individual heterotopic bones.....	87
TABLE 31. Length measurements of vertebrae of unknown type and articulation.....	88
TABLE 32. Length measurements of cervical vertebrae of unknown articulation.....	90
TABLE 33. Length measurements of dorsal vertebrae of unknown articulation.....	91
TABLE 34. Length measurements of caudal vertebrae of unknown articulation.....	91
TABLE 35. Averaged length measurements of ribs on caudal vertebrae of unknown articulation.....	92
TABLE 36. Length measurements of appendicular long bones of unknown articulation.....	92
TABLE 37. Matrix of the character states used in the cladistic analysis of Protorosauria and selected archosauromorphs.....	100

INTRODUCTION

A redescription of *Tanytrachelos ahynis*, a small, aquatic protorosaur from the Triassic sediments of the Cow Branch Formation of the Newark Supergroup, is important for two main reasons. The redescription includes nearly 200 more specimens than did the preliminary description of *Tanytrachelos* by Olsen (1979). This increased sample size, along with the availability of CT imaging of specimens that cannot be prepared from the matrix, allow for the creation of a detailed, quantitative resource regarding this taxon. This in turn fills in missing data for *Tanytrachelos* in previous cladistic analyses of Protorosauria, allowing for the creation of a new, more robust cladistic analysis to determine if Protorosauria is monophyletic or paraphyletic. A paraphyletic Protorosauria would noticeably impact the structure of its parent group Archosauromorpha, as protosaurs would then have to be intercalated among archosauromorph clades. On the other hand, a monophyletic Protorosauria would not affect the cladistic structure of Archosauromorpha, as Protorosauria would consist of a single clade within the overall group.

The overwhelming majority of *Tanytrachelos ahynis* specimens are found in the Solite Quarry near Cascade, Virginia. This locality exposes roughly thirty Triassic lacustrine cycles of the Cow Branch Formation, and is a Konzentrat and Konservat Lagerstätte that yields a variety of plant, vertebrate, and insect fossils. The Cow Branch Formation is part of the Dan Diver Group, which is a series of fluvially-transported siliclastics and lacustrine members within the Newark Supergroup. Overall, this supergroup consists of thirteen Triassic rift basins that follow the east coast of North America, spanning from Nova Scotia to South Carolina.

Although this study presents the first in-depth qualitative and quantitative description of *Tanytrachelos*, two previous publications have discussed this taxon. In 1979, P. E. Olsen published a preliminary description of the animal based on just over one hundred specimens. The description included an overview of postcranial elements, vertebral counts, limb proportions, and comparisons to its proposed sister taxon *Tanystropheus*. The second publication involving *Tanytrachelos* (Casey et al. 2007), discussed the taphonomic processes involved in its preservation within the second, third, and sixteenth lacustrine cycles of the Solite Quarry.

Information from this redescription fills in data that were missing for *Tanytrachelos* in previous cladistic analyses of Protorosauria. Protorosauria, a group within Archosauromorpha that includes the families Drepanosauridae (*Drepanosaurus*, *Hypuronector*, *Megalancosaurus*, and *Vallesaurus*) and Tanystropheidae (*Amotosaurus* (Fraser and Rieppel 2006), *Dinocephalosaurus*, *Tanystropheus*, and *Tanytrachelos*), as well as the genera *Boreoprincea*, *Cosesaurus*, *Kadimakara*, *Langobardisaurus*, *Malerisaurus*, *Macrocnemus*, *Prolacerta*, *Prolacertoides*, *Protorosaurus*, *Trachelosaurus*, (Rieppel et al. 2003), *Czatkowiella* (Borsuk-Bialnicka and Evans 2009), and *Rhombopholis* (Benton and Allen 1997), has been presented as monophyletic by some authors and paraphyletic by other authors. Benton and Allen (1997), Jalil (1997), and Hone and Benton (2008) concluded that Protorosauria is monophyletic, whereas Dilkes (1998), Rieppel et al. (2003), and Modesto and Sues (2004) concluded that Protorosauria is paraphyletic.

A morphological and morphometric redescription of *Tanytrachelos ahynis*

ABSTRACT

Tanytrachelos ahynis is a small (averaging 21 cm long), aquatic protorosaur from the Triassic rift sediments of the Cow Branch Formation (Dan River Group, Newark Supergroup) exposed in the Solite Quarry (Dan River Basin) near Cascade, Virginia. Although a preliminary description of *Tanytrachelos*, based on just over 100 specimens, had been published in 1979 by P. E. Olsen, a significant increase in sample size to nearly three hundred specimens (and counting) and the current availability of CT imaging allow for a new, detailed redescription. For this redescription, two hundred and ninety specimens and CT scans of two specimens of *Tanytrachelos ahynis* from the Solite Quarry were examined. Seventy linear measurements, four angle measurements, and 5 derived variables were taken from individual elements.

Tanytrachelos can be characterized by relatively large orbits (occupying 11% to 13% of the lateral area of the skull), an axis fused to the atlas, procoelous cervical centra that are subequal in length, a homodont dentition, non-sigmoidal femora, subequally long metatarsals I through IV, and paired curved heterotopic bones in some specimens. The heterotopic bones are signs of sexual dimorphism, but it is not entirely clear if they were used as claspers in the male or to support a brood pouch in the male or female. Thirteen elongate cervical vertebrae constitute 25% of the vertebral length, followed by thirteen dorsal vertebrae (21% of the vertebral length), two sacral vertebrae (4% of the vertebral length), and thirty-one caudal vertebrae (50% of the vertebral length). The cervical ribs are dichoccephalous, and the dorsal ribs are holocephalous and unfused to the vertebrae. Traces of soft tissue have been preserved on a few specimens over the ribcage, around the femora of a juvenile specimen, and around individual caudal vertebrae, suggesting the presence of caudal muscles.

Gwyneddosaurus, a small protorosaur discovered in the Triassic lacustrine sediments of the Locketong formation (Newark Supergroup) in Montgomery County, Pennsylvania, has elements that share morphological and morphometric similarities with those of *Tanytrachelos*. These similarities indicate that both *Gwyneddosaurus* and *Tanytrachelos* are the same genus. Although the name *Gwyneddosaurus* was established before *Tanytrachelos*, *Tanytrachelos* should retain its generic name, as *Gwyneddosaurus* is too fragmentary to be unequivocally diagnosed.

INTRODUCTION

First described in 1979 by P.E. Olsen, *Tanytrachelos ahynis* is a small, lizard-like aquatic diapsid of Triassic age found in various locations within the Newark Supergroup, including basins in southeastern Pennsylvania (Olsen and Flynn 1989), southern Virginia, and central North Carolina (Olsen 1979). Approximately 200 additional specimens of *Tanytrachelos* have been collected from the Solite Quarry near Cascade, Virginia since its original description which, in addition to the current availability of CT imaging and the common use of quantitative morphometrics, allow for a new, more detailed redescription of this animal.

The Newark Supergroup and the Dan River Basin

The Newark Supergroup consists of a collection of thirteen Triassic rift basins that were created just before the breakup of Laurasia. The supergroup extends from Nova Scotia to South Carolina along the east coast of North America (Olsen and Flynn 1989), as partly shown in Figure 1. The Newark Supergroup arguably offers the greatest opportunity of all Triassic-Jurassic sequences in the world to test hypotheses of early Mesozoic faunal change. The collection of formations within this supergroup span from the Carnian of the Triassic into the Hettangian of the early Jurassic, with the Triassic-Jurassic boundary occurring right above the lowest basalt from the Central Atlantic magmatic province. These ages are rather precise because they are derived from a combination of on radiometric dating, palynology, and magnetostratigraphy, and isotopic traces (Lucas and Tanner 2007). The Dan River Basin, shown in red on Figure 1, exposes the Dan River Group within the Newark Supergroup (Olsen et al. 1978) This group consists of fluviially transported siliclastics as well as the Cow Branch Formation, the lacustrine middle member of the group (Liutkus et al. 2010).

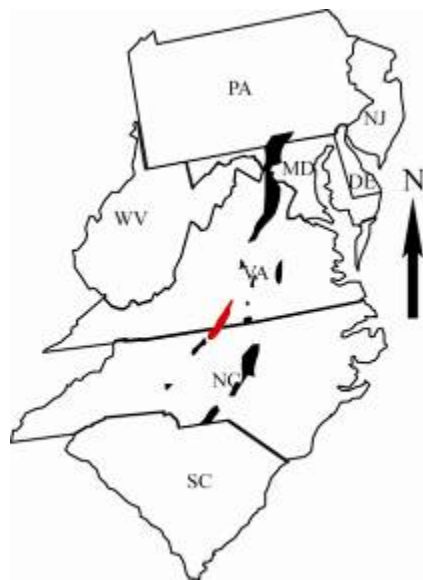


FIGURE 1. Locations of the southernmost basins of the Newark Supergroup. The Dan River Basin, which crosses the Virginia-North Carolina boundary, is marked in red.

The Cow Branch Formation of the Dan River Group

The Cow Branch Formation is a part of the Dan River Group (Olsen and Johansson 1994) that consists of mudrocks, fine-grained feldspathic sandstones, and coal from the Norian (Liutkus et al. 2010). The majority of its deposits are mud shale, whereas only a few of the deposits are sandstones, which are unfossiliferous (Meyertons 1963). The Cow Branch Formation is comprised of two lacustrine complexes that are interbedded with the fluvial and deltaic sediments from the Pine Hall and Stoneville Formations. Well-developed Van Houten cycles are present within the Cow Branch Formation (Olsen and Johansson 1994), and each cycle can be divided into three phases: a transgressive phase, a highstand phase, and a regressive phase. Most macrofossils from this formation are found in cycles 2, 3, and 16, with the highstand phase of cycle 2 being an extremely fossiliferous sequence (Casey et al. 2007).

Tanytrachelos Locality within the Dan River Basin

Specimens of *Tanytrachelos ahynis* are most abundant within the Solite Quarry in Cascade, Virginia, which is located in a Triassic rift basin at the border between Virginia and North Carolina (see Figure 2). The Solite Quarry is the best and most accessible exposure of the Cow Branch Formation (Meyertons 1963), showcasing roughly thirty lacustrine cycles (Fraser et al. 1996) and laterally spanning several hundred meters (Olsen and Johansson 1994).

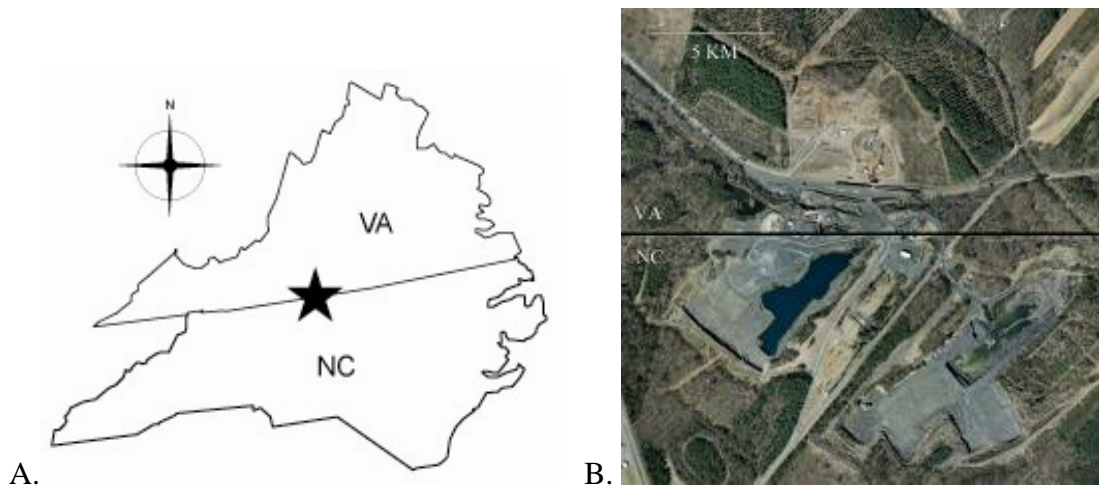


FIGURE 2. The Solite Quarry. A. Location of the Solite Quarry along the Virginia-North Carolina Border (marked by the star). B. Aerial view of the Solite Quarry (satellite image taken from Google Earth).

The Solite Quarry was once thought to be largely unfossiliferous (Meyertons, 1963) until later, more careful examination of the area was made (Olsen et al 1978; Olsen and Johansson, 1994; Fraser et al, 1996; Fraser and Grimaldi 2003). Since then, the quarry has yielded an array of vertebrate fossils, which includes the archosauromorph *Tanytrachelos*, the gliding reptile *Mecistotrachelos apeoros* (Fraser et al. 2007), the fish *Turseodus*, *Semionotus*, *Parlostegus*, *Cionichthyes*, and *Synorichthyes*, the phytosaur ichnofossil *Apatopus*, and the ornithischian ichnofossil *Atripus cf. milfordensis*. The

Solite Quarry is unique in that it is the only locality that has yielded specimens of *Mecistotrachelos apeoros* and yields the most specimens of *Tanytrachelos ahynis* in the world (Fraser et al. 2007). Other fossils found at the Solite Quarry include a variety of insects that span seven orders, as well as many plant fossils (Casey et al. 2007). These and other fossils are preserved in high abundance: for example: to date over 3000 insect specimens (Fraser and Grimaldi 2003) and nearly 300 specimens of *Tanytrachelos* have been excavated. Many fossil specimens are also in exceptional quality, often displaying articulation of elements and sometimes even traces of soft tissue (Olsen and Johansson 1994, Casey et al. 2007). These conditions categorize the Solite Quarry as a *Konzentrat* and *Konservat Lagerstätte*.

Tanytrachelos specimens have been found in the second, third, and sixteenth Van Houten cycles within the Solite Quarry (Casey et al. 2007), diagrammed in Figure 3A. These specimens have been found at the base of the second division (highstand phase) of the cycles (shown in Figure 3B, stratigraphic unit B), where strata are finely laminated, compressed (due to past tectonic activity near the area), and have a high content of organic carbon (Olsen and Johansson 1994).

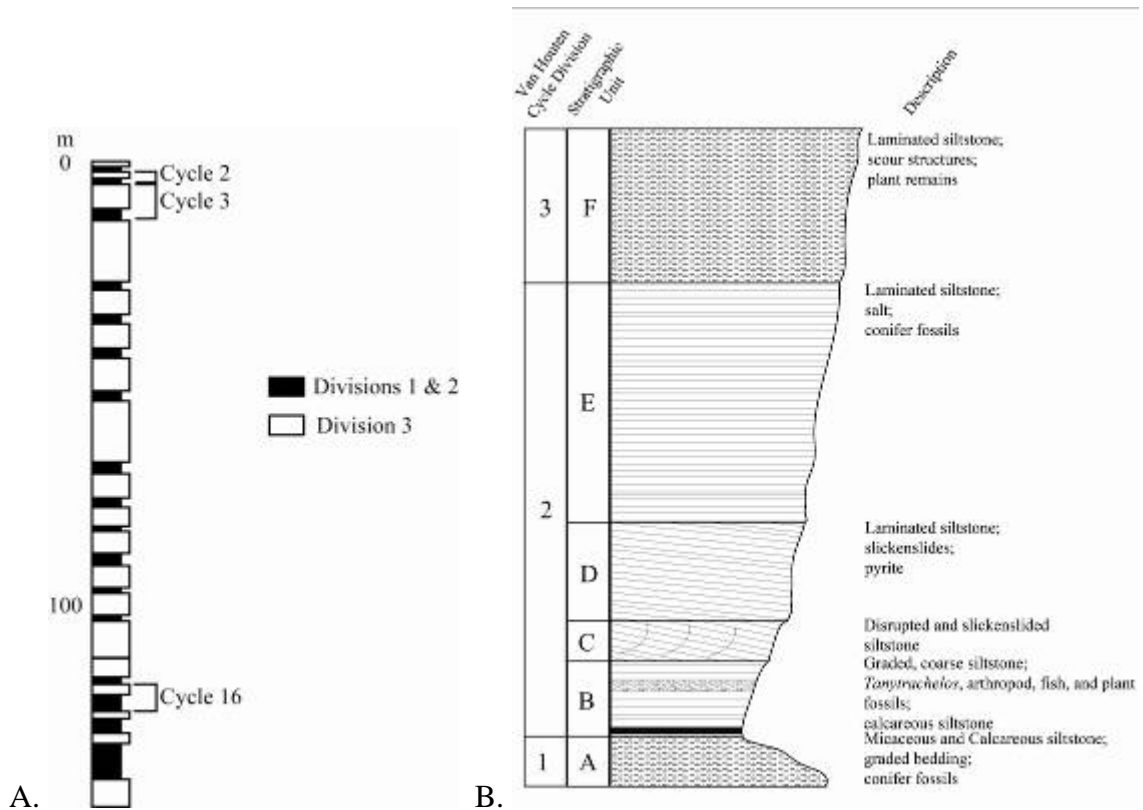


FIGURE 3. Diagrams of the Van Houten Cycles of the Solite Quarry. A. Stratigraphic representation of the collective Van Houten Cycles of the Solite Quarry, numbered from the top downwards. B. Stratigraphic reconstruction of Cycle 2. Division 1 represents the transgressive phase, Division 2 represents the highstand phase, and Division 3 represents the regressive phase. (Information from Olsen et al. 1978.)

Two models have been proposed to describe the lake depths of the Solite during the Triassic. The first model proposed that the lake was deep, environmentally quiet, and

anoxic at the lake bottom. Olsen (1979) and Olsen and Johansson (1994) suggested these conditions are supported by a lack of bioturbation at the bottom (a result from anoxia) and the chemical stratification, a condition found in deep lakes, necessary for this anoxia. If present, this chemical stratification could have been the result of the inability of wind currents to mix the water all the way down to the base of the lake (Olsen and Johansson 1994). Such a deep, quiet lake with no bioturbation at the bottom might conceivably allow high levels of soft tissue and articulation occurrence among preserved fossil specimens among the thinly laminate siltstones at the Solite Quarry.

Although the presence of lamination, high amount and quality of insect preservation, and lack of bioturbation might suggest that the Solite had been a deep lake, it is now also suggested that the depositional environment for the Solite may instead have been a shallow lake with low environmental energy. Liutkus et al (2010) suggested three lines of evidence support a shallow lake scenario. First, the chemistry in the water necessary to support the deposition of dolomitic laminites present in the Solite would have prohibited bioturbation due to toxicity as a result of high alkalinity levels. Secondly, it is possible that the high fluorine concentration in the insect layer of the Solite quarry originated from lake seepage. Finally, the high rates of articulation and low rates of consumption of insects and specimens of *Tanytrachelos* indicate a rapid burial, a condition that would not be met had these animals fallen to the floor of a deep lake (Liutkus et al. 2010).

Casey et al. (2007) also suggested that the bottom of the lake was toxic (due to high levels of alkalinity), and proposed an anoxic lake bottom as well. The presence of soft tissues within various specimens from the Solite Quarry supports both of these conditions. Anoxic water at the lake bottom, possibly caused by lack of lake mixing as a result of no water input from outside sources, would have facilitated the precipitation of diagenetic minerals that coat the fragile tissues within specimens shortly after their reaching the lake bottom. In turn, anoxia may also have slowed the rates of decay sufficiently to prevent decaying bodies from outgassing and floating in the water. With these supporting points, Casey et al. (2007) also suggested that the Solite was a shallow lake at highstand, with the lake connecting to and disconnecting from outside water sources during transgressive-regressive phases.

Previous Work on *Tanytrachelos*

In 1979, P.E. Olsen first described *Tanytrachelos ahynis* based on over 100 specimens. This description outlined details of many of the postcranial elements, vertebral counts, and limb proportions. This publication also described the family Tanystropheidae, and discussed differences and similarities between *Tanytrachelos* and its proposed sister taxon *Tanystropheus*.

A second publication regarding *Tanytrachelos* (Casey et al. 2007) had more of a taphonomic perspective. This work used quantitative methods to describe the frequency of specimen completeness, degree of articulation, and soft tissue preservation within a sample taken from the second, third, and sixteenth lake cycles of the Solite Quarry. Length measurements were taken from bones of the appendicular skeleton and the heterotopic bones, the latter of which were only present in some specimens. However, these lengths were neither presented nor were they compared to each other for morphological purposes. Instead, these data indicated that this sample had a low

frequency of specimen completeness and articulation, a result that was used to support a description of the depositional environment of the Solite Quarry. However, although the main focus of the work by Casey et al. (2007) is on the taphonomy of *Tanytrachelos* and its implications for its depositional environment, the presence of heterotopic bones in some of the studied specimens lead to a discussion of the possibility that *Tanytrachelos* was sexually dimorphic, as it was found that absence of these bones was not a significant taphonomic signal.

MATERIALS AND METHODS

Specimens Studied

A total of two hundred and ninety specimens of *Tanytrachelos* were studied for this project. Two hundred and eighty-three of these specimens belong to The Virginia Museum of Natural History in Martinsville, Virginia, and the remaining seven specimens belong to the Yale Peabody Museum in New Haven, Connecticut. There is a range of degrees of articulation and completeness among specimens. For example, some specimens comprise a single isolated bone within the rock matrix, others consist of several bones within the rock which are very jumbled, while still others exhibit nearly full articulation of the skeleton.

It is extremely difficult to prepare the Solite specimens by traditional mechanical techniques. Consequently, two specimens (Lot 30.221 and Lot 30.277), previously CT scanned by VMNH, were of considerable value. CT imaging of these specimens provided a view of structures within *Tanytrachelos* that would otherwise be masked by sediment. This imaging method has been successfully used by Fraser et al. (2007) to examine the two specimens of *Mecistotrachelos* found at the same locality, revealing details of the specimens that could not otherwise be observed.

Photograph Acquisition

Photographs of *Tanytrachelos* specimens were taken in order to facilitate measuring the specimens with digital imaging software. All photos of the *Tanytrachelos* specimens were taken using a Canon Powershot A560 digital camera. Due to the small features present within this taxon (for example, a typical femur spans roughly 2 cm in length) as well as the problem of photographing gray fossils or fossil imprints within gray shale, a macro lens (10x) was combined with a polarizing lens in order to achieve an adequate resolution of features and to enhance visual contrast between the fossil or imprints and the surrounding rock matrix.

Contrast Enhancement in Photographs

Because the specimens of *Tanytrachelos* were all compressed within fine-grained shales (most within unweathered gray shales, and the rest were in heavily weathered shales that were now brown), they could not be prepared or separated from the rock matrix. Furthermore, many specimens were either permineralized bones that were the same color as the surrounding rock matrix, or were simply indentations of once existing bone within the rock. Thus, it was occasionally necessary to enhance the contrast between the bones and/or bone impressions and the surrounding rock matrix as much as possible in order to determine exactly where the borders of the fossils were located.

All contrast enhancements were performed uniformly for each photograph in Adobe Photoshop CS4. In the cases of *Tanytrachelos* specimens within gray shale, contrast was optimized by selecting the red, green, and blue channels in sequence and adjusting the Brightness/Contrast for each Channel (Image>Adjustments...>Brightness/Contrast...). Specimens whose colors were almost

identical to the color of the surrounding rock underwent the creation of a new channel through the Image Calculations function (Image>Calculations...). In most cases, this new channel was created by subtracting the inverted green channel from the red channel, with differing offset values depending on the particular photograph (method taken from Bengston 2000). In other cases, the multiply function more efficiently optimized the contrast within the photograph. Photographs of specimens within gray shale that were not adequately optimized by these methods underwent direct adjustments through the Apply Image function (Image>Apply Image) using either the overlay or the multiply option on the RGB channel, as demonstrated in Figure 4.

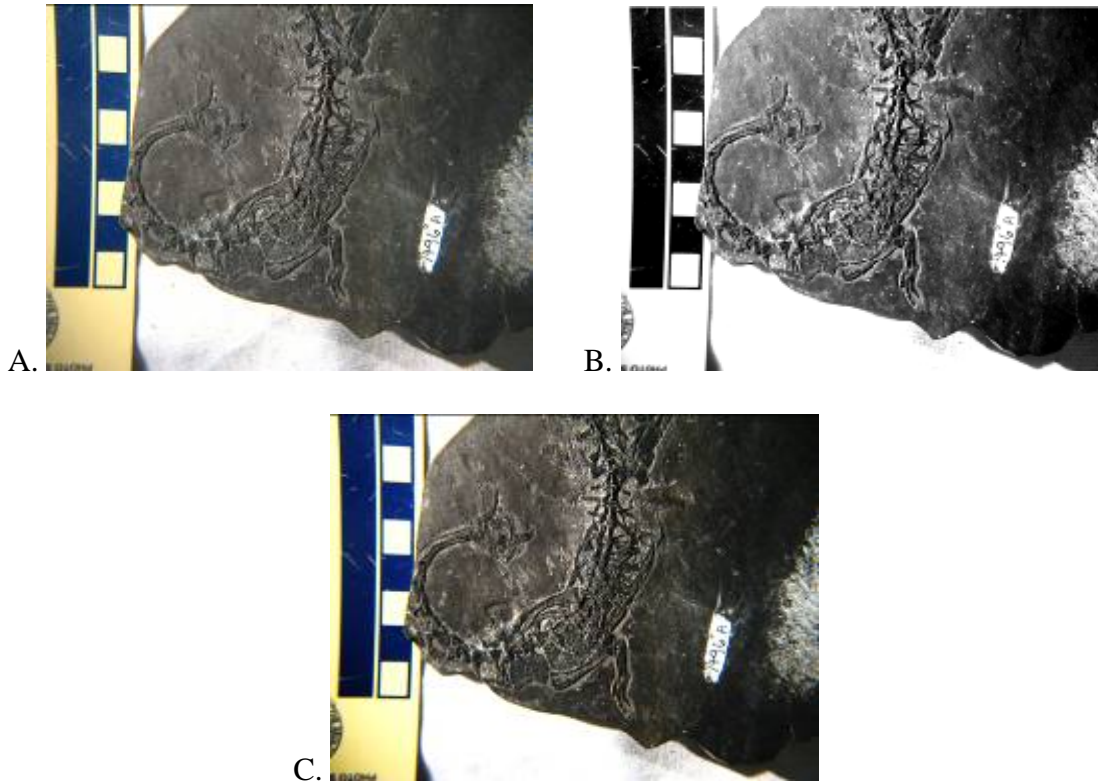


FIGURE 4. Photograph of YPM7496A demonstrating the Image>Calculations function (in this case, the subtract inverted green channel from red channel option is used) as well as the Apply Image function (using the overlay option). A. Before adjustments. B. New channel created with Image Calculations. C. Adjustment of photograph using Apply Image.

Some photographs inherently had more contrast than those of specimens in gray shale because the contained fossils were brown in a lighter tan matrix. Photographs of these specimens that could not adequately be adjusted by the Brightness/Contrast function underwent the Apply Image function, where the multiply option was used on the red channel, demonstrated in Figure 5. This reduced the amount of reddish noise from the tan rock matrix.

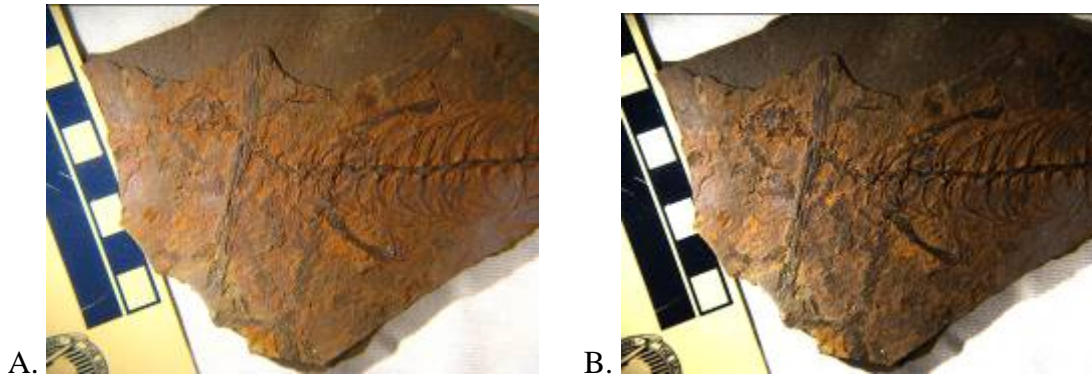


FIGURE 5. Photograph of VMNH120016 demonstrating the Apply Image>Multiply>Red channel adjustment. A. Before adjustment. B. After adjustment.

Gathering Qualitative Data

Qualitative observations were made by identifying individual elements within the specimens and by describing their shapes without the use of morphometrics. For partly articulated or complete specimens, vertebrae were differentiated into cervical, dorsal, sacral, and caudal; phalangeal formulas for the pes and manus were recorded; individual tarsal and carpal bones were identified; finally, the overall shapes of all elements were described. These observations were made from the three hundred and sixteen hand samples and from digital CT scans of the two specimens Lot 30.221 and Lot 30.277, which were examined in ImageJ.

Gathering Quantitative Data

Quantitative data were gathered from the actual specimens and scaled specimen photographs, and consisted of numbers of element types, length measurements, width measurements, and morphometric variables derived from the raw measurements. First, cervical vertebrae, dorsal vertebrae, sacral vertebrae, caudal vertebrae, upper and lower teeth, digits, phalanges, metacarpals, and metatarsals, were counted on specimens. This categorization of elements was important because specific element numbers, such as the number of cervical vertebrae, have significant implications for future studies of evolutionary relationships involving *Tanytrachelos*.

Linear measurements were taken from photographs of specimens digitally in Adobe Photoshop CS4. For each photograph, the scale was calibrated to match the centimeter scale in the photograph with the Set Measurement Scale function in the Analysis menu. Using the ruler tool, a total of seventy different linear measurements were taken of the vertebrae, individual elements of the appendicular skeleton (excluding the carpals and tarsals), the dentary, the heterotopic bones, and the diameters of the skull and orbit. Next, the angles of the paired heterotopic bones in reference to the vertebral column were measured. These specific measurements are illustrated in Figure 6.

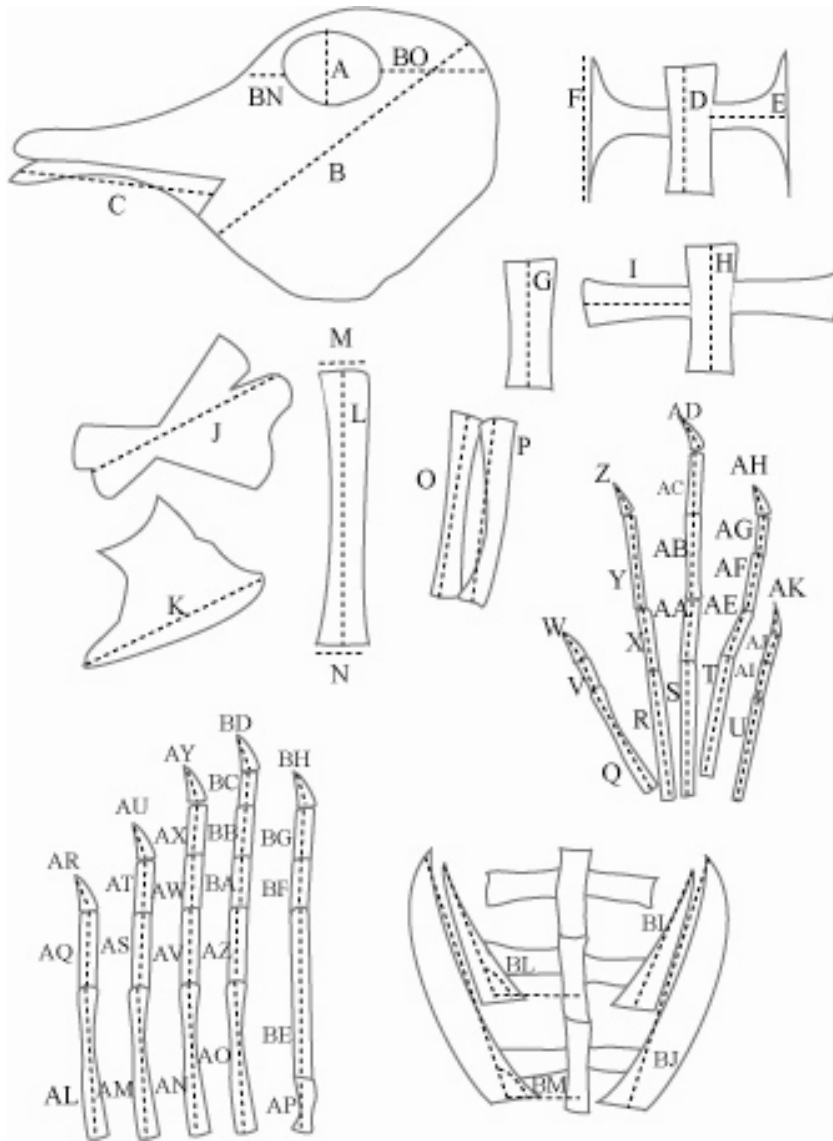


FIGURE 6. Linear and angle measurements taken from individual elements of *Tanytrachelos*. Linear measurements were recorded in centimeters, and angle measurements were recorded in degrees. Sketches of elements are generalized and not to scale. A, orbit diameter; B, skull diameter; C, dentary length; D, length of cervical vertebra centra; E, width of cervical vertebra ribs; F, length of cervical vertebra ribs; G, length of centra of dorsal vertebrae and caudal vertebrae 7 through 31; H, length of centra of sacral vertebrae and caudal vertebrae 1 through 6; I, length of transverse processes on sacral vertebrae and caudal vertebrae 1 through 6; J, ischium length; K, ilium length; L, lengths of femur and humerus; M, proximal widths of femur and humerus; N, distal widths of femur and humerus; O, lengths of the fibula and radius; P, lengths of the tibia and ulna; Q through T, lengths of metacarpals I through V; V and W, phalanx lengths of first manus digit; X through Z, phalanx lengths of second manus digit; AA through AD, phalanx lengths of third manus digit; AE through AH, phalanx lengths of fourth manus digit; AI through AK, phalanx lengths of fifth manus digit; AL through AP, length measurements of metatarsals I through V; AQ and AR, phalanx lengths of first pes digit; AS through AU, phalanx lengths of second pes digit; AV through AY, phalanx lengths of third pes digit; AZ through BD, phalanx lengths of fourth pes digit; BE through BH, phalanx lengths of fifth pes digit; BI, length of the medial heterotopic bone; BH, length of the lateral heterotopic bone; BL, angle of the medial heterotopic bone with respect to the vertebral column; BM, angle of the lateral heterotopic bone with respect to the vertebral column; BN, distance from orbit to front of skull; BO, distance from orbit to back of skull.

An additional five morphometric variables were derived from the length measurements. The diameters of the skull and orbit were used to calculate the skull and orbit areas (Equation 1A), which were then used to calculate the percentage of the skull area occupied by the orbit (Equation 1B).

$$\text{A. area} = \pi \left(\frac{\text{diameter}}{2} \right)^2 \qquad \text{B. \% occupied} = \left(\frac{\text{orbit area}}{\text{skull area}} \right) \bullet 100$$

EQUATION 1. Stepwise procedures calculating skull occupancy by the orbit. A. Surface area of skull or orbit. B. Percentage of skull occupied by orbit.

Aspect ratios were calculated for the humerus and femur by dividing the average of the widths of the distal and proximal ends of each bone by the length of the bone, as shown in Equation 2.

$$\text{aspect ratio} = \frac{\left(\frac{\text{distal width} + \text{proximal width}}{2} \right)}{\text{length of bone}}$$

EQUATION 2. Aspect ratio of the humerus or femur.

RESULTS

Articulated specimens of *Tanytrachelos* averaged around 21 centimeters in length from the head to the posterior end of the 31st caudal vertebra, as approximated by composites of eighteen specimens. The type specimen of *Tanytrachelos*, YPM7496A, is a Yale specimen that was described in the original description by Olsen (1979). Shown and illustrated in Figure 7, this specimen is articulated and mostly complete except for the distal caudal vertebrae and pedes.

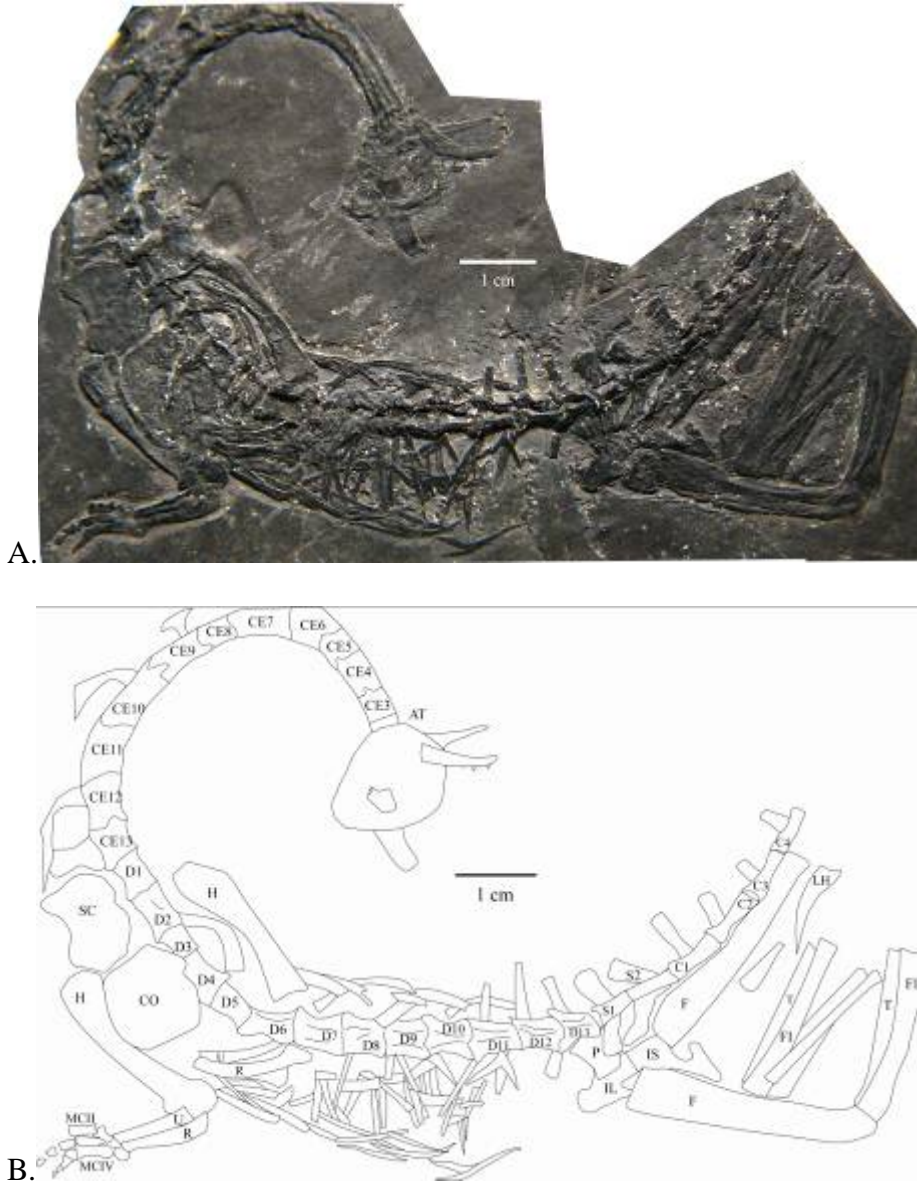


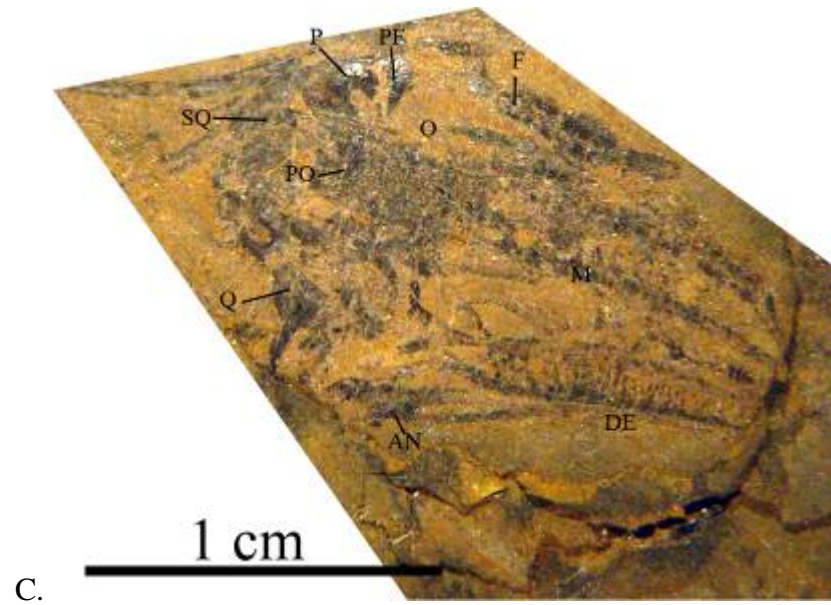
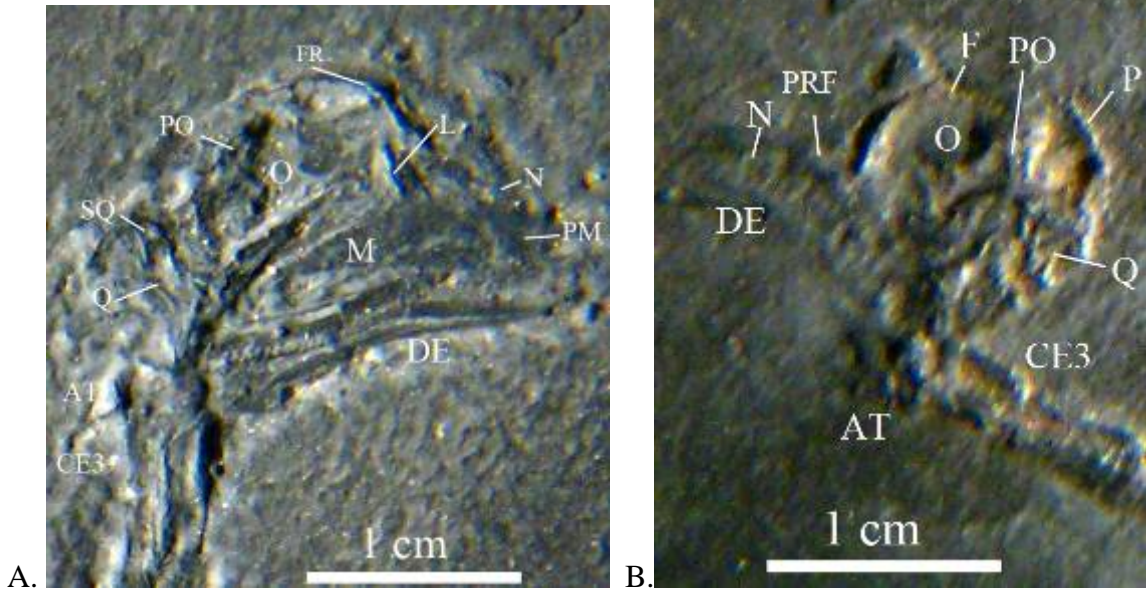
FIGURE 7. The type specimen of *Tanytrachelos ahynis*, YPM7496. A. Photograph of the type specimen. B. Labeled sketch of the type specimen. AT, axis and atlas; C1-4, caudal vertebrae; CE3-13, cervical vertebrae; CO, coracoid; D1-13, dorsal vertebrae; LH, distal heterotopic bone; F, femur; FI, fibula; H, humerus; IL, ilium; IS, ischium; MCII-MCIV, metacarpals; P, pubis; R, radius; S1-2, sacral vertebrae; SC, scapula; T, tibia; U, ulna.

Skull

Of the two hundred and ninety specimens studied, only eleven had the skull still present, and all skulls except one were preserved in strictly lateral views. The dentition is homodont, and there are no less than ten seemingly pleurodont teeth present on each the dentary and the maxilla, the latter containing the most posterior tooth. The teeth are flattened, recurved, and have a single point, as shown in Figures 8A and 8C.

Due to the poor preservation of the skulls, the exact labeling of individual skull bones is uncertain, and suture locations are difficult to indentify. Furthermore, the postparietals, articular, stapedial foramen, paroccipital, external naris, quadratojugal, supratemporal, occipital condyle, crista prootica, and pila antotica cannot be discerned due to poor preservation. In lateral view, the skull is mostly round with a rostrum that comprises roughly one half of the skull length. The premaxilla is reduced, and contacts the maxilla. The nasals are slightly longer than the frontals (Figure 8B), which extend nearly to the back of the dorsal rim of the orbit. There is apparently no pineal foramen. The prefrontal is a slender bone that occupies the anterior 12% of the dorsal rim of the orbit, contacting the small (under 50% the area of the nasal bone) lacrimal, which is confined to the anterior rim of the orbit. The upper temporal fenestra (see Figure 8E) is bordered anteriorly by the postfrontal and triradiate postorbital, dorsally by the parietal, and posteriorly/ventrally by the quadrate. The ventral flange of the squamosal is reduced and does not seem to extend lower than where the upper part of the lower temporal fenestra would be (Figures 8A, 8C, and 8E). The quadrate does not seem to be emarginated, which may be due to specimen compression within the rock. The jugal's posterior process does not reach the posterior margin of the skull.

The type specimen (Figure 8D) possesses a lower jaw that shows the long dentary, small angular (under half the length of the dentary), and tiny splenial. The ventral surface of the dentary in this as well as most other specimens shows a subtle downturn, seen best in figures 8A, 8B, and 8D. However, the ventral surface of the dentary of WS02-120 (Figure 8C) is straight and exhibits no such downturn. The curved dentaries of the other specimens may be a result of taphonomic processes, as they do not consistently occur within each and every specimen. On the other hand, because there are more specimens with curved dentaries than with a straight dentary, a curved dentary may have been the normal condition, and the straight dentary may have been the outlier.



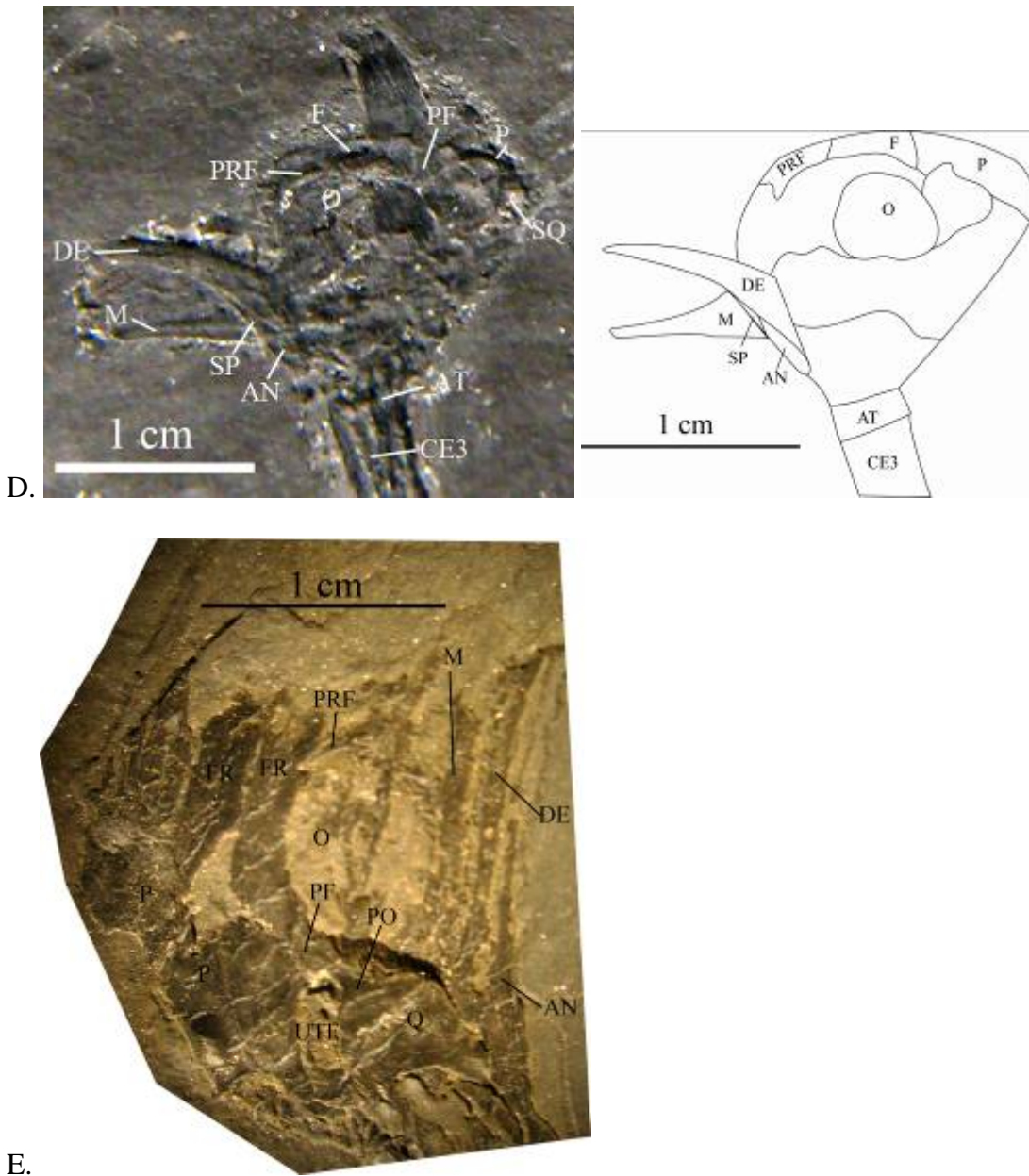


FIGURE 8. Skulls of *Tanytrachelos*. A. Skull of VMNH982 in lateral view. B. Skull of VMNH3651 in lateral view. C. Lateral view of the skull of WS02-120. D. Photograph and illustration of the type specimen skull YPM7496A. E. Photograph of the skull of VMNH2826 in dorsolateral view. AN, angular; AT, axis/atlas; CE3, cervical vertebra 3; DE, dentary; FR, frontal; L, lacrimal; M, maxilla; N, nasals; O, orbit; P, parietal; PF, postfrontal; PM, premaxilla; PO, postorbital; PRF, prefrontal; Q, quadrate; SQ, squamosal; SP, splenial; UTF, upper temporal fenestra.

Four specimens clearly demonstrate that the orbit of *Tanytrachelos* is large and consistently occupies between 11.7% and 13.7% of the lateral skull area, as shown in Figure 9. Furthermore, in three of the four measured specimens, the distance between the anterior orbit rim and the front of the skull is between 81.6% and 83.7% of the distance between the posterior orbit rim and the back of the skull, indicating that the orbit is forwardly placed in these specimens. However, VMNH3651 has a distance from the front

of the skull to the anterior rim of the orbit that is only 54.9% of the distance between the posterior rim of the orbit and the back of the skull. This outlier may be the result of distortion of the skull through depositional and tectonic processes. These statistics are summarized in Table 1.

Specimen	Orbit Area (cm ²)	Skull Area (cm ²)	Ratio of Orbit Area to Skull Area	Ratio of Front Distance to Back Distance
YPM7496A	0.151976	1.2661265	0.12003224	0.816326531
7622	0.0572265	0.4899185	0.116808204	0.818181818
VMNH982	0.2205065	1.813664	0.121580679	0.837209302
VMNH3651	0.1256	0.915624	0.137174211	0.549019608

TABLE 1. Skull morphometrics of the four measured specimens.

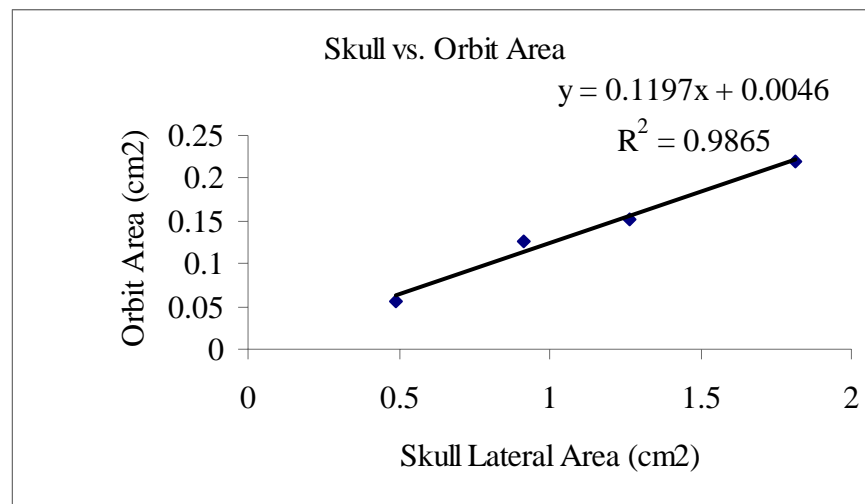


FIGURE 9. Comparison of the area of the orbit to the lateral area of the skull, with the linear equation and correlation coefficient.

Vertebral Column and Ribs

The neck of *Tanytrachelos* is comprised of thirteen cervical vertebrae, which together form roughly 25% of the total length of the animal. The centra are procoelous and altogether average 0.43 cm long (based on eighteen specimens). No one vertebral articulation consistently possesses the longest or shortest centrum of the cervical series, as the cervical centra are all subequal in length.

The axis lacks a centrum and is fused to the atlas (Figure 10A). The following eleven vertebrae have a dichocoelous cervical rib on either side that is longer than and as wide as or less wide than the centrum. Parallel to the centrum, these ribs possess a small overhanging process anteriorly and a larger overhanging process (twice as long as the anterior process) posteriorly. This posterior overhang slightly overlaps the rib of the following vertebra by approximately 0.1 cm. The width and length of cervical ribs increase overall posteriorly, but show no consistent trends in size compared to specific

articulations. Due to the compression of the specimens, neural spine height, width, and shape cannot be determined.

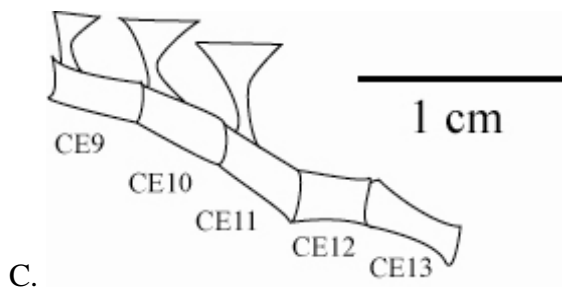
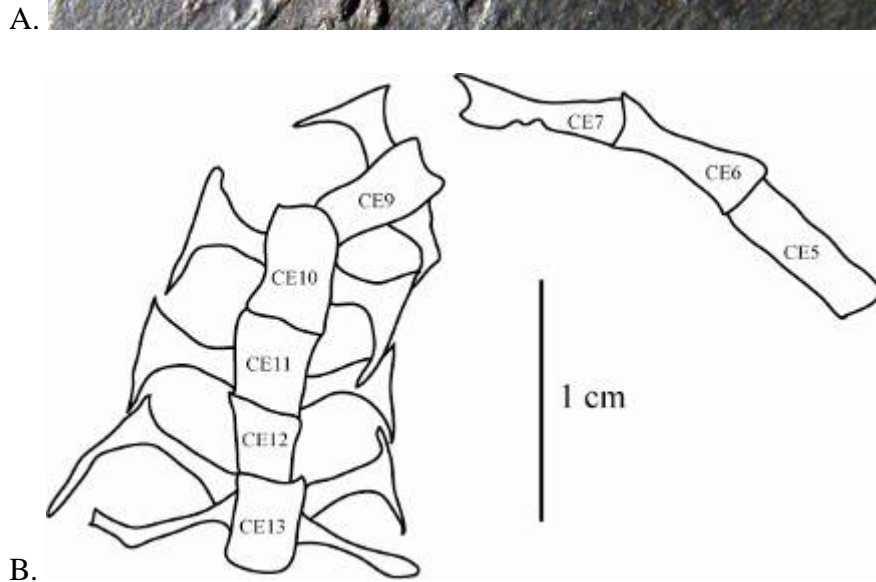
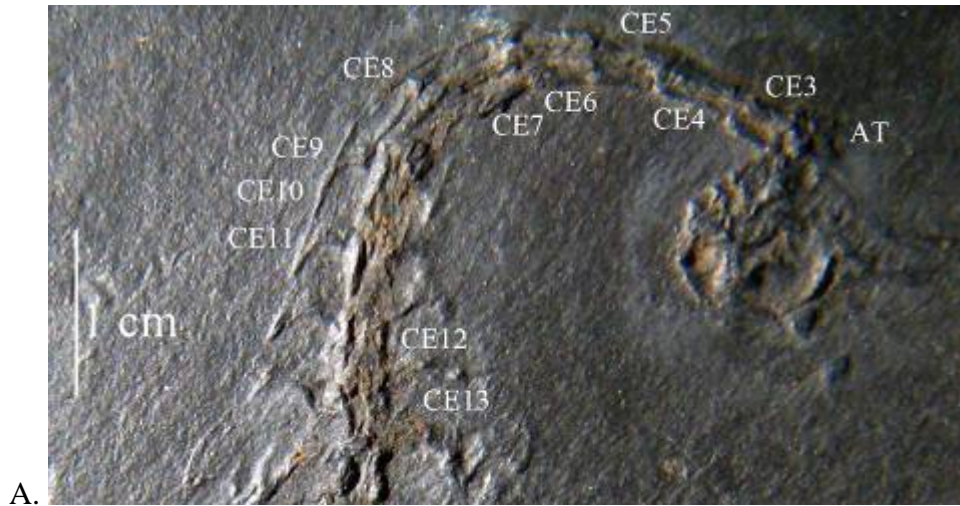
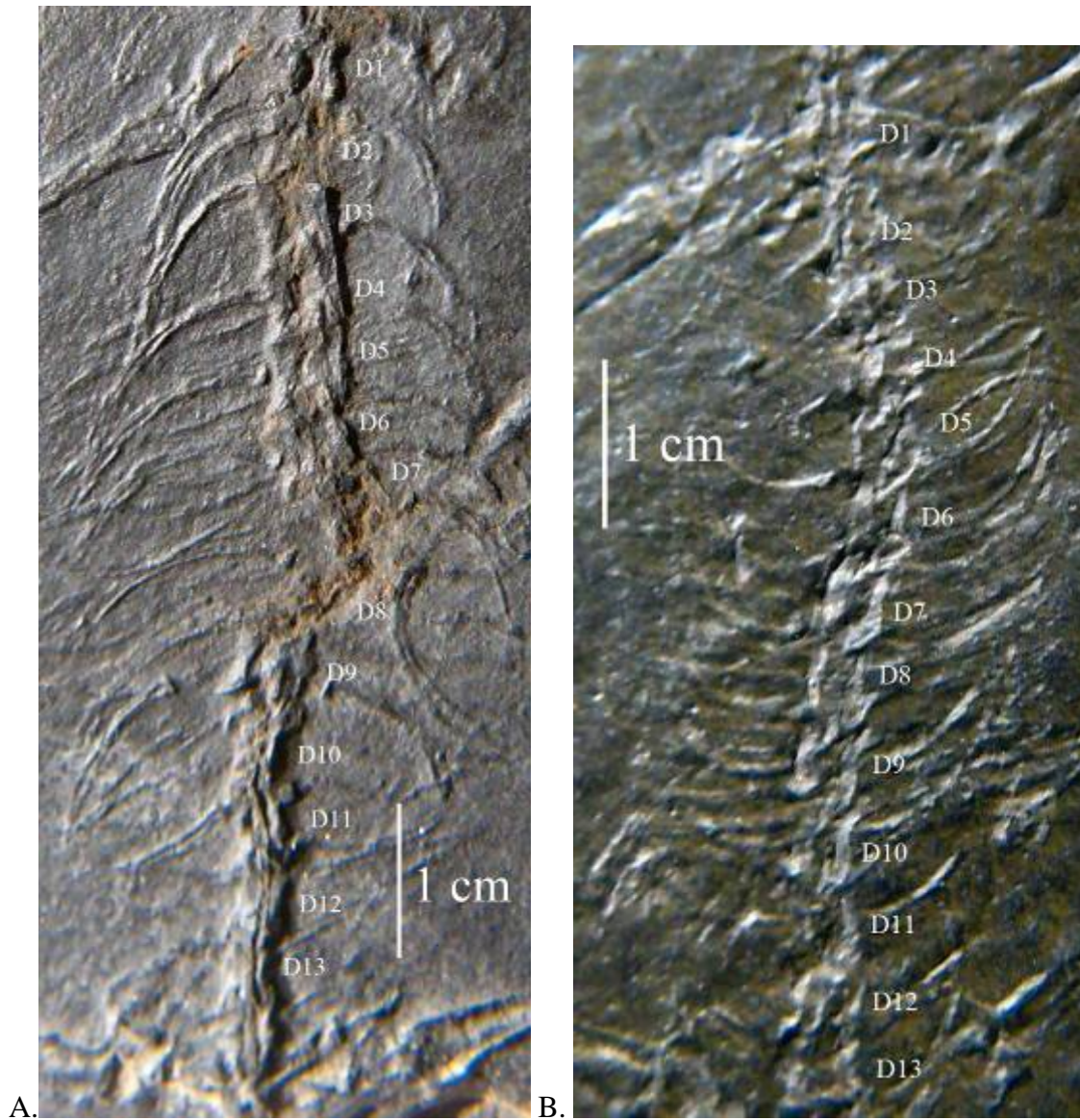


FIGURE 10. Sequences of cervical vertebrae of *Tanytrachelos*. A. Entire cervical vertebral sequence of VMNH3651. B. Illustration of the partial cervical vertebral sequence of VMNH120023. This specimen is slightly disarticulated, weathered, and has several structures obscured by sediment. C. Illustration of a partial imprint of the latter cervical vertebral sequence of VMNH120042. *AT*, axis/atlas; *CE3-13*, cervical vertebrae.

Following the cervical vertebrae are a total of thirteen procoelous dorsal vertebrae. On average, the dorsal vertebrae collectively span approximately 21% of the total body length. Dorsal centra share the same basic shape as cervical centra, and the average centrum of a dorsal vertebra is 0.374 cm long (based on twenty specimens). Although the centra are subequal in length, the anterior 8 dorsal centra are generally slightly longer than the posterior five dorsal centra. As is the case for the cervical vertebrae, the neural spines on the dorsal vertebrae are impossible to discern due to the compression of the specimens.



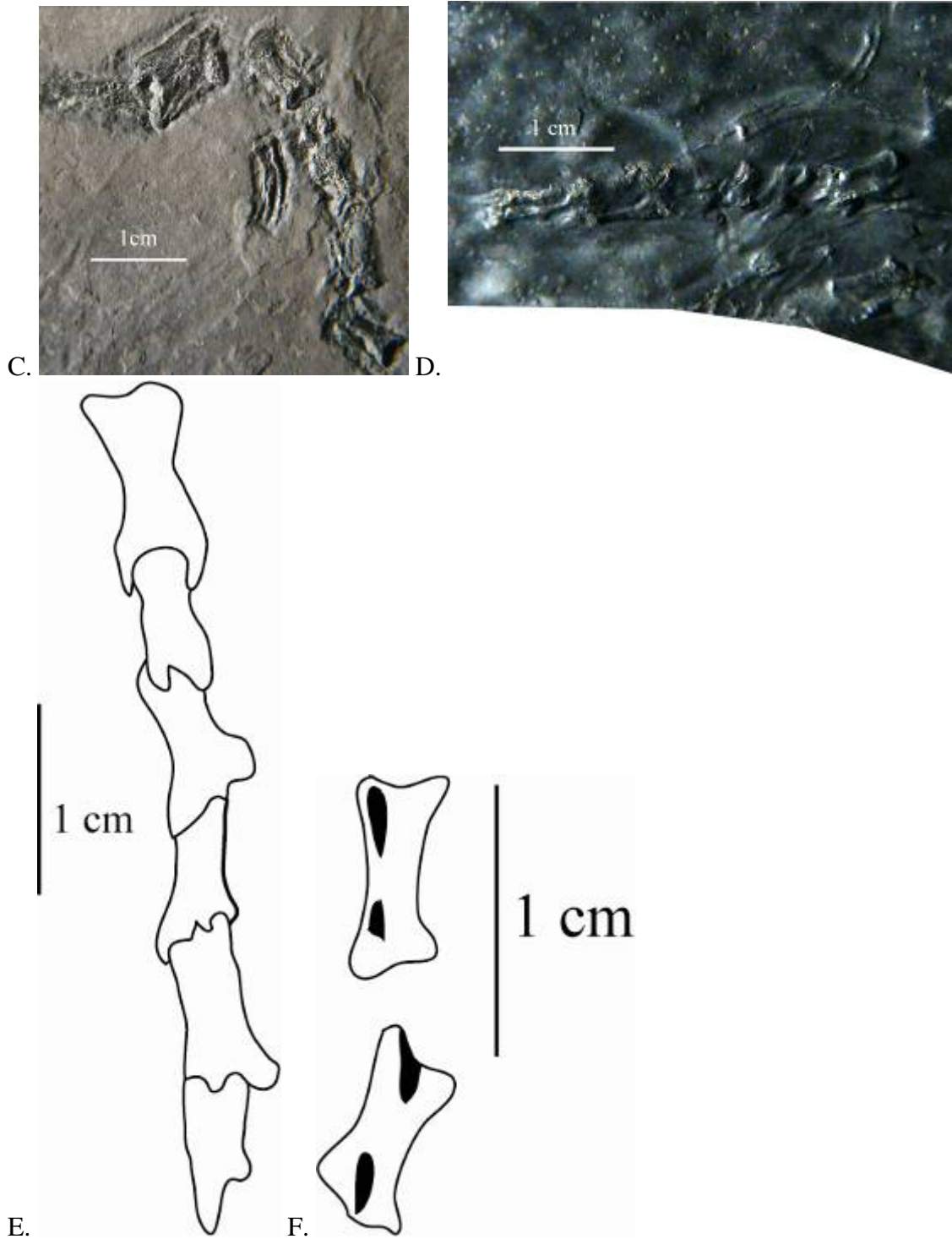
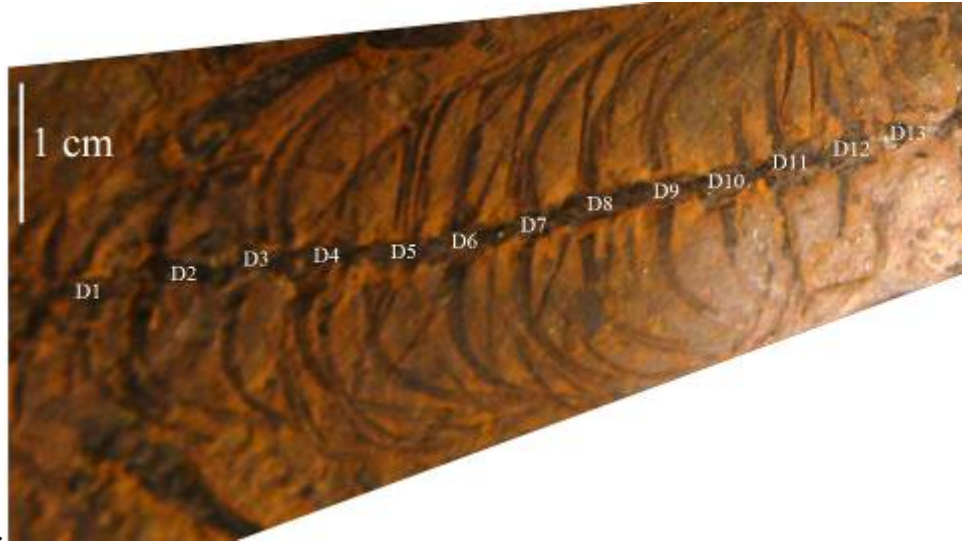
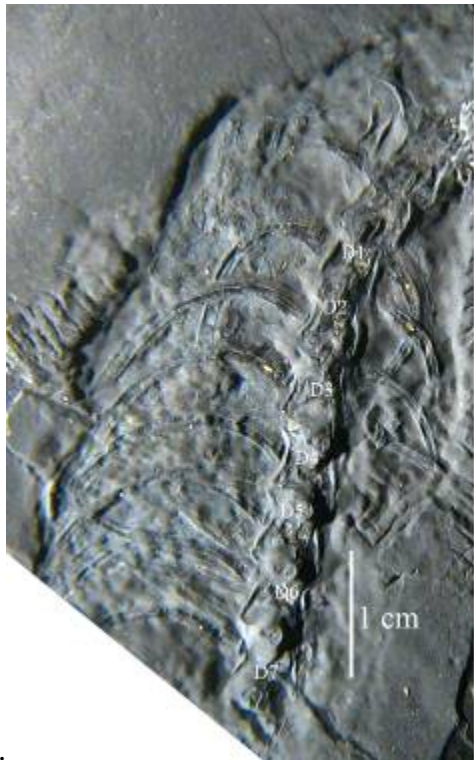


FIGURE 11. Articulated and disarticulated dorsal vertebrae of *Tanytrachelos*. A. Articulated dorsal vertebrae of VMNH3651. B. Articulated dorsal vertebrae of 7622A. C. Several disarticulated dorsal vertebrae and a dorsal rib of lot 30.240. D. Several articulated dorsal vertebrae of VMNH3240. E. Illustration of several articulated dorsal vertebrae of lot 30.251. F. Illustration of two disarticulated dorsal vertebrae of VMNH3221. D1-13, dorsal vertebrae.

Each of the dorsal vertebrae supports an unfused pair of long, curved ribs, as shown in Figures 11A, 11B, and 12. Although these dorsal ribs are holocephalous, a few individual ribs of unknown articulation have been found with a wavy surface on the end of the head, as shown in Figures 12E and 12F. In addition to these curved ribs, which decrease in length posteriorly, dorsal vertebra 11 through 13 each possess a pair of short, straight transverse processes, as shown in Figures 7, 11A, 11B, and 12A.



A.



B.



C.

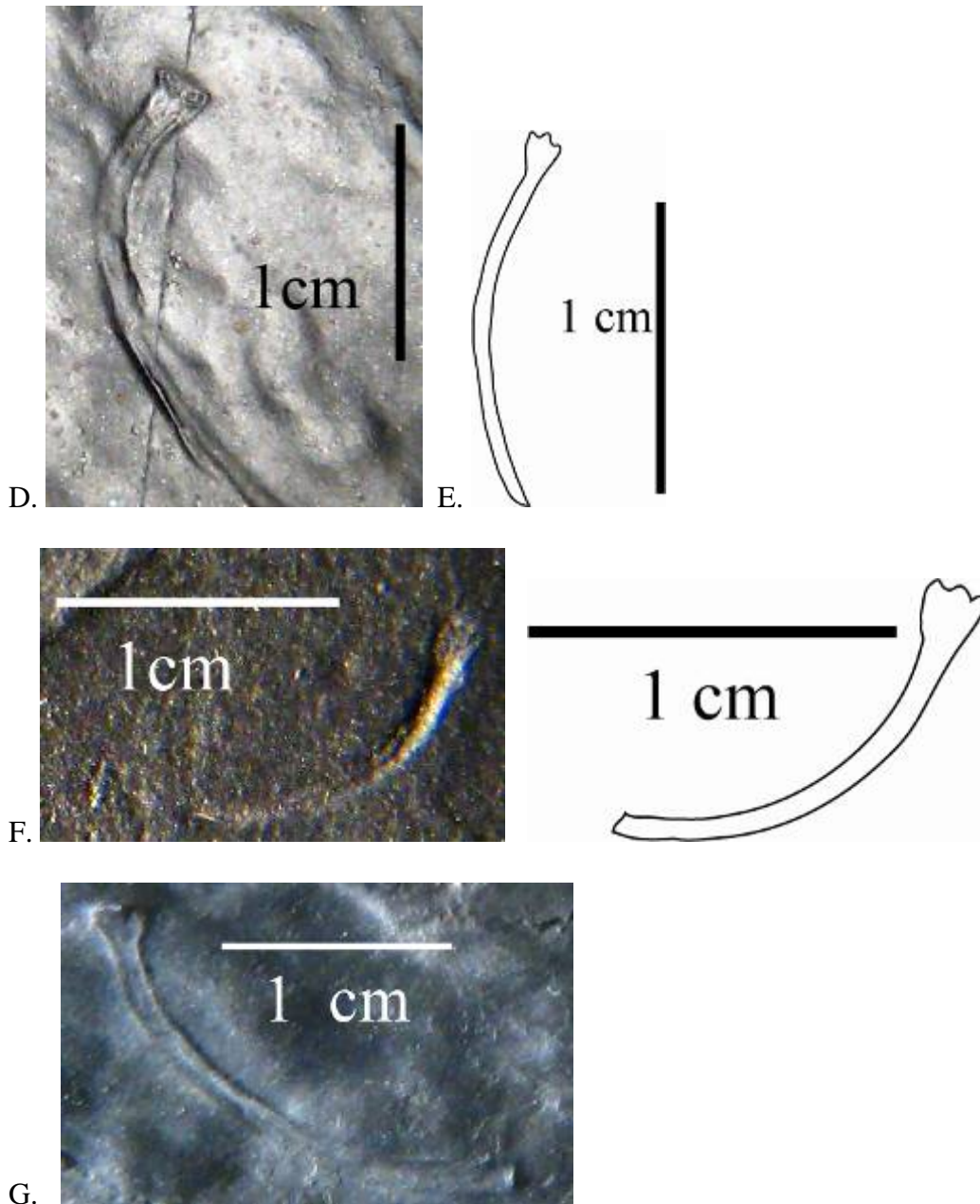


FIGURE 12. Articulated and disarticulated ribs of *Tanytrachelos*. A. Dorsal vertebrae and ribs of VMNH120016. B. First seven dorsal vertebrae and ribs of VMNH2850. C. Disarticulated ribs of YPM7621. D. Single rib of FN17A4. E. Illustration of single rib of lot 30.762. F. Photograph and illustration of single rib of lot 30.271. G. Single rib of VMNH3239. *D1-D13*, dorsal vertebrae; *RI*, rib.

Two sacral vertebrae, shown in Figure 13, support the pelvis and comprise approximately 4% of the total vertebral length. The transverse processes of the first sacral vertebra are oriented roughly perpendicular to the centrum (in dorsal view), and the transverse processes of the second sacral vertebra are angled anteriorly to meet the distal ends of the first sacral's transverse processes.

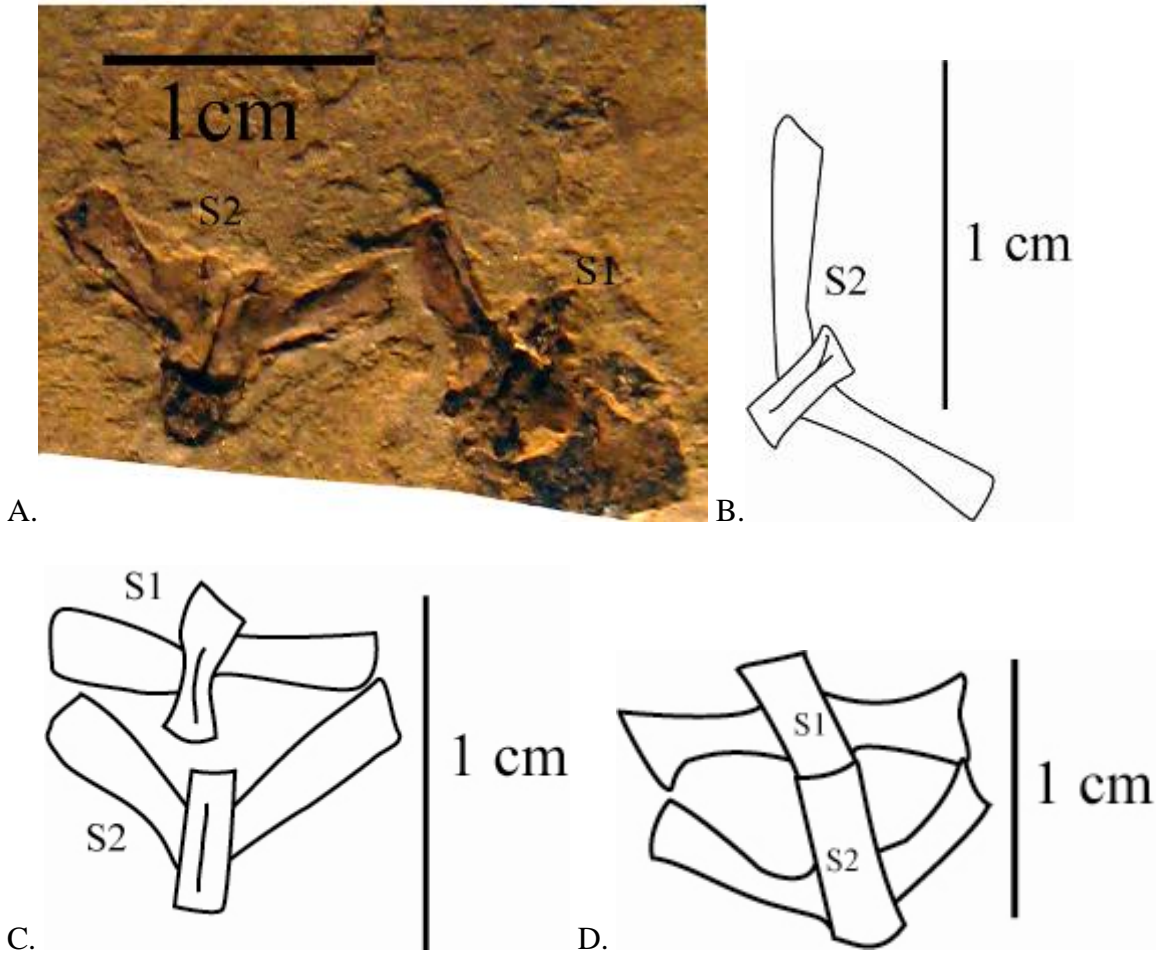


FIGURE 13. The sacral vertebrae of *Tanytrachelos*. A. Disarticulated sacral vertebrae of lot 30.245. B. Illustration of the second disarticulated vertebra of Lot 30.712. C. Diagram of the somewhat articulated sacral vertebrae of VMNH977. D. Diagram of the articulated vertebrae of VMNH120048. S1-2, sacral vertebrae.

The tail of *Tanytrachelos* is distinctly long, making up half of the total vertebral length. It is comprised of at least thirty-one procoelous caudal vertebrae, shown completely only in one specimen (Lot 30.267, Figure 14A). The first six caudal vertebrae each possess a short, straight transverse process on either side of the centrum, as illustrated in Figure 14. The caudal centra collectively average 0.436 cm in length (based on twenty-eight specimens), and the transverse processes collectively average 0.479 cm long (based on eighteen specimens). In many cases, the transverse processes are longer than the centrum with which they articulate. However, other specimens seem to demonstrate no such correlation of lengths, and have various pairs of transverse processes that are longer than their corresponding centrum. The caudal centra are mostly subequal in length; however, caudal centra 6 through 9 are generally the shortest, and caudal centra 20 through 24 are generally the longest.



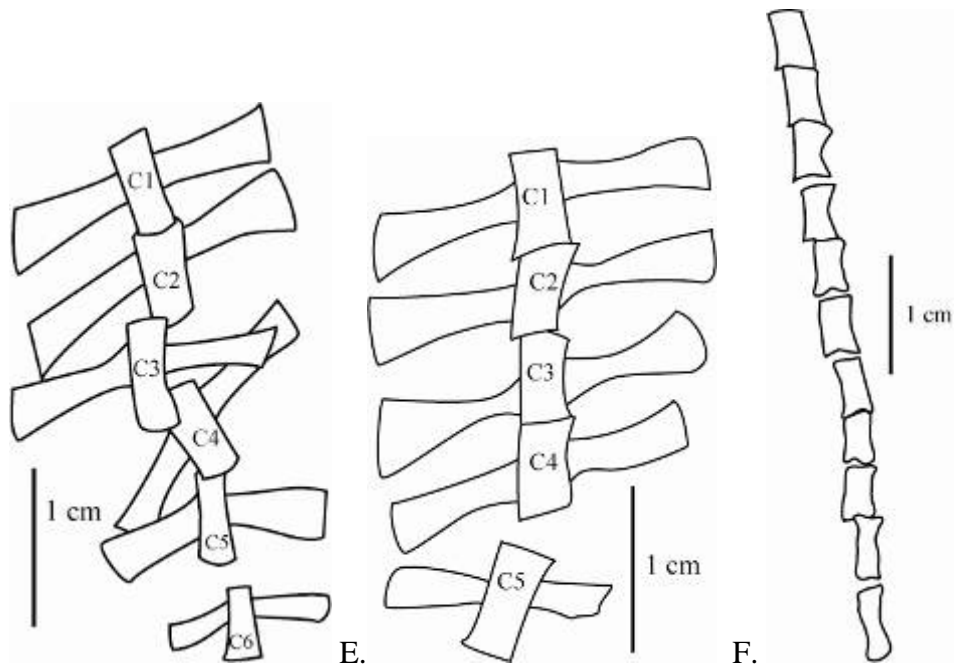
A.



B.



C.



D.

E.

F.

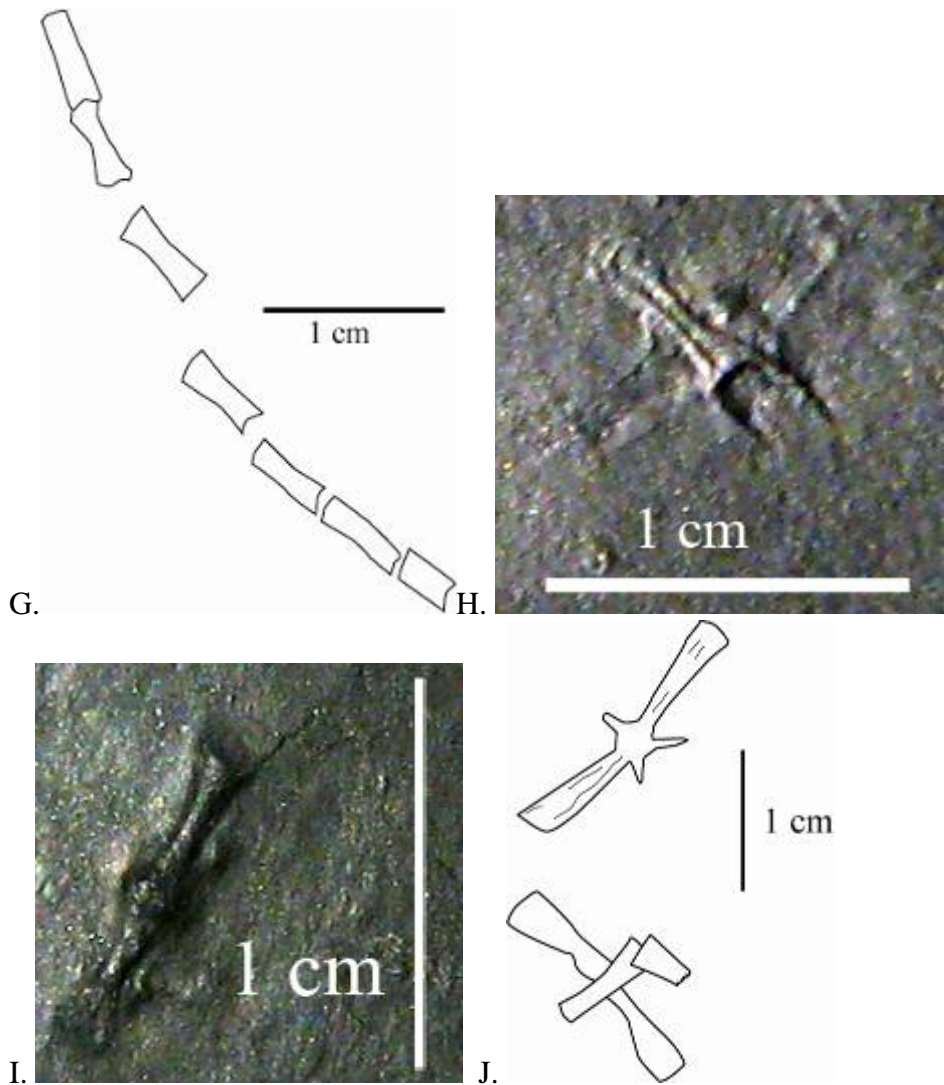


FIGURE 14. Caudal vertebrae of *Tanytrachelos*. A. Second sacral and first 31 caudal vertebrae of Lot 30.267. B. First 21 vertebrae of specimen VMNH2827. C. Second sacral and first four caudal vertebrae of YPM7621. D. Illustration of the first five caudal vertebrae of VMNH3059. E. Illustration of the isolated first five caudal vertebrae of VMNH3238. The right transverse process of the fifth caudal vertebrae is partly obscured by sediment. F. Illustration of distal caudal vertebrae of VMNH965. Exact articulations are unknown. G. Illustration of impression of a sequence of distal caudal vertebrae of Lot 30.269. H. Caudal vertebrae of lot 30.227 247. Although exact articulation is unknown, the transverse processes indicate that it is one of the first seven caudal vertebrae. I. Two articulated distal caudal vertebrae of VMNH991. J. Illustration of two proximal caudal vertebrae of Lot 30.325 23. *CI-31*, caudal vertebrae; *S2*, second sacral vertebra.

Pectoral Girdle and Anterior Limbs

An unfused scapula and coracoid occupy each side of the pectoral girdle. As shown in Figure 15, the coracoid is slightly larger than the scapula. They also differ in shape, as the coracoid is mostly oval in shape (with its long axis perpendicular to the vertebral column), whereas the scapula is fan-shaped. No coracoid foramen can be discerned.

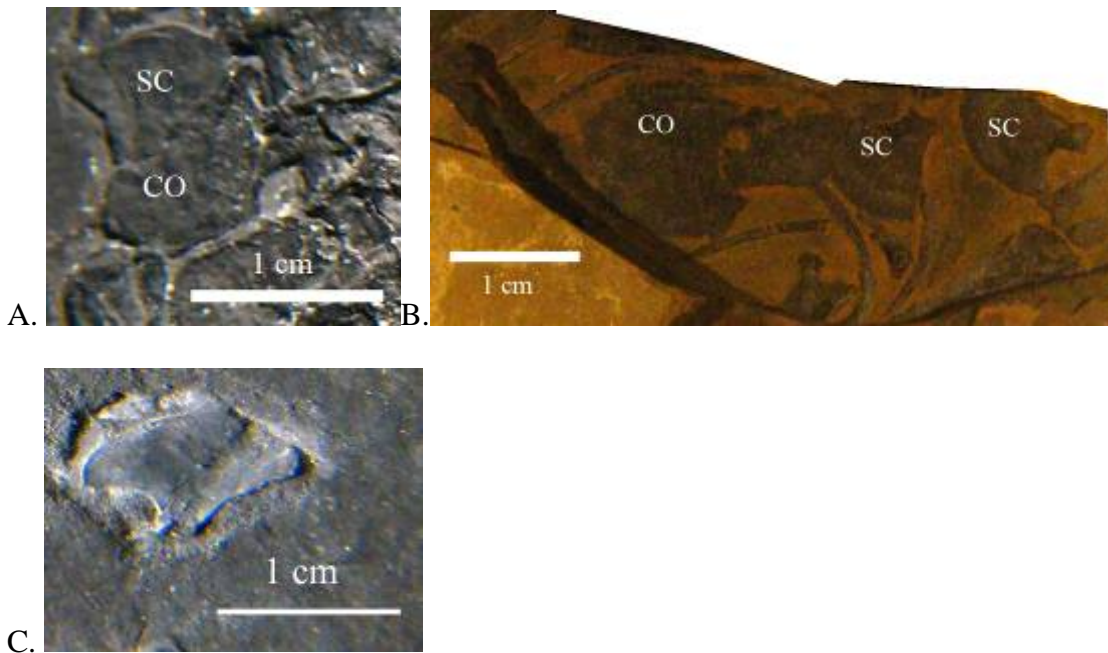
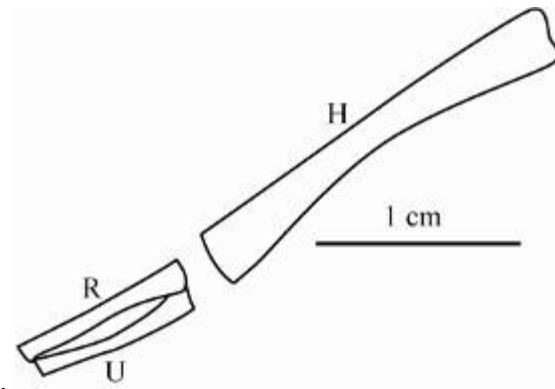
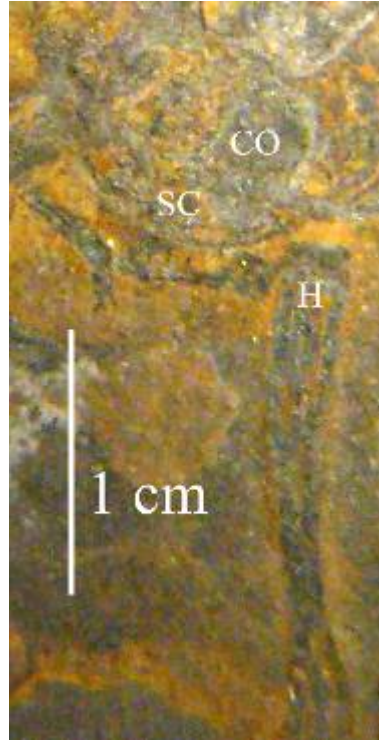
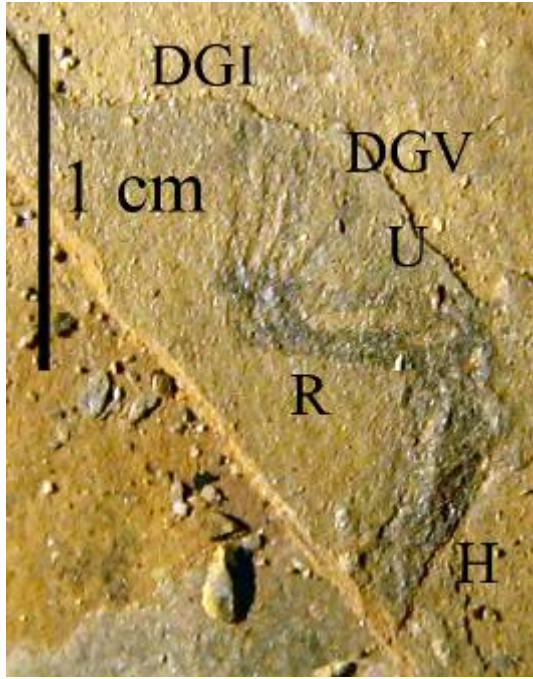


FIGURE 15. Scapulae and coracoids of *Tanytrachelos*. A. Articulated and unfused left coracoid and scapula from YPM7496A. B. Disarticulated scapulae and coracoid from VMNH120046. C. Scapula from disarticulated specimen YPM7621. SC, scapula; CO, coracoid.

In the forelimb (shown in Figure 16), the average radius length (0.864 cm, based on twenty-one specimens) is 92% of the average length of the ulna (0.910 cm, based on nineteen specimens) and 41% of the average length of the humerus (2.15 cm, based on twenty-five specimens). The middle of the humeral shaft is straight and narrower than its proximal and distal ends. In some specimens, the distal end of the humerus is wider, but in others, the proximal end is wider, and both width measurements averaged to be 0.30 cm long. No entepicondylar or ectepicondylar grooves or foramina can be discerned, which may be a result of fossil distortion through local tectonic activity rather than absence of these structures.



A.

B.

C.

D.

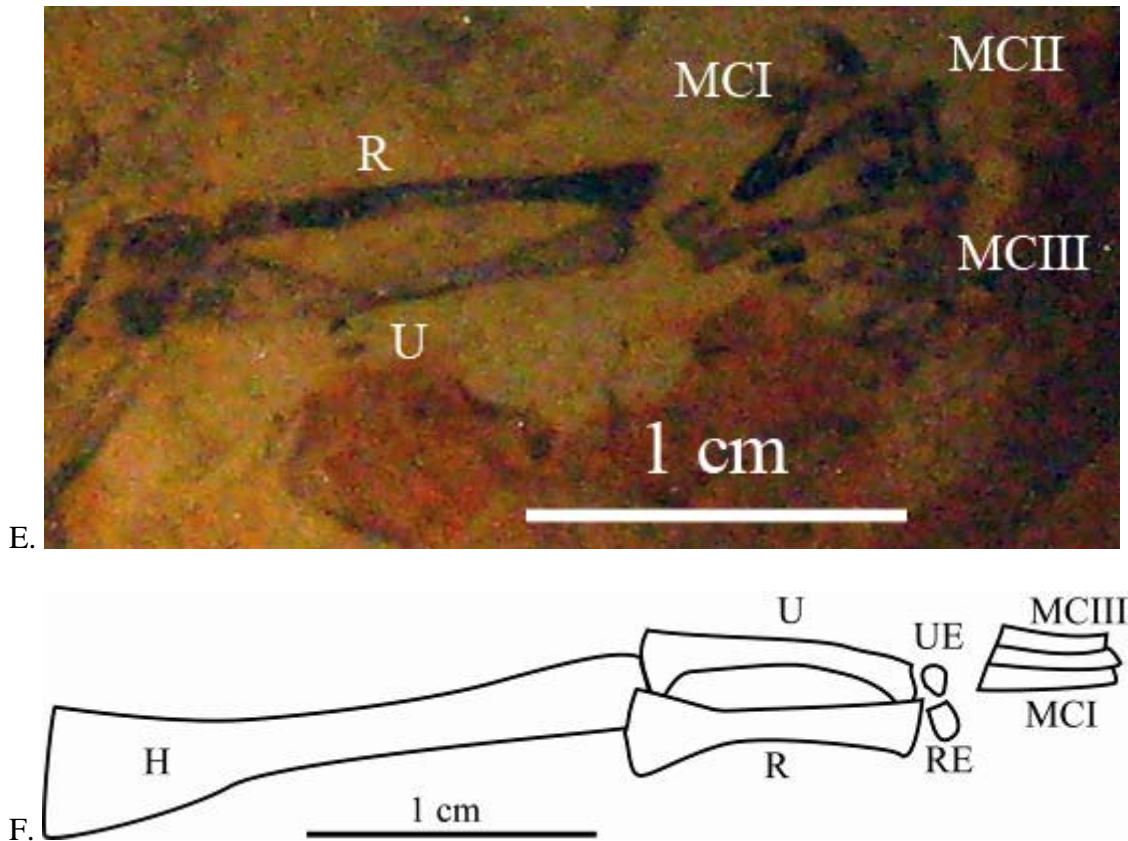


FIGURE 16. The anterior limb of *Tanytrachelos*. A. The articulated forelimb of 04-23. Only the distal half of the humerus is present. B. The left pectoral girdle and humerus of VMNH120023. C. Disarticulated humerus and proximal ends of radius and ulna of VMNH3184. D. Illustration of the left forelimb of VMNH3651. The manus was disarticulated beyond recognition. E. Right somewhat articulated distal forelimb of VMNH120049. F. Illustration of the right forelimb of Lot 30.267. The manus is greatly disarticulated. *DGI-DGV*, digits I through V; *H*, humerus; *MCI-MCIII*, metacarpals I through III; *R*, radius; *RE*, radiale; *U*, ulna; *UE*, ulnare.

The manus has five metacarpals and five digits, with the phalangeal formula 2-3-4-4-3. The carpals are comprised of an ulnare, a radiale, and two distal carpals, as diagrammed in Figure 17. The metacarpals are similar to each other in length, and the digit lengths are roughly symmetrical with the third digit being the longest. For example, the specimen Lot 30.315 (Figure 17) possesses a second digit with three phalanges that total 0.8 cm in length and a fourth digit with four phalanges that total 0.88 cm in length. This similarity in total digits length can be explained by phalanges 1 and 2 of the second digit, which are both longer than those of the fourth digit. The third digit of this specimen measures 119% the length of the fourth digit.

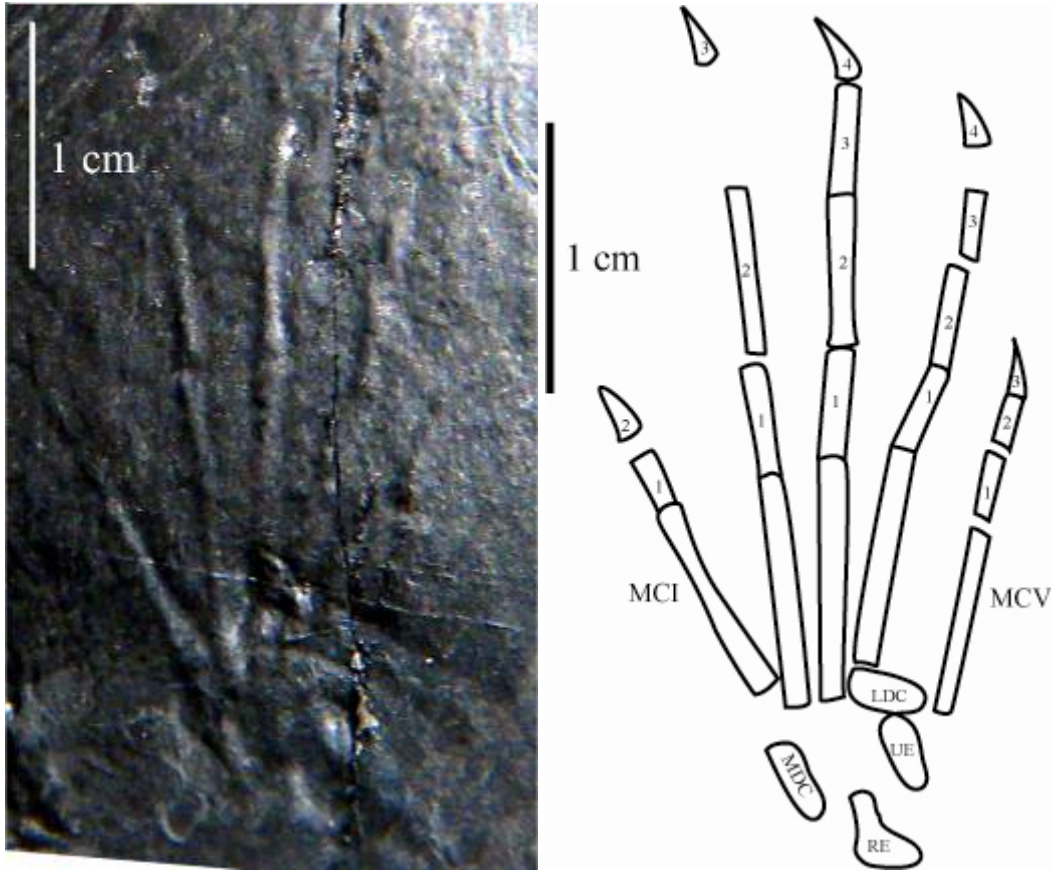


FIGURE 17. The right manus of *Tanytrachelos*, shown in the photograph and illustration of Lot 30.315. 1-4, individual phalanges; LDC, lateral distal carpal; MCI-V, metacarpals I through V; MDC, medial distal carpal; RE, radiale; UE, ulnare.

Pelvic Girdle and Posterior Limbs

Like the pectoral girdle, the pelvic girdle is difficult to discern from the surrounding matrix and other elements (most often the sacral vertebrae) in the vast majority of specimens. However, specimens YPM7621 and VMNH120048 most clearly show the pelvic elements of *Tanytrachelos* (Figure 18). The ilia and pubes are similar in average length (0.84 cm based on the only measurable specimen and 0.85 cm based on two specimens respectively), and the ischia have the longest average length at 1.19 cm (based on two specimens). No preacetabular buttress can be discerned on the ilium, and no obturator foramen can be seen in the pelvis.

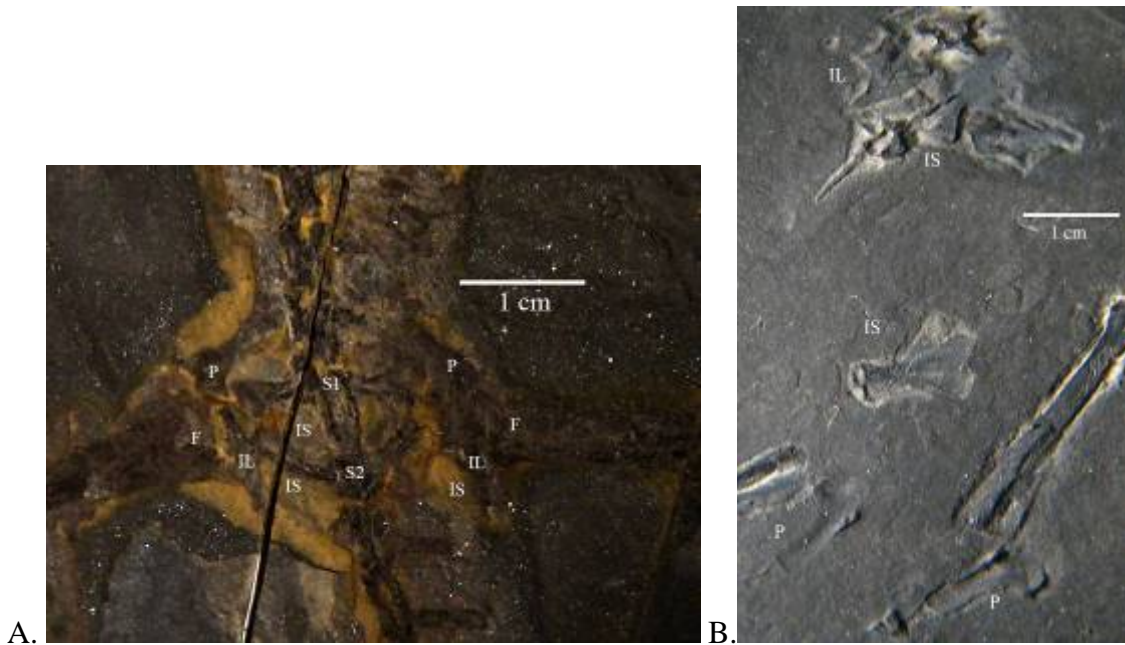


FIGURE 18. The pelvic girdle of *Tanytrachelos* in various states of articulation. A. The articulated pelvic girdle of VMNH120048. B. Disarticulated ilium, ischiums, and pubises of specimen YPM7621. *F*, femur; *IL*, ilium; *IS*, ischium; *P*, pubis; *S1-2*, sacral vertebrae.

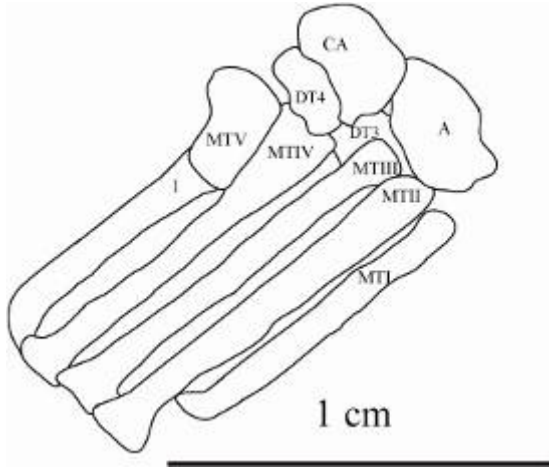
The hind limb, shown in Figure 19, is noticeably longer and larger than the forelimb, and contains a straight, non-sigmoidal femur averaging 2.67 cm in length (based on forty-one specimens). The middle of its shaft is narrower than the widths of its proximal and distal ends, which average 0.383 cm and 0.276 cm respectively. As in the case of the humeral proximal and distal widths, one end is not consistently wider than the other and vice versa.

The fibula and tibia are both shorter than the femur (average lengths at 1.69 cm based on thirty-four specimens and 1.79 cm based on thirty-seven specimens respectively), and in most specimens, the fibula is shorter than the tibia, as it ranges from 81% to 97% the length of the tibia. In contrast, three of the nineteen measured specimens have a fibula with a length that ranges from 106% to 110% the length of the tibia.

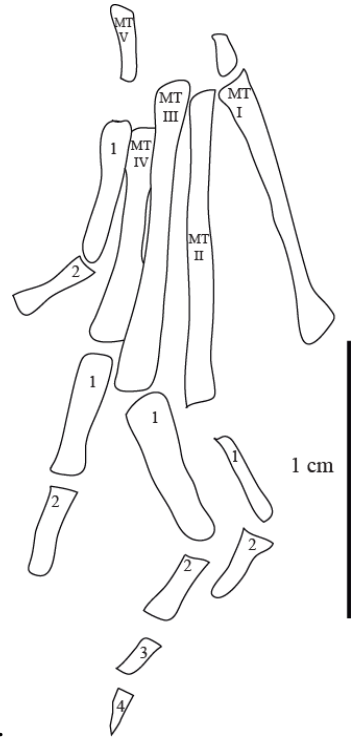


FIGURE 19. The right hindlimb and partial left hindlimb of *Tanytrachelos* (VMNH120049). A, astragalus; CA, calcaneum; DT4, distal tarsal 4; F, femur; FI, fibula; T, tibia.

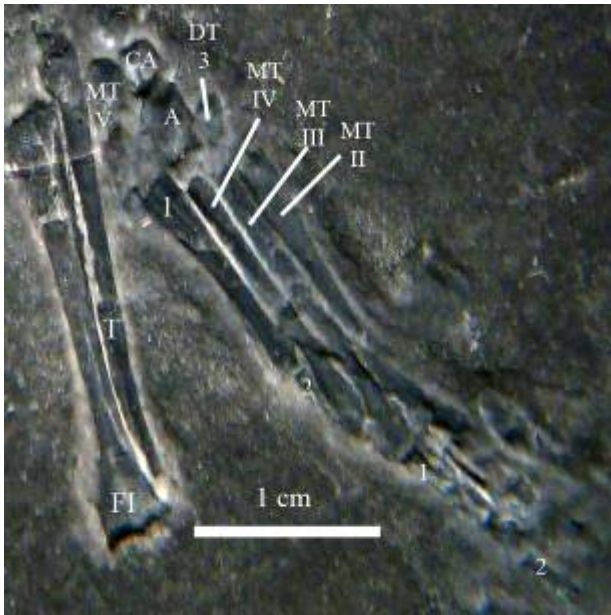
The tarsals include the proximal astragalus and calcaneum, as well as distal tarsal 3 and distal tarsal 4. A space is visible between the unfused astragalus and the calcaneum of Lot 30.245, as shown in Figure 20A. This space could not be discerned in the other specimens, which may be a result of taphonomy. The pes of *Tanytrachelos*, shown in Figure 20, has five metatarsals, the first four being subequal in length. Metatarsal V is greatly reduced in length, spanning less than one half the length of any of the other metatarsals. It is straight with a slight hook to its proximal end as shown in Figure 20A. There are five digits on the pes, which has the phalangeal formula 2-3-4-5-4. The phalanges are progressively shorter within each digit, so that, for example, within digit 4, the fourth phalanx is shorter than the third phalanx, which is shorter than the second phalanx. The fifth digit has an extraordinarily long first phalanx, averaging 0.887 cm long (based on three specimens). The two specimens that had both the fifth pes metatarsal and its first phalanx preserved showed that the length of the first phalanx averages between 3.6 to 4 times the length of the fifth metatarsal. The three specimens that had the first phalanx of digit V and the third metatarsal preserved showed that the length of the first phalanx of digit V was between 70% and 91% of the length of the third metatarsal.



A.



B.



C.

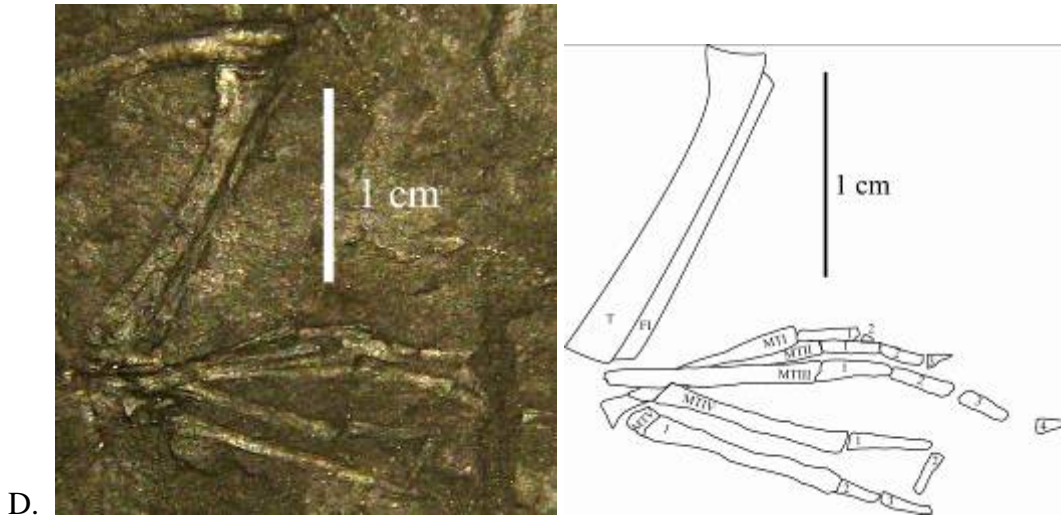


FIGURE 20. Illustrations and photographs of the pes of *Tanytrachelos*. A. Illustration of the right pes of specimen Lot 30.245. B. Illustration of the right pes of VMNH2827. C. Photograph of the left pes of YPM7621. D. Photograph of the left pes of YPM7540. *I-4*, individual phalanges; *A*, astragalus; *CA*, calcaneum; *DT3-4*, distal tarsals 3 and 4; *FI*, fibula; *MTI-V*, metatarsals I through V; *T*, tibia.

Although the pes of *Tanytrachelos* is noticeably larger than the manus, the disparity of size is not present in the corresponding digit lengths. The total digit lengths (phalanges only) as approximated by a composite of incomplete specimens show a disparity under 0.1 cm, with exception to the lengths of the first digits of the manus and pes, which differ by 0.16 cm. Instead, the extreme difference in lengths between the overall manus and pes is caused by the noticeable differences in lengths between the shorter metacarpals and their corresponding longer metatarsals. The ratio of the lengths of the metacarpals to those of the metatarsals are 0.337, 0.423, 0.438, 0.426, and 1.781 for digits I through V respectively. The unusually large ratio of the length of metacarpal V to the length of metatarsal V is a result of the unusually short length of metatarsal V in comparison to the other four metatarsals. However, the ratio of the length of metacarpal V to the combined lengths of metatarsal V and its first phalanx, which is nearly as long as the other metatarsals, is 0.442.

Gastralia and Heterotopic Bones

Masses of curved, densely clustered gastralia are present in the ventral region of the more complete and articulated specimens. They are preserved as a series of thin straight to arc-shaped impressions compressed under the rest of the body in the matrix, as shown in Figure 21. The series of gastralia begins at the fourth dorsal vertebra and ends anterior to the first sacral vertebra. All individual gastralia are thinner than the body ribs attached to the vertebrae. Although all occurrences of gastralia are heavily compressed under other bones, it seems that there are two pairs of gastralia per vertebra, which is a typical condition among protorosaurs. This is most easily seen in Figure 21B.



FIGURE 21. Sets of gastralia found in *Tanytrachelos*. A. Specimen 04-22 has gastralia (the thin, straight lines clustered under the ribs) from the fourth dorsal vertebra to before the first sacral vertebra. B The torso of specimen Lot 30.267, showing masses of gastralia from the fourth dorsal vertebra onwards. C. A cluster of gastralia in the middle trunk region of specimen Lot 30.217:52.

Several of the articulated specimens have a pair of curved, parallel heterotopic (Olsen 1979) bones on each side of the tail, articulating with caudal vertebrae 4 and 5 (shown in Figure 22A). The lateral bone within the pair is larger than the medial bone, whose length ranges between 45% and 83% of the length of the medial bone. Together, these pairs of bones have a broad base posteriorly, and end in a pointed base anteriorly. No bones or structures can be seen fusing the heterotopic bones to the vertebral column, a case that is particularly noticeable in specimen 04-23, shown in Figure 22B. In this specimen, the heterotopic bones and femora have been pushed towards the anterior end of

the body presumably by forces during burial, because the distal ends of the femora are pointing anteriorly. Furthermore, the heterotopic bones are located between caudal vertebrae 2 and 3, not caudal vertebrae 4 and 5 as is the case for other specimens. The force that pushed the femora and heterotopic bones forwards was apparently strong enough to move the absolute positions of the unattached heterotopic bones, but not strong enough to detach the femora from the hip. Additionally, in articulated specimens of *Tanytrachelos*, the heterotopic bones' angles with respect to the body median range from 94.8 degrees to 128.9 degrees, again suggesting that the heterotopic bones are not fused to the caudal vertebra.

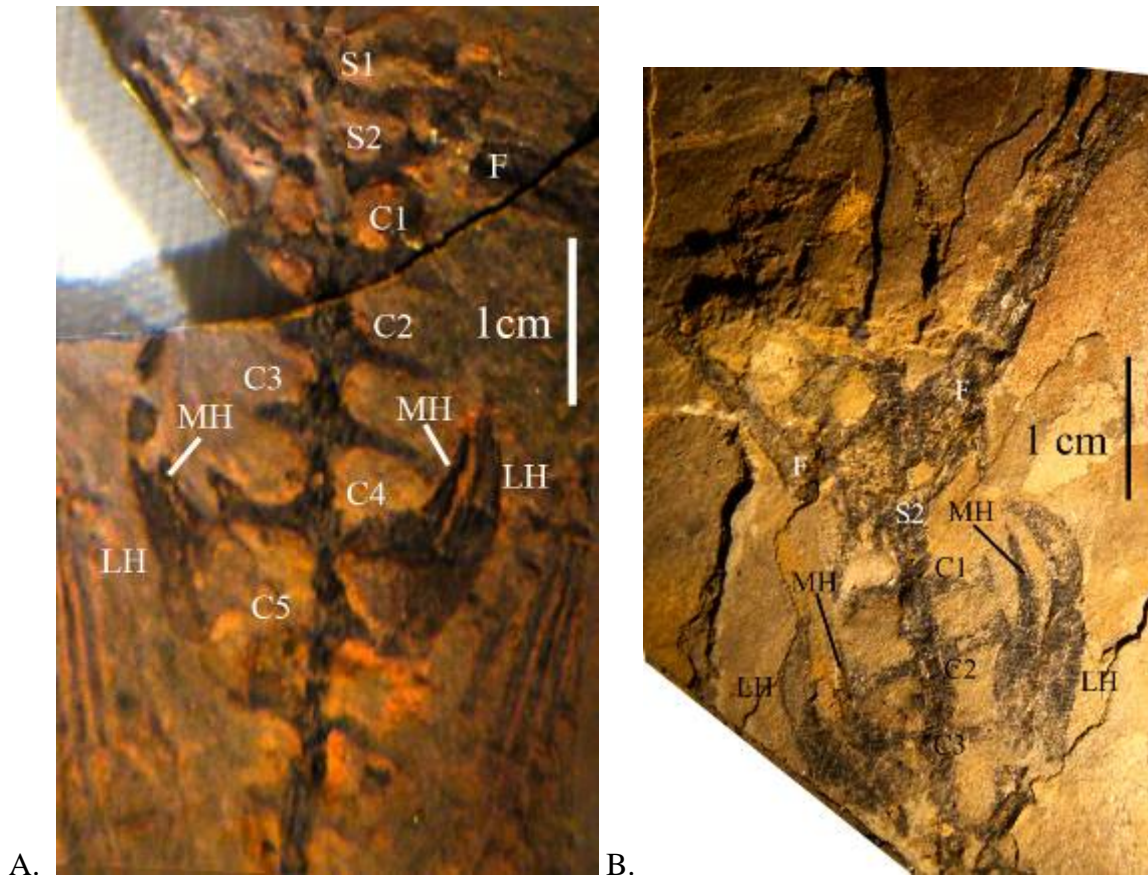


FIGURE 22. Heterotopic bones found in *Tanytrachelos*. A. Paired heterotopic bones located at caudal vertebrae 4 and 5 (VMNH120016). The anterior end is towards the top of the page. B. Slightly disarticulated pair of heterotopic bones in specimen 04-23. A post-mortem force has pushed the attached femora and unattached heterotopic bones anteriorly during preservation.

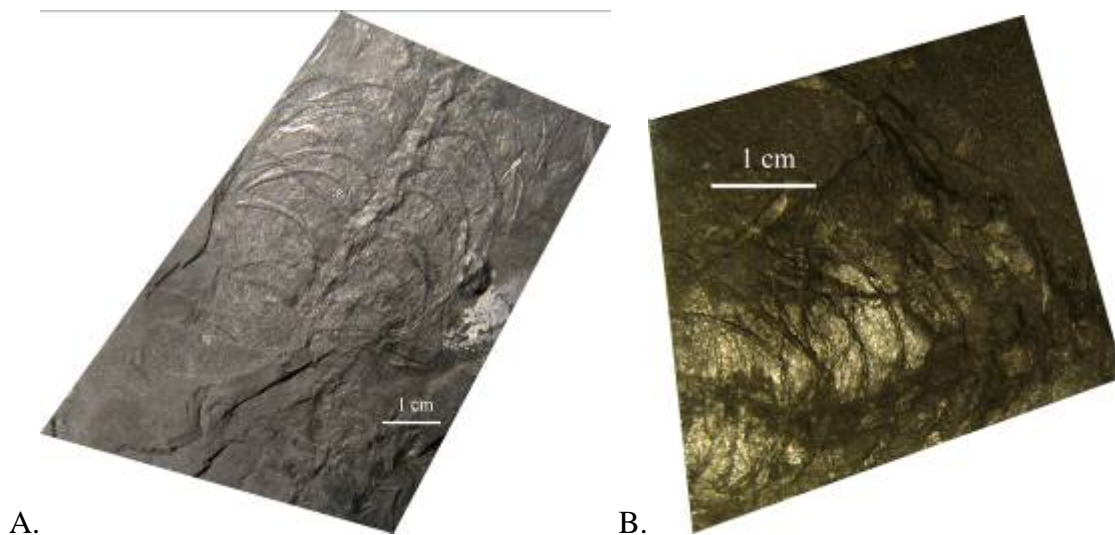
A nonparametric Wilcoxon two-tailed test comparing the femur lengths (as an approximation to body size) to the presence and absence of paired heterotopic bones (using the data found in Table 2), yielded a chi square value of 0.5357 with a p value of 0.4642. These results indicate that there is no significant difference between the body sizes of specimens with heterotopic bones and the specimens without heterotopic bones, by not rejecting the null hypothesis that both samples have the same average body size.

Sample	Specimen	Average Femur Length (cm)
Sample 1: Heterotopic Bones Absent	VMNH988	2.925
	YPM7496A	2.76
	VMNH2852	1.68
	VMNH2827	1.62
	4	2.92
	VMNH3059	3.31
	19	3.035
	VMNH2826	3.02
Sample 2: Heterotopic Bones Present	#1	2.81
	04-19	2.33
	04-23	2.83
	Lot 30.235-70	2.285
	YPM7621	2.95

TABLE 2. Data used in the nonparametric test comparing the presence of heterotopic bones to body size through femur length.

Soft Tissue Traces

Traces of soft tissue are visible on the ribcages and/or tails on some of the more exceptionally preserved specimens of *Tanytrachelos*. The specimens shown in Figures 23A through 23C show soft tissue traces over the ribcage, and Figure 23C demonstrates where the body tapered posteriorly towards the pelvis. This specimen also shows traces of segmented tissues on either side of the tail, evidenced by lighter grey areas in contrast with the darker grey sediment (see Figure 23D). VMNH776 also has traces of segmented tissues on either side of several caudal vertebrae, shown in Figure 23E as light grey markings around each vertebra. Because these traces of muscle blocks are segmented so that each block has its anterior and posterior edges meeting at the middle of each centrum, they were most likely used for lateral or dorsoventral flexion of the tail. An alternative explanation for these traces is that they are remains of color patterns along the tail.



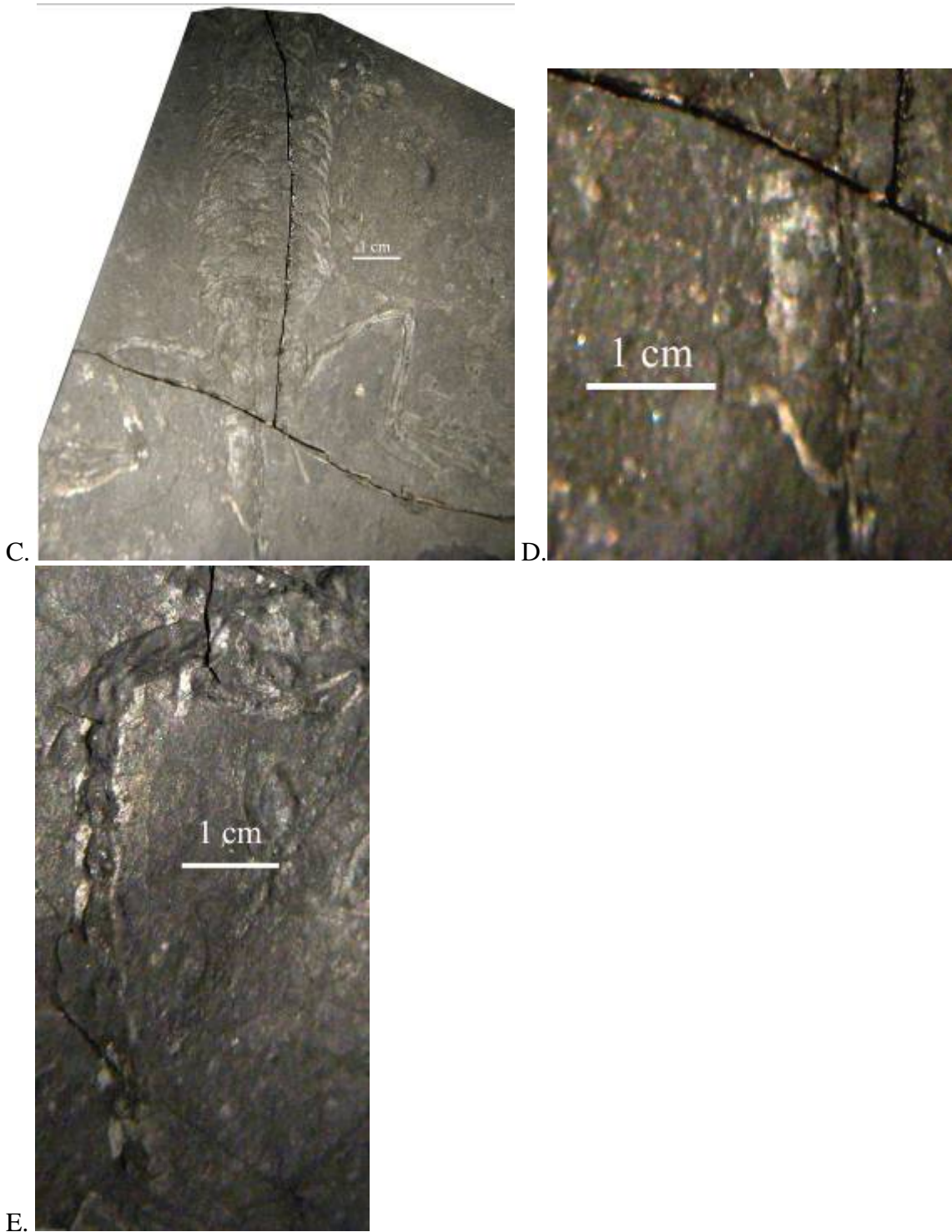


FIGURE 23. Traces of soft tissue in specimens of *Tanytrachelos*. A. Lot 30.251 showing traces of soft tissue around the ribcage. B. Lot 30.625 with traces of soft tissue around the rib cage, shown as the very light grey area under the ribs. C. VMNH963 showing traces of soft tissue around the ribcage, as well as blocks of soft tissue around the caudal vertebrae. D. The tail of VMNH963, enlarged. The soft tissue is most easily seen around the second caudal vertebra. E. The tail of VMNH776 with rounded, segmented tissue traces corresponding to individual vertebrae (shown as light grey traces around the sides of the vertebrae).

Specimens with Noticeably Wide Bodies

A few specimens possess ribcages that are noticeably wider than the average specimens of *Tanytrachelos*. VMNH3059, shown in Figure 24A, has a wide ribcage, as well as femora that measure 3.44 cm and 3.18 cm long. These are the longest femora of the forty-five measured specimens. VMNH3243 (Figure 24B) has a distinctly wide ribcage, as well as a right humerus that measures 2.28 cm long and a left humerus that measures 2.30 cm long. These are not the greatest lengths among specimen humeri, and they fall at the median of the sample of humerus lengths, being longer than ten of the eighteen measured specimens. With only the trunk portion of this specimen preserved, it is difficult to determine beyond the humerus if the overall specimen was larger than average. Another factor that may explain the noticeable wideness of these ribcages is that the ribs of these specimens are considerably straighter than those of other specimens, such as those shown in Figure 11A and Figure 12B. This straightening out of the ribs may have been caused by compressive forces during and/or after burial.

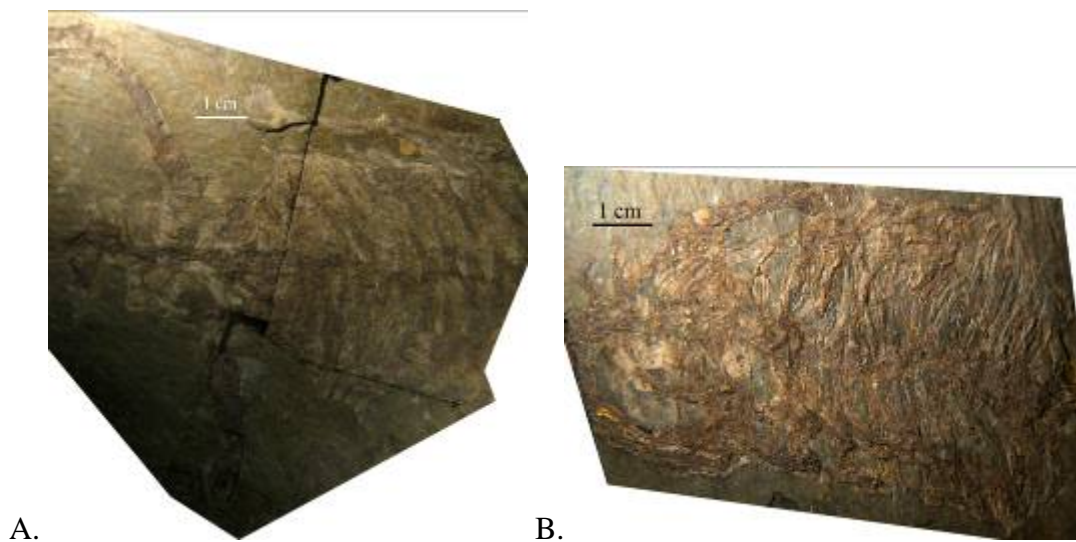


FIGURE 24. Specimens of *Tanytrachelos* that have wider ribcages than average specimens. A. VMNH3059 possesses the longest femora of all measured specimens, and is considered to be one of the largest individuals in the study. B. VMNH3243 possesses a right humerus that is 2.28 cm long, which is in the median range of humeri lengths the study.

Juvenile Specimens of *Tanytrachelos*

The two smallest juvenile specimens yet found, shown in Figure 25, are specimens that show traces of soft tissue. The more complete of the two (Figure 25A) is articulated and lacking the skull, neck, and left half of the pectoral girdle. This specimen retains its soft tissue body outline, which masks the details of individual bones, assuming that the bones had fully ossified before deposition and had not been chemically leached away after deposition. Its measured length from its first dorsal vertebra to the end of its tail measures 3.65 cm long, and its total length is approximated between four and five centimeters. Directly behind the pelvis is a mass of soft tissue that follows the tail for the first 5 mm. This length occupies 23.4% of the total caudal length, which is 21.4 mm long.

The first 23.4% of the caudal vertebrae length reaches the posterior end of the seventh caudal vertebra in larger specimens, and marks the posterior edge of paired heterotopic bones in specimens that possess these. Thus, this soft tissue mass can likely be interpreted as the location of paired heterotopic bones within this juvenile specimen. Otherwise, the mass could be a flap of skin that came loose during burial. Another excellent example of soft tissue preservation found within this juvenile takes the form of large soft tissue masses around the femora. Most easily seen in the right leg, the soft tissue around the femur is significantly wider than would be the femur by itself, and is wider than the lower leg and forelimb.

The second juvenile specimen, shown in Figure 25B, is articulated but less clearly preserved. It also seems to have less soft tissue preserved than does VMNH120045, as the tibia and fibula can be differentiated from each other, and no large ovals of soft tissue traces can be seen around the femora as is the case of VMNH120045 (Figure 25A). VMNH2768 seems to be missing all elements anterior from the posterior two-thirds of the ribcage, as well as the most posterior portion of its tail. Although the anterior portion of the tail is preserved, it is difficult to determine if this specimen shows the same sac-like structure that is present in VMNH120045, possibly due to the lack of soft tissue preservation. The pedes of VMNH2768 are more clearly shown than those of VMNH120045, but do not show any signs of webbing. The right femur and tibia/fibula of VMNH2768 are 9.02 mm and 6.62 mm respectively (see Table 3), which are longer than the lengths of the same structures in VMNH120045 (5.4 mm and 4.8 mm respectively). This indicates that VMNH2768 is a larger specimen than VMNH120045, possibly as a result of being older at the time of death.

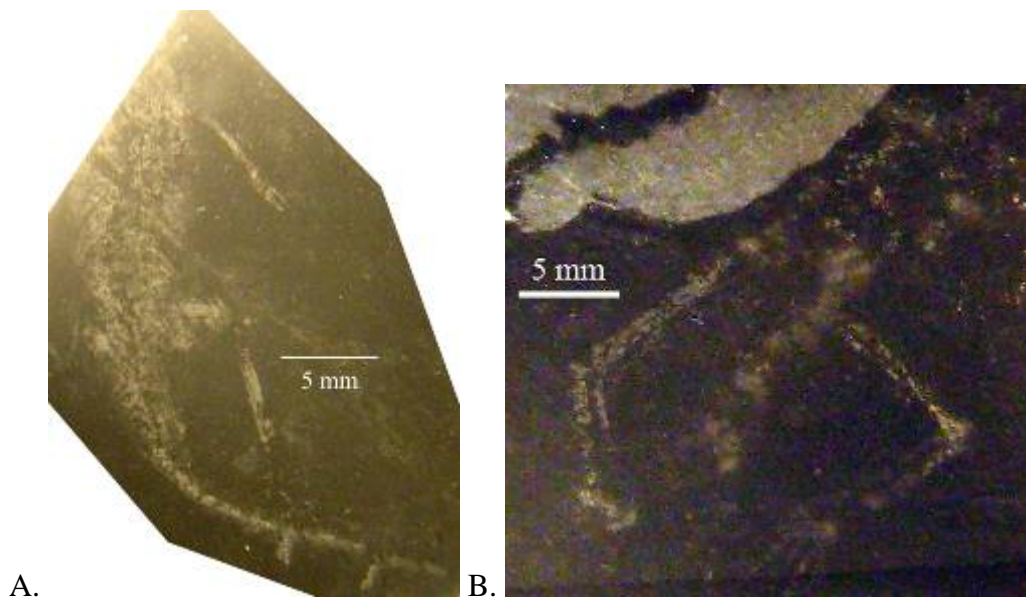


FIGURE 25. The two smallest juvenile specimens of *Tanytrachelos* found to date, showing soft tissue outlines. A. VMNH120045 shows a distinctive sac-like structure composed of soft tissue that may be indicative of heterotopic bones. B. VMNH2768 shows clearer details in the pes than does VMNH120045.

	VMNH120045	VMNH2768
Combined Right Humerus and Radius/Ulna Length (mm)	6.41	
Right Manus Length (mm)	1.47	
Right Femur (mm)	5.4	9.02
Left Femur (mm)		9.06
Right Tibia/Fibula (mm)	3.8	6.62
Left Tibia/Fibula (mm)		6.65
Right Pes Length (mm)	2.09	4.52
Heterotopic Region Length (mm)	5	
Tail Length (mm)	21.4	

TABLE 3. Measurements of elements from the two smallest specimens of *Tanytrachelos* yet found, VMNH120045 and VMNH2768.

Quantitative Results

The seventy length measurements taken from elements of *Tanytrachelos* are summarized in Tables 4 through 8:

Element	Measurement Type	Sample Size	Mean (cm)	Minimum (cm)	Maximum (cm)	Variance (cm ²)	Standard Deviation (cm)
Skull	Diameter	4	1.165	0.79	1.52	0.095	0.308
	Area	4	1.12133	0.4899	1.266	0.314	0.560
Orbit	Diameter	4	0.41	0.27	0.53	0.012	0.108
	Area	4	0.13883	0.05722	0.221	0.005	0.068
Dentary	Length	3	1.05	0.89	1.24	0.031	0.177
Atlas	Length	6	0.48857	0.34	0.7	0.019	0.139
Cervical Vertebra 3	Length	7	0.47375	0.36	0.61	0.008	0.087
Cervical Vertebra 4	Length	8	0.45667	0.34	0.56	0.006	0.078
Cervical Vertebra 5	Length	8	0.43111	0.33	0.6	0.008	0.090
Cervical Vertebra 6	Length	12	0.41077	0.21	0.52	0.009	0.094
Cervical Vertebra 7	Length	13	0.42846	0.17	0.74	0.023	0.151
Cervical Vertebra 8	Length	13	0.41615	0.19	0.62	0.011	0.103
Cervical Vertebra 9	Length	12	0.43417	0.2	0.57	0.009	0.097
Cervical Vertebra 10	Length	12	0.425	0.19	0.56	0.012	0.107
Cervical Vertebra 11	Length	15	0.43133	0.2	0.67	0.010	0.101
Cervical Vertebra 12	Length	15	0.39933	0.16	0.6	0.013	0.114
Cervical Vertebra 13	Length	15	0.38067	0.19	0.53	0.007	0.081
Cervical Rib 5	Averaged Length	1	0.56	0.56	0.56	N/A	N/A
	Averaged Width	1	0.29	0.29	0.29	N/A	N/A
Cervical Rib 6	Averaged Length	2	0.55	0.48	0.62	0.010	0.099
	Averaged Width	2	0.165	0.12	0.21	0.004	0.064
Cervical Rib 7	Averaged Length	1	0.55	0.55	0.55	N/A	N/A
	Averaged Width	1	0.14	0.14	0.14	N/A	N/A
Cervical Rib 8	Averaged Length	2	0.555	0.48	0.63	0.011	0.106
	Averaged Width	2	0.21	0.19	0.23	0.001	0.028
Cervical Rib 9	Averaged Length	3	0.4867	0.35	0.56	0.014	0.118
	Averaged Width	3	0.2367	0.21	0.25	0.001	0.023
Cervical Rib 10	Averaged Length	4	0.4875	0.28	0.56	0.019	0.138
	Averaged Width	4	0.2925	0.26	0.34	0.001	0.036
Cervical Rib 11	Averaged Length	4	0.4575	0.38	0.56	0.007	0.083
	Averaged Width	4	0.3725	0.31	0.43	0.003	0.057
Cervical Rib 12	Averaged Length	4	0.455	0.39	0.53	0.004	0.060
	Averaged Width	4	0.42	0.36	0.5	0.004	0.063
Cervical Rib 13	Averaged Length	1	0.31	0.21	0.31	N/A	N/A
	Averaged Width	3	0.4533	0.33	0.57	0.014	0.120

TABLE 4. Summary statistics of morphometric measurements of the skull and cervical vertebrae.

Element	Measurement Type	Sample Size	Mean (cm)	Minimum (cm)	Maximum (cm)	Variance (cm ²)	Standard Deviation (cm)
Dorsal Vertebra 1	Length	13	0.414	0.33	0.53	0.004	0.062
Dorsal Vertebra 2	Length	16	0.382	0.21	0.48	0.005	0.071
Dorsal Vertebra 3	Length	15	0.396	0.34	0.46	0.002	0.042
Dorsal Vertebra 4	Length	15	0.397	0.27	0.55	0.005	0.073
Dorsal Vertebra 5	Length	16	0.389	0.24	0.56	0.006	0.078
Dorsal Vertebra 6	Length	15	0.386	0.24	0.53	0.005	0.072
Dorsal Vertebra 7	Length	14	0.38	0.24	0.48	0.005	0.069
Dorsal Vertebra 8	Length	14	0.346	0.23	0.44	0.004	0.061
Dorsal Vertebra 9	Length	14	0.349	0.22	0.45	0.005	0.072
Dorsal Vertebra 10	Length	14	0.367	0.23	0.5	0.006	0.080
Dorsal Vertebra 11	Length	15	0.347	0.25	0.44	0.003	0.058
Dorsal Vertebra 12	Length	15	0.352	0.25	0.46	0.003	0.057
Dorsal Vertebra 13	Length	14	0.351	0.22	0.41	0.003	0.058
Sacral Vertebra 1	Length	14	0.381	0.27	0.59	0.009	0.094
Sacral Vertebra 2	Length	17	0.361	0.25	0.62	0.010	0.099
Sacral Rib 1	Averaged Length	7	0.506	0.46	0.64	0.004	0.063
Sacral Rib 2	Averaged Length	12	0.541	0.44	0.67	0.005	0.072

TABLE 5. Summary statistics of morphometric measurements of the dorsal and sacral vertebrae.

Element	Measurement Type	Sample Size	Mean (cm)	Minimum (cm)	Maximum (cm)	Variance (cm ²)	Standard Deviation (cm)	
Humerus	Length	25	2.1512	1.6	2.92	0.091	0.302	
	Proximal Width	27	0.3037037	0.16	0.53	0.010	0.099	
	Distal Width	26	0.3096154	0.14	0.5	0.010	0.100	
Radius	Length	21	0.9095238	0.71	1.19	0.019	0.139	
Ulna	Length	19	0.8642105	0.67	1.21	0.019	0.139	
Metacarpal I	Length	5	0.32	0.13	0.47	0.023	0.152	
Metacarpal II	Length	6	0.4733333	0.18	1.09	0.117	0.342	
Metacarpal III	Length	6	0.49	0.22	1.16	0.130	0.360	
Metacarpal IV	Length	2	0.42	0.24	0.6	0.065	0.255	
Metacarpal V	Length	1	0.52	0.52	0.52	N/A	N/A	
M a n u s	Digit I Phalanx 1	Length	2	0.18	0.16	0.2	0.001	0.028
	Digit I Phalanx 2	Length	2	0.085	0.08	0.09	0.000	0.007
	Digit II Phalanx 1	Length	2	0.285	0.19	0.38	0.018	0.134
	Digit II Phalanx 2	Length	2	0.225	0.15	0.3	0.011	0.106
	Digit II Phalanx 3	Length	2	0.12	0.12	0.12	0.000	0.000
	Digit III Phalanx 1	Length	3	0.2766667	0.11	0.41	0.023	0.153
	Digit III Phalanx 2	Length	3	0.2066667	0.12	0.27	0.006	0.078
	Digit III Phalanx 3	Length	2	0.15	0.08	0.22	0.010	0.099
	Digit III Phalanx 4	Length	1	0.15	0.15	0.15	N/A	N/A
	Digit IV Phalanx 1	Length	1	0.33	0.33	0.33	N/A	N/A
	Digit IV Phalanx 2	Length	1	0.22	0.22	0.22	N/A	N/A
	Digit IV Phalanx 3	Length	1	0.18	0.18	0.18	N/A	N/A
	Digit IV Phalanx 4	Length	1	0.15	0.15	0.15	N/A	N/A
	Digit V Phalanx 1	Length	1	0.24	0.24	0.24	N/A	N/A
	Digit V Phalanx 2	Length	1	0.18	0.18	0.18	N/A	N/A
Digit V Phalanx 3	Length	1	0.12	0.12	0.12	N/A	N/A	

TABLE 6. Summary statistics of morphometric measurements of the forelimb elements.

Element	Measurement Type	Sample Size	Mean (cm)	Minimum (cm)	Maximum (cm)	Variance (cm ²)	Standard Deviation (cm)
Caudal Vertebra 1	Length	23	0.403	0.23	0.67	0.010	0.100
Caudal Vertebra 2	Length	24	0.403	0.24	0.71	0.012	0.111
Caudal Vertebra 3	Length	20	0.389	0.23	0.53	0.006	0.075
Caudal Vertebra 4	Length	15	0.411	0.24	0.55	0.009	0.092
Caudal Vertebra 5	Length	11	0.419	0.25	0.59	0.010	0.100
Caudal Vertebra 6	Length	6	0.455	0.27	0.72	0.033	0.183
Caudal Vertebra 7	Length	5	0.438	0.37	0.66	0.016	0.125
Caudal Vertebra 8	Length	3	0.39	0.26	0.55	0.022	0.147
Caudal Vertebra 9	Length	3	0.393	0.33	0.46	0.004	0.065
Caudal Vertebra 10	Length	2	0.39	0.35	0.43	0.003	0.057
Caudal Vertebra 11	Length	2	0.44	0.37	0.51	0.010	0.099
Caudal Vertebra 12	Length	2	0.39	0.34	0.44	0.005	0.071
Caudal Vertebra 13	Length	2	0.41	0.37	0.45	0.003	0.057
Caudal Vertebra 14	Length	2	0.43	0.38	0.48	0.005	0.071
Caudal Vertebra 15	Length	2	0.42	0.38	0.46	0.003	0.057
Caudal Vertebra 16	Length	2	0.41	0.36	0.46	0.005	0.071
Caudal Vertebra 17	Length	2	0.34	0.22	0.46	0.029	0.170
Caudal Vertebra 18	Length	2	0.4	0.32	0.48	0.013	0.113
Caudal Vertebra 19	Length	2	0.415	0.36	0.47	0.006	0.078
Caudal Vertebra 20	Length	1	0.52	0.52	0.52	N/A	N/A
Caudal Vertebra 21	Length	1	0.57	0.57	0.57	N/A	N/A
Caudal Vertebra 22	Length	1	0.56	0.56	0.56	N/A	N/A
Caudal Vertebra 23	Length	1	0.57	0.57	0.57	N/A	N/A
Caudal Vertebra 24	Length	1	0.54	0.54	0.54	N/A	N/A
Caudal Vertebra 25	Length	1	0.45	0.45	0.45	N/A	N/A
Caudal Vertebra 26	Length	1	0.49	0.49	0.49	N/A	N/A
Caudal Vertebra 27	Length	1	0.47	0.47	0.47	N/A	N/A
Caudal Vertebra 28	Length	1	0.38	0.38	0.38	N/A	N/A
Caudal Vertebra 29	Length	1	0.44	0.44	0.44	N/A	N/A
Caudal Vertebra 30	Length	1	0.41	0.41	0.41	N/A	N/A
Caudal Vertebra 31	Length	1	0.4	0.4	0.4	N/A	N/A
Caudal Vertebra 32	Length	1	0.4	0.4	0.4	N/A	N/A
Medial Heterotopic Bone	Length	8	1.166	0.64	1.57	0.091	0.301
Distal Heterotopic Bone	Length	10	1.764	1.4	2.33	0.114	0.337

TABLE 7. Summary statistics of morphometric measurements of the caudal vertebrae and heterotopic bones.

Element	Measurement Type	Sample Size	Mean (cm)	Minimum (cm)	Maximum (cm)	Variance (cm ²)	Standard Deviation (cm)	
Femur	Length	41	2.674634	1.62	3.44	0.163	0.404	
	Proximal Width	43	0.383721	0.12	0.64	0.012	0.109	
	Distal Width	41	0.27561	0.14	0.44	0.006	0.075	
Tibia	Length	37	1.789189	0.4	2.54	0.171	0.414	
Fibula	Length	34	1.690588	0.17	2.8	0.217	0.466	
Metatarsal I	Length	11	0.950909	0.6	1.57	8.474	2.911	
Metatarsal II	Length	11	1.093636	0.76	1.54	8.233	2.869	
Metatarsal III	Length	10	1.119	0.84	1.6	7.220	2.687	
Metatarsal IV	Length	10	0.987	0.74	1.23	7.408	2.722	
Metatarsal V	Length	9	0.292222	0.21	0.55	7.593	2.755	
P e s	Digit I Phalanx 1	Length	2	0.305	0.29	0.32	0.000	0.021
	Digit II Phalanx 1	Length	3	0.303333	0.18	0.38	0.012	0.108
	Digit II Phalanx 2	Length	3	0.203333	0.18	0.23	0.001	0.025
	Digit III Phalanx 1	Length	4	0.405	0.25	0.5	0.012	0.108
	Digit III Phalanx 2	Length	3	0.24	0.17	0.31	0.005	0.070
	Digit III Phalanx 3	Length	2	0.155	0.07	0.24	0.014	0.120
	Digit III Phalanx 4	Length	2	0.09	0.06	0.12	0.002	0.042
	Digit IV Phalanx 1	Length	2	0.395	0.36	0.43	0.002	0.049
	Digit IV Phalanx 2	Length	2	0.265	0.25	0.28	0.000	0.021
	Digit IV Phalanx 3	Length	1	0.2	0.2	0.2	N/A	N/A
	Digit IV Phalanx 4	Length	1	0.08	0.08	0.08	N/A	N/A
	Digit V Phalanx 1	Length	3	0.886667	0.59	1.14	0.077	0.278
	Digit V Phalanx 2	Length	2	0.365	0.29	0.44	0.011	0.106

TABLE 8. Summary statistics of morphometric measurements of the hindlimb elements.

DISCUSSION

Diagnostic Qualities of *Tanytrachelos*

Tanytrachelos ahynis is a small protorosaur, possessing more than seven cervical vertebrae with long, slender cervical ribs, cervical centra that are longer than the dorsal centra (Benton and Allen 1997), and a snout that comprises roughly 50% of the entire skull length (Dilkes 1998). Several characteristics of *Tanytrachelos* place it within the family Tanystropheidae. As in other tanystropheids, the skull contains no quadratojugal, and the postfrontal is a reduced element that lacks distinct processes (Benton and Allen 1997). The lower jaw displays a concave profile caudal to the coronoid (Dilkes 1998). There are more than twelve cervical vertebrae present (Jalil 1997), and the transverse processes of the caudal vertebrae are longer than their corresponding centra (Dilkes 1998). The scapula is fan-shaped, with a concave surface on its caudal border (Dilkes 1998), and there is no distal carpal 1 in the carpus (Jalil 1997). The ilium, pubis, and ischium equally contribute to the acetabulum. The tarsus contains an elongate astragalus and lacks the second distal tarsal. The fifth metatarsal is remarkably short and hooked without deflection (Dilkes 1998), and articulates with an elongate first phalanx that is nearly as long as the first four metatarsals (Jalil 1997). Several specimens possess paired post-cloacal bones on either side of the tail (Jalil 1997).

Tanytrachelos can be diagnosed as a small (approximated at 21 cm long by a composite of specimens) tanystropheid with 13 cervical vertebrae, 13 dorsal vertebrae, 2 sacral vertebrae, and 31 caudal vertebrae, the latter which comprise 50% of the entire vertebral length. Several features distinguish *Tanytrachelos* from other tanystropheids. Its neck contains an atlas that is fused to the axis, the centra are subequal in length, and its cervical ribs are relatively shorter than those of other tanystropheids, only slightly overlapping the next cervical rib in the sequence. The vertebrae are procoelous, and the posterior dorsal ribs are not fused to the centra. The teeth of *Tanytrachelos* are homodont and seemingly pleurodont. Its femur is non-sigmoidal, and the metatarsals I through IV are subequal in length. The paired post-cloacal bones found in some specimens of *Tanytrachelos* are shaped like pointed arcs, and differ from those in *Tanystropheus*.

Possible Function of Paired Heterotopic Bones

Although the presence or absence of heterotopic bones did not statistically correlate to body size, the distribution of heterotopic bones among some but not all specimens is still likely due to sexual dimorphism, as said distribution was shown to not be a taphonomic signal by Casey et al. (2007). They are decidedly members of the same species, as specimens with and without these paired bones shared qualities diagnostic for *Tanytrachelos*. Although heterotopic bones are not found in 50% of all specimens due to varying degrees of articulation (that is to say, many specimens do not have a posterior end preserved or they consist of a single element), evidences against a taphonomic signal as an explanation for the absence of heterotopic bones are that they are always present as pairs, they have not been found in VMNH2828, which is preserved so well that it shows soft tissue traces, and there was no increase in specimen disarticulation in the study (Casey et al 2007). However, the exact function of these heterotopic bones is unclear.

Although some members of *Tanystropheus*, the proposed sister group of *Tanytrachelos*, also possess pairs of heterotopic bones behind the pelvis, those of *Tanystropheus* differ from those of *Tanytrachelos* in that they show a sigmoidal curve instead of an arc shape, possess a large bump in the posterior portion of the larger heterotopic bone, and the anterior end of the bones have blunt tips in contrast to the pointy tips found at the anterior ends of those of *Tanytrachelos* (Rieppel et al. 2010).

The heterotopic bones of *Tanytrachelos* also cannot be compared to the cloacal bones of extant geckos (Burt 1935), as the latter pairs of bones are external and completely different in shape than the heterotopic bones of *Tanytrachelos*. The heterotopic bones also show no similarities with the external hemipenes of extant monitor lizards (Card and Kluge 1995). Although extant xantusiids (night lizards) also have paired postcloacal bones, they are not considered homologous to those of *Tanytrachelos* due to the extreme differences in size, shape, number, and orientation (Kluge 1982).

Although it has been suggested that the heterotopic bones of *Tanystropheus longobardicus* are primitive forms of the L-shaped post cloacal bones that are seen in geckos and night lizards today (Rieppel 1976), this is unlikely to explain the function of the heterotopic bones of *Tanytrachelos*, as these are shaped too differently. Any sort of external claspers or hemipenes are also improbable explanations, as the juvenile specimen in Figure 25A shows soft tissue traces completely covering its paired heterotopic bones, if they are indeed present within this specimen. However, if the claspers could function together within a single flap of skin as internal structures, then members of *Tanytrachelos* with heterotopic bones may have been decidedly male. Alternatively, the heterotopic bones in the juvenile specimen in Figure 25A may simply be in an early stage of ontogeny, and these structures may project externally over the course of the organism's development. An alternative explanation that might fit this internal condition is that these pairs of bones support a brood pouch in the female, or in the male if the reproductive roles of *Tanytrachelos* followed those of modern seahorses, whose male members carry the young. This idea in turn leads to the question of *Tanytrachelos* oviparity, which is demonstrated by the overwhelming majority of reptiles throughout Earth's history, or ovoviviparity, demonstrated only by a select few reptiles (e.g., ichthyosaurs and snakes). Such a question can not be sufficiently addressed with the current specimens and data.

The Relationship of *Gwyneddosaurus* to *Tanytrachelos*

Gwyneddosaurus, a small reptile found in Montgomery County, Pennsylvania, shares several morphological similarities with *Tanytrachelos* that suggest that they might be congeneric. *Gwyneddosaurus* was found within the Upper Triassic Lockatong Formation of the Newark Supergroup (Bock 1945). The ichnofossils *Gwyneddichnium majore*, *Gwyneddichnium elongatum*, and *Gwyneddichnium minore* have also been found in the Lockatong Formation (Bock 1952). It has been suggested that these three ichnofossils were made by specimens of *Gwyneddosaurus* (Olsen and Flynn 1989).

Although the preserved elements of *Gwyneddosaurus* show some morphological similarities to those of *Tanytrachelos*, the remains are fragmentary and disarticulated. Bock (1945) noted that the vertebrae of *Gwyneddosaurus* have a procoelous ball and socket articulation with each other, which is congruent with the procoelous vertebrae

seen in *Tanytrachelos*. The scapula and coracoid of *Gwyneddosaurus* are also morphologically similar to those of *Tanytrachelos*, as the scapula exhibits a fan-shaped profile, while the coracoid is larger than the scapula. The disarticulated dorsal ribs of *Gwyneddosaurus* are holocephalous like those of *Tanytrachelos*, and both taxa possess straight, non-sigmoidal femora.

With the exception of the humerus, the sizes of individual elements are also congruent between *Tanytrachelos ahynis* and *Gwyneddosaurus*. Bock (1945) reported *Gwyneddosaurus* to have a humerus that is 0.7 cm long, a femur that is 2.3 cm long, a largest finger that is 1 cm long, and toes that range from 0.8 cm to 1.3 cm long. In comparison, the humerus of *Tanytrachelos* averages at 2.15 cm long, the femur averages at 2.67 cm long, the largest finger (which is the third finger of Lot 30.315) is 1.05 cm long, and the toes range from 0.74 cm long to 1.37 cm long (as observed in three specimens). It is likely that the measured humerus of *Gwyneddosaurus* was in fact some other long bone, such as a metacarpal or phalanx, or was truncated due to partial preservation, as the femur of *Gwyneddosaurus* was measured to be over 3 times the length of its humerus. This would also explain the difference in lengths between the humerus of *Gwyneddosaurus* and that of *Tanytrachelos*. However, other more diagnostic features such as the cervical vertebrae and ribs are not preserved in *Gwyneddosaurus*.

It is possible that *Gwyneddosaurus* and *Tanytrachelos* belong to the same genus, and if so the question arises of which generic name should be kept to describe both. Although *Gwyneddosaurus* was established first (Bock 1945), it is represented by a disarticulated holotype with no distinguishing characteristics that would allow for a proper diagnosis. Furthermore, it was considered to be a composite by Olsen and Flynn (1989) that included tetrapod and fish elements, the accumulation possibly representing a result of a gastric ejection. The inability to properly diagnose the fossil and the ambiguity as to exactly which creature the name *Gwyneddosaurus* refers to renders *Gwyneddosaurus* a nomen dubium, allowing *Tanytrachelos* to be retained as a generic name.

There are three species of the ichnofossil *Gwyneddichnium* found in Pennsylvania that are proposed to have been made by *Gwyneddosaurus*. *Gwyneddichnium majore*, the only *Gwyneddichnium* found in Pennsylvania with manus prints, has five manus digits, with the third digit as the longest. Table 9 indicates that the digits of the manus of *Tanytrachelos* averaged remarkably close in length to those of *Gwyneddichnium majore*. The pes of *Gwyneddichnium majore* is larger than its manus, as is the case for *Tanytrachelos*, but is hypothesized to have a phalangeal formula of 2-3-4-4-3 or 2-3-4-3-3 (Bock 1952). This contrasts with *Tanytrachelos*, whose pes phalangeal formula is 2-3-4-5-4. The pes of *Gwyneddichnium majore* is also noticeably larger than that of *Tanytrachelos* (shown in Table 9), as well as the size ranges for the pes and manus digits of *Gwyneddosaurus*. The difference of digit lengths and pes phalangeal formulas between *Gwyneddichnium majore* and *Gwyneddosaurus/Tanytrachelos*, as well as the size disparities between the pes and manus traces of *Gwyneddichnium majore* (in contrast with the disparities between the sizes of the pes and manus in *Gwyneddosaurus/Tanytrachelos*) may suggest that this ichnofossil was made by a different species within the genus, or of a different tetrapod taxon altogether.

Gwyneddichnium elongatum and *Gwyneddichnium minore* also have five digits on the pes, with the third digit being the longest. The pes phalangeal formula of

Gwyneddichnium elongatum is unknown, but the formula for *Gwyneddichnium minore* is hypothesized to be 2-3-4-4-2. The pes digit lengths of *Gwyneddichnium elongatum* are slightly longer than the average pes digit lengths of *Tanytrachelos*, whereas those of *Gwyneddichnium minore* are slightly shorter. Due to the relatively small range between the two ichnotaxa with *Tanytrachelos* in the middle, it is possible that these two taxa actually represent traces from younger (the smaller *Gwyneddichnium minore*) and older (the larger *Gwyneddichnium elongatum*) specimens of *Gwyneddosaurus*, and are not results of two different species. The difference in phalangeal formulas may be a result of either unclear preservation of the ichnofossils, or it may be an indication of a different species within the genus.

	Digit I Average Length (Phalanges Only) (cm)	Digit II Average Length (Phalanges Only) (cm)	Digit III Average Length (Phalanges Only) (cm)	Digit IV Average Length (Phalanges Only) (cm)	Digit V Average Length (Phalanges Only) (cm)
<i>Tanytrachelos</i> Manus	.25	0.8	1.05	0.88	0.54
<i>Gwyneddichnium majore</i> Manus	0.63	0.73	0.97	0.8	0.55
<i>Tanytrachelos</i> Pes	0.41	0.73	1.1	0.98	1.43
<i>Gwyneddichnium majore</i> Pes	1.4	1.62	1.98	1.85	1.28
<i>Gwyneddichnium elongatum</i> Pes	0.5	0.9	1.3	0.8	0.6
<i>Gwyneddichnium minore</i> Pes	0.3	0.6	0.7	0.5	0.4

TABLE 9. Comparisons of the average lengths of *Gwyneddichnium* digits to the lengths of *Tanytrachelos* digits. *Gwyneddichnium* measurements are taken from Bock (1952).

A pair of manus prints labeled as *Gwyneddichnium* (VMNH3668), shown in Figure 26, has been found in the Solite Quarry. They are considered to be manus imprints as opposed to pes imprints because they have a third digit that is the longest of all five digits, and they are significantly smaller than the pes of *Tanytrachelos*. The lengths of the digits, shown in Table 10, are shorter than their homologs in the manus and pes of *Tanytrachelos* and *Gwyneddichnium*. Although they are closest in length to their homologs in the pes of *Gwyneddichnium minore*, the digits of these traces from the Solite Quarry are still noticeably shorter. It is impossible to discern individual phalanges within the digits, and curvature at the base of the digits may be an indication of webbing. The right manus imprint is placed more forwards than the left one, and the width between them is 4.17 cm. Due to the size of the imprints, the presence of five digits on each manus, and the ichnofossil having been found in the Solite quarry, these tracks were most likely made by a young *Tanytrachelos ahynis*.



FIGURE 26. VMNH3668, the specimen of *Gwyneddichnium* found in the Solite Quarry. A left and right manus print are preserved.

	Digit I Length (cm)	Digit II Length (cm)	Digit III Length (cm)	Digit IV Length (cm)	Digit V Length (cm)
Left Manus	0.24	0.29	0.37	0.31	0.30
Right Manus	0.38	0.40	0.43	0.34	0.39

TABLE 10. Lengths of manus digits of the *Gwyneddichnium* specimen found in the Solite Quarry (VMNH3668).

Locomotion of *Tanytrachelos*

Tanytrachelos was an aquatic reptile that spent much of its time in the water. The sizes of the pedes and hind limbs, as well as soft tissue evidence, indicate that propulsion through the water was likely accomplished with the back legs. The hind limb of *Tanytrachelos* averages roughly 1.7 times the length of the fore limb, and likewise, the pes length averages 1.3 times the length of the manus. This size disparity indicates that of the two pairs of limbs, the hind limbs would more likely perform propulsion. Another piece of evidence for propulsion by the hind limbs is the soft tissue preserved around the femora of the juvenile specimen in Figure 25A. The right femur shows a wide area of soft tissue not seen around the lower hind limb or the fore limb, and can be interpreted as a collection of robust muscles around the femur. Such thigh muscles would have been a useful adaptation for propelling the animal through the water, if the hind feet were webbed. Although no specimens to date have shown webbed feet, this absence may be a result of soft tissue loss before preservation. It is unlikely that the tail was not used for aquatic propulsion, as the caudal soft tissue shown in Figures 23C, 23D, and 23E are not broad and are instead restricted to the perimeter of the tail, and no elongate chevrons were found with any specimens.

It is also reasonable to assume that *Tanytrachelos* could walk either on land or in shallow water, as an ichnofossil (see Figure 26) that matches the structure of the two manus of *Tanytrachelos* has been found in the Solite Quarry. The presence of manus prints within the rock confirms that *Tanytrachelos* was quadrupedal. However, this specimen gives little other information about the taxon's activities on land or in shallow water. There are concave curves between the bases of the digits of these manus imprints,

which may indicate subtle webbing between the digits. Such subtle webbing may have been used for stabilization, but not propulsion, in the water.

The Possibility of Neoteny in *Tanytrachelos*

Two pieces of evidence introduce the possibility that *Tanytrachelos* may have been neotenic. First, specimens that retained their skull show a consistently large orbit that occupies between 11% and 13% of the skull’s lateral area. In addition to the possibility that a large orbit was the result of selective pressures, such as the need to see insect prey, a large orbit is congruent with the large eyes typically found in juvenile animals. The more compelling piece of evidence is found in the juvenile specimen VMNH120045 (Figure 25A). As previously discussed, this specimen shows a mass of soft tissue that may possibly be interpreted as paired heterotopic bones. If these were indeed heterotopic bones and they had served some function during reproduction, then this soft tissue mass is evidence of reproductive structures found within a very young juvenile. However, it should be kept in mind that it is impossible to determine if they were functional within this specimen.

Essentially, the main physical development that *Tanytrachelos* would have undergone throughout its lifetime would be an increase in size. Table 11 shows the ratio of various measured element lengths to the femora of the two juvenile specimens and four average sized, presumably adult specimens. The ratio of the forearm length to the femur length show little variability, ranging from 1.19 in the smaller juvenile to 1.13 in one of the adult specimens. Likewise, the adult ratio of manus length to femur length is only 0.06 less than that of the small juvenile. Although the ratio of the lower leg length to the femur shows a great range of variability between specimens (between 0.6 and 0.89), this disparity does not correlate to overall body size. The ratio of the pes length to femur length differs between the two juvenile specimens by 0.11, likely as a result of a small sample size.

Specimen	Femur Length (cm)	Forearm/Femur	Manus/Femur	Tibia & Fibula/Femur	Pes/Femur
VMNH120045	0.54	1.19	0.27	0.89	0.39
VMNH2768	0.90			0.73	0.50
YPM7496A	2.76	1.05	0.21	0.80	
YPM7621	2.95			0.79	
VMNH3059	3.31			0.76	
VMNH120006	2.81	1.13		0.60	

TABLE 11. Ratios of element lengths of the two smallest juvenile specimens of *Tanytrachelos* found (VMNH120045 and VMNH2768) and four distinctly larger (presumably adult) specimens. Femur length is used as a proxy of overall specimen size.

In most cases of neoteny, the high rates of growth of juveniles are retained through adulthood, resulting in larger animals. *Tanytrachelos*, being the small protorosaur that it is, might argue against the case for neoteny due to its small stature. However, other factors may have limited the size of *Tanytrachelos*. The lake that occupied the area that is now the Solite Quarry was a fairly small and isolated environment. Such a restricted environment may have impacted the upper limits of body

size in *Tanytrachelos*. Another factor to consider is the difference in size between the smallest specimen (VMNH120045), that has a 0.54 cm long femur, and the largest found specimen (VMNH3059) that has a femur that is 3.31 cm long. Using femoral length as a proxy for body size, the largest adult specimen can be estimated at six times the size of the smallest juvenile. It is impossible to determine the average lifespan for *Tanytrachelos*, but if sexual maturity were reached early in life, the average lifespan may have been reasonably short (a few years, for instance). This temporal brevity would truncate growth of *Tanytrachelos* body sizes. A third possibility is that the entire found population of *Tanytrachelos* represents only juveniles, and that adult specimens, which may have lived elsewhere, have not yet been found.

Comparison and Contrast between *Tanytrachelos* and its proposed sister taxon *Tanytropheus*

Tanytrachelos and its sister taxon *Tanytropheus* share several characteristics that are considered diagnostic for the family Tanytropheidae. Both taxa have thirteen cervical vertebrae with dichocoephalous ribs, a quantity that was previously counted as twelve in the original description of *Tanytrachelos* (Olsen 1979). Both taxa also have thirteen dorsal vertebrae, the last three of which possess short, straight transverse processes. The scapulae of *Tanytrachelos* and *Tanytropheus* are both fan-shaped, and both taxa have the same phalangeal formulae on the manus (2-3-4-4-3) and pes (2-3-4-5-4). The carpus of both taxa consists of a radiale, ulnare, and two distal carpals, and the tarsus consists of an astragalus, calcaneum, and distal tarsals 3 and 4. The taxa also share an extremely short metatarsal V that is slightly hooked at its proximal end. Articulating with this metatarsal is a remarkably long first phalanx, which is almost as long as the first through fourth metatarsals. As mentioned previously, some specimens of *Tanytrachelos* and *Tanytropheus* have paired heterotopic bones behind the pelvis. These ossifications differ noticeably in size and shape between the taxa, although their sizes proportionate to the rest of their bodies are congruent (spanning the length of four caudal centra in both taxa).

Several morphological differences make the distinction between these taxa quite clear. The most noticeable difference is the size disparity; the average length of *Tanytrachelos* is 21 cm, whereas *Tanytropheus* is substantially longer at approximately 5 m. In contrast with the homodont teeth possessed by *Tanytrachelos*, *Tanytropheus* has a heterodont dentition that is comprised of conical, recurved teeth in the front of the jaw and tricuspid teeth in the back (Nosotti 2007).

Although the atlas and axis are the shortest vertebrae within *Tanytropheus* (Nosotti 2007), they are not fused to each other as they are in specimens of *Tanytrachelos*. Although the ribs of *Tanytrachelos* and *Tanytropheus* are both dichocoephalous, their cervical ribs differ greatly in length. *Tanytropheus* possesses cervical ribs that are extremely long, spanning the length of three centra, thus overlapping each other and forming rigid, spindly bundles (Rieppel et al. 2010). In contrast, the cervical ribs of *Tanytrachelos* are just slightly longer than the length of the centrum, and only a millimeter or two of the posterior end of the rib overlaps the anterior end of the following cervical rib. *Tanytropheus* also differs in dorsal vertebral structure, having amphicoelous dorsal vertebrae in contrast with the procoelous dorsal vertebrae possessed

by *Tanytrachelos* (Wild 1973). The first three dorsal ribs of *Tanystropheus* are dichoccephalous (Nosotti 2007), whereas all of the dorsal ribs of *Tanytrachelos* are holocephalous. Furthermore, the dorsal ribs of *Tanystropheus* are fused to the posterior vertebrae, whereas those of *Tanytrachelos* are unfused. *Tanystropheus* has at least 41 caudal vertebrae (Nosotti 2007), which is ten more than the most complete tail known from *Tanytrachelos*.

Unlike *Tanystropheus*, the pelvis of *Tanytrachelos* lacks an obturator foramen. The shapes of the femora also differ between the taxa, as the femur of *Tanytrachelos* is straight whereas the femur of *Tanystropheus* is sigmoidal. Although the pedes and manus of these taxa contain the same phalangeal formulae and both taxa have the same tarsal and carpal bones, metacarpals I through IV of *Tanytrachelos* are roughly equal in length, whereas metacarpals I and V of *Tanystropheus* are noticeably shorter than metacarpals II through IV (Nosotti 2007). Furthermore, the concavo-convex astragalo-calcaneal contact present in the tarsus of *Tanystropheus* is not seen in that of *Tanytrachelos*.

Potential Sources of Error in Morphometric Measurements

Although it would seem that length measurements are simple and easy to accurately obtain, when specimens cannot be removed from the surrounding matrix, accurate morphometric measurements are sometimes impossible to guarantee. Length measurements taken from compressed skeletons trapped in a fine-grained matrix would be shorter than the actual lengths of elements if one or both true ends of the bone in question are covered by the sediment. These measurements would also be inconsistent if the elements are not laying flat with respect to their exposed surfaces. Even if some of the elements are flat along this surface, comparison between the lengths of two bones, such as the right and left femora, can be inaccurate if the distal side of the left femur is exposed, whereas the dorsal side of the right femur is exposed. Furthermore, many of the measured bones were bent, possibly caused by the tectonic compression that all fossils in the Solite Quarry underwent (Olsen and Johansson 1994). This compression can distort the fossils to a small degree that is imperceptible on a qualitative scale, but can skew measurements taken from its elements. For these reasons, it should be emphasized that the qualitative description of *Tanytrachelos* presented in this work is the main, diagnostic description, whereas the morphometric measurements and calculations are tangential additions.

LITERATURE CITED

- BENGSTON, S. 2000. Teasing Fossils out of Shales with Cameras and Computers. *Paleaeontologica Electronica*, 3(1):1-14.
- BOCK, W., 1952. Triassic reptilian tracks and trends of locomotive evolution: with remarks on correlation. *Journal of Paleontology* 26:395-433.
- BOCK, W., 1945. A new small reptile from the Triassic of Pennsylvania. *Notulae Naturae of the Academy of Natural Sciences of Philadelphia*. 154:1-8.
- BURT, C. E. 1935. A Key to the Lizards of the United States and Canada. *Transactions of the Kansas Academy of Science*, 38: 255-305.
- CARD, W. AND A. G. KLUGE. 1995. Hemipenial Skeleton and Varanid Lizard Systematics. *Journal of Herpetology*, 29(2): 275-280.
- CASEY, M. M., N. C. FRASER, AND M. KOWALEWSKI. 2007. Quantitative taphonomy of a Triassic reptile *Tanytrachelos ahynis* from the Cow Branch Formation, Dan River Basin, Solite Quarry, Virginia. *Palaios*, 22:598-611.
- FRASER, N. C., D. A. GRIMALDI, P. E. OLSEN, AND B. AXSMITH. 1996. A Triassic Lagerstätte from eastern North America. *Nature*, 380(18):615-619.
- FRASER, N. C., AND D. A. GRIMALDI. 2003. Late Triassic Continental Faunal Change: New Perspectives on Triassic Insect Diversity as Revealed by a Locality in the Danville Basin, Virginia, Newark Supergroup, p. 192-205. *In* P. M. LeTourneau and P. E. Olsen (eds.), *The Great Rift Valleys of Pangea in Eastern North America, Volume 2: Sedimentology, Stratigraphy, and Paleontology*. Columbia University Press, New York.
- FRASER, N. C., P. E. OLSEN, A. C. DOOLEY JR., AND T. R. RYAN. 2007. A new gliding tetrapod (Diapsida: ?Archosauromorpha) from the Upper Triassic (Carnian) of Virginia. *Journal of Vertebrate Paleontology*, 27(2):261-265.
- KLUGE, A. G. 1982. Cloacal bones and sacs as evidence of gekkonoid lizard relationships. *Herpetologica*, 38(3): 348-355.
- LIUTKUS, C. M., J. S. BEARD, N. C. FRASER, and P. C. RAGLAND, 2010. Use of fine-scale stratigraphy and chemostratigraphy to evaluate conditions of deposition and preservation of a Triassic Lagerstätte, south-central Virginia. *Journal of Paleolimnology* 44:645-666.
- LUCAS, S. G., AND L. H. TANNER. 2007. The nonmarine Triassic-Jurassic boundary in the Newark Supergroup of eastern North America. *Earth-Science Reviews*, 84:1-20.

- MEYERTONS, C. T. 1963. Triassic Formations of the Danville Basin. Commonwealth of Virginia Department of Conservation and Economic Development: Division of Mineral Resources, Charlottesville, 6.
- NOSOTTI, S. 2007. *Tanystropheus longobardicus* (Reptilia, Protorosauria): re-interpretations of the anatomy based on new specimens from the Middle Triassic of Besano (Lombardy, northern Italy). *Memorie della Società Italiana di Scienze Naturali e del Museo Civico di Storia Naturale di Milano*, 35: 1-88.
- OLSEN, P. E. 1979. A New Aquatic Eosuchian form the Newark Supergroup (Late Triassic-Early Jurassic) of North Carolina and Virginia. *Postilla*, 176:1-14.
- OLSEN, P. E., C. L. REMINGTON, B. CORNET, and K. S. THOMSON. 1978. Cyclic Change in Late Triassic Lacustrine Communities. *Science*, 201 (4357): 729-733.
- OLSEN, P. E. and J. FLYNN, 1989. Field guide to the vertebrate paleontology of Late Triassic rocks in the southwestern Newark basin (Newark Supergroup, New Jersey and Pennsylvania). *The Mosasaur* 4:1-35.
- OLSEN, P. E., AND A. K. JOHANSSON. 1994. Field guide to Late Triassic tetrapod sites in Virginia and North Carolina, p. 408-430. *In* N. C. Fraser and H.-D. Sues (eds.), *In the Shadow of the Dinosaurs: Early Mesozoic Tetrapods*. Cambridge University Press, New York.
- RIEPEL, O. 1976. On the presence and function of post-cloacal bones in the Lacertilia. *Monitore zoologico italiano*, 10(1): 7-13.
- RIEPEL, O., D. JIANG, N. C. FRASER, W. HAO, R. MOTANI, Y. SUN, AND Z. SUN. 2010. *Tanystropheus* cf. *T. longobardicus* from the Early Late Triassic of Guizhou Province, Southwestern China. *Journal of Vertebrate Paleontology*, 30(4): 1082-1089.
- SUES, H. D. AND N. FRASER. 2010. *Triassic Life on Land*. New York, NY, Columbia University Press.

A reanalysis of protorosaur cladistics and its impact on archosauromorph evolutionary relationships

ABSTRACT

Protorosauria is a group of archosauromorphs that contains the families Drepanosauridae and Tanystropheidae and eleven other genera. The monophyly versus paraphyly of this group has been debated through several cladistic analyses. The result of this debate would greatly impact the cladistic structure of Archosauromorpha if Protorosauria were found to be paraphyletic, as this would require protorosaurs to be intercalated among archosauromorph clades. On the other hand, a monophyletic Protorosauria would not change the structure of Archosauromorpha.

Benton and Allen (1997), Jalil (1997), and Hone and Benton (2008) have presented a monophyletic Protorosauria, whereas Dilkes (1998), Rieppel et al. (2003), and Modesto and Sues (2004) have presented a paraphyletic Protorosauria. The most basal protorosaur within these analyses has varied, but has most commonly been *Protorosaurus* or *Boreopricea*. The status of *Prolacerta* as a member of Protorosauria is also unresolved, as Dilkes (1998), Modesto and Sues (2004), and Hone and Benton (2008) have proposed that *Prolacerta* is not a protorosaur.

Two new cladistic analyses were performed to test the monophyly of Protorosauria. The first analysis included the outgroup *Petrolacosaurus*, twenty-one members of Protorosauria, and nine other archosauromorphs, regardless of their percentage of data completion. The second analysis tested only the twenty taxa from this sample that had data completeness of 50% or higher. Both analyses used 201 characters, which were adapted from Benton and Allen (1997), Jalil (1997), and Dilkes (1998). These characters were coded based on published descriptions, with exception to *Tanytrachelos*, which was directly observed, and *Prolacertoides*, which utilized character states from Rieppel et al. (2003).

Each analysis rendered a single most parsimonious cladogram presenting a paraphyletic Protorosauria. Both results also placed *Prolacerta* within the confines of Protorosauria, pairing it with *Macrocnemus bassanii* in the analysis of all taxa, and placing it as the most primitive protorosaur within a clade containing eight protorosaurs in the second analysis. In spite of these commonalities, the exact structures and details of the two trees differed. The analysis of all taxa presented *Boreopricea* as the most basal protorosaur, while the analysis of the twenty most complete taxa presented *Protorosaurus* as the most basal protorosaur. When compared to previous analyses, neither tree agrees fully with any previously published data, partly due to differences in taxa sampling between studies. This may be addressed in future works, which would also benefit from direct observation of most or all specimens as the source for character coding.

INTRODUCTION

Archosauromorpha contains the group Protorosauria (also known as Prolacertiformes), which is comprised of the families Drepanosauridae (*Drepanosaurus*, *Hypuronector*, *Megalancosaurus*, and *Vallesaurus*) and Tanystropheidae (*Amotosaurus* (Fraser and Rieppel 2006), *Dinocephalosaurus*, *Tanystropheus*, and *Tanytrachelos*), as well as the genera *Boreoprincea*, *Cosesaurus*, *Kadimakara*, *Langobardisaurus*, *Macrocnemus*, *Malerisaurus*, *Prolacerta*, *Prolacertoides*, *Protorosaurus*, *Trachelosaurus*, (Rieppel et al. 2003), *Czatkowiella* (Borsuk-Bialnicka and Evans 2009), and *Rhombopholis* (Benton and Allen 1997). The monophyly versus paraphyly of Protorosauria has been debated through several publications. While analyses performed by Benton and Allen (1997), Jalil (1997), and Hone and Benton (2008) presented a monophyletic Protorosauria, analyses by Dilkes (1998), Rieppel et al. (2003), and Modesto and Sues (2004) presented Protorosauria as paraphyletic. A reanalysis of the group with previously missing data filled in could ultimately impact the structure of the parent clade Archosauromorpha, as a paraphyletic Protorosauria would necessitate the intercalation of protorosaurs among various archosauromorph clades.

Previous Studies of Protorosaur Phylogeny

The debate of a monophyletic Protorosauria versus a paraphyletic Protorosauria has spanned several publications, beginning in 1997 with the cladistic analyses of Protorosauria performed independently by Jalil and by Benton and Allen. Benton and Allen (1997) used *Rhynchosaurus*, *Youngina*, and *Trilophosaurus* as outgroups for their analysis. Of the protorosaurs, *Kadimakara*, *Megalancosaurus*, *Malerisaurus robinsonae* and *Trachelosaurus* were excluded from the analysis due to insufficient data. The resulting Reduced Adams Consensus tree (Figure 27) had a Consistency Index of 0.577 and a Retention Index of 0.629. It presented a monophyletic Protorosauria with *Trilophosaurus* and *Rhynchosaurus* as its sister clade. *Protorosaurus* was not found to be the most basal protorosaur; instead, the most basal clade within Protorosauria was occupied by *Boreoprincea* and *Prolacerta*. Additionally, although Benton and Allen's (1997) study found the family Tanystropheidae to be monophyletic, the genus *Tanystropheus* was paraphyletic within that family, as *Tanytrachelos* and *Tanystropheus longibardicus* formed a sister clade to *Tanystropheus meridensis*.

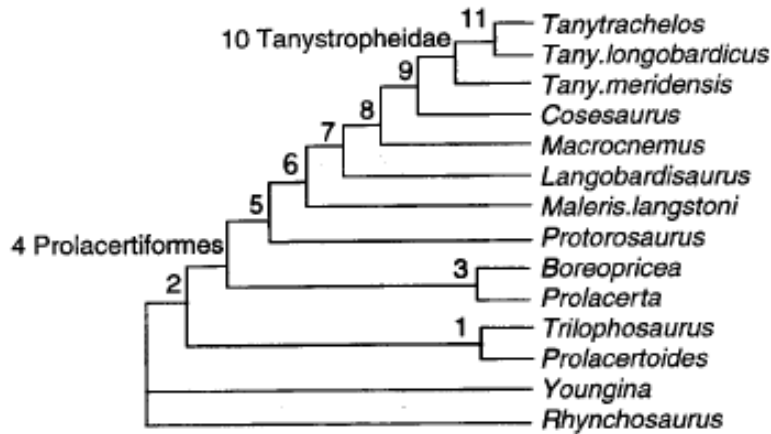


FIGURE 27. The cladistic analysis of Protorosauria as presented by Benton and Allen (1997).

Jalil (1997) included *Petrolacosaurus* and *Youngina* as outgroups in his cladistic analysis of Protorosauria. As in Benton and Allen's (1997) study, poorly known protosaurs were excluded from the analysis. The result was a single cladogram (Figure 28) that presented a monophyletic Protorosauria with *Proterosuchus* as its sister clade. The cladogram had a Consistency Index of 0.538, and presented *Protorosaurus* as the most basal protosaurus. Tanytropheidae was monophyletic, and formed a sister clade to *Cosesaurus*.

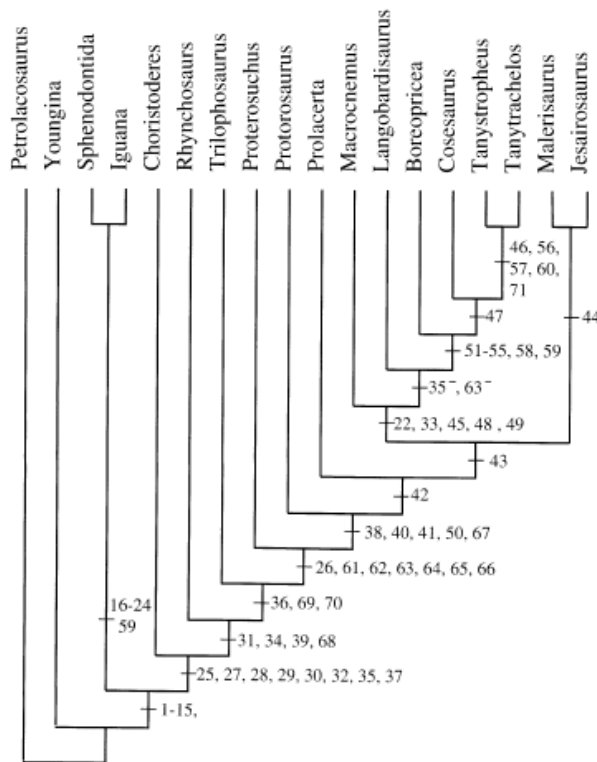


FIGURE 28. The cladistic analysis of Protorosauria and members of Archosauromorpha as presented by Jalil (1997).

In contrast to the results of these two studies, Dilkes (1998) presented a paraphyletic Protorosauria with a single most parsimonious tree (Figure 29) 354 steps long (CI = 0.479, rescaled CI = 0.326, RI = 0.662). This paraphyly arose as a result of *Prolacerta* being the sister taxon to the *Proterosuchus-Euparkeria* clade. Alternatively, this result may suggest that *Prolacerta* is not a member of Protorosauria (Dilkes 1998). Within Protorosauria, Drepanosauridae was monophyletic, and *Protorosaurus* was the most basal protorosaur.

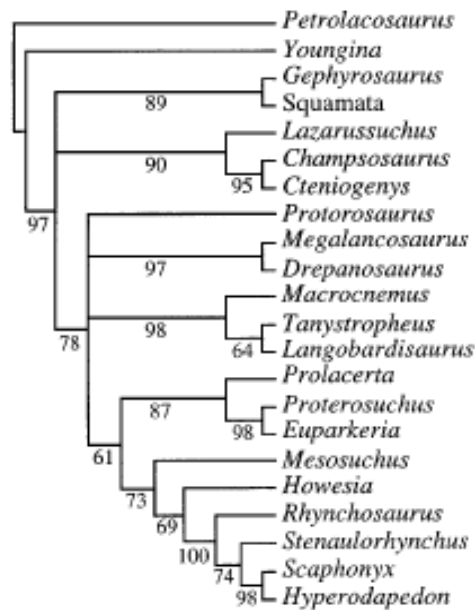


FIGURE 29. The cladistic analysis of Protorosauria and members of Archosauromorpha as presented by Dilkes (1998).

In 2003, Rieppel et al. tested the monophyly of Protorosauria by combining the characters used in analyses performed by Benton and Allen (1997), Jalil (1997), and Dilkes (1998). The resulting most parsimonious tree (Figure 30; CI = 0.515, RI = 0.558) supported the paraphyletic Protorosauria presented by Dilkes (1998). This paraphyly was caused by the presence of *Proterosuchus* and *Euparkeria* as a sister clade to *Prolacerta*. The family Drepanosauridae was found to be monophyletic, and *Boreopricea* was identified as the most basal protorosaur. *Rhynchosaurus* and *Trilophosaurus* formed the sister clade to Protorosauria.

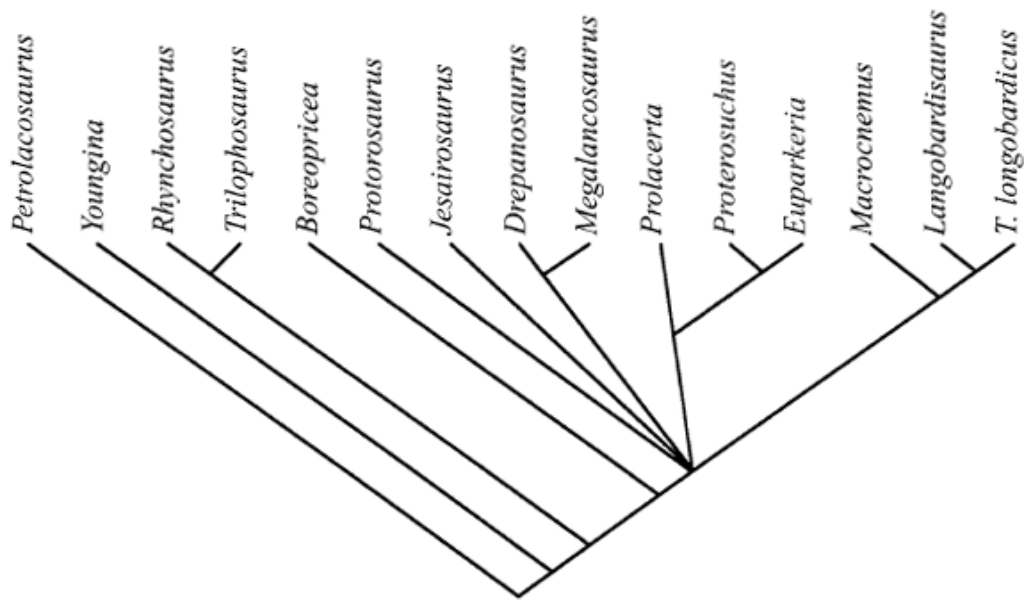


FIGURE 30. The cladistic analysis of Protorosauria as presented by Rieppel et al. (2003).

Modesto and Sues (2004) also presented evidence for a paraphyletic Protorosauria. Their strict consensus tree (Figure 31), which was a composite of two equally parsimonious trees 310 steps long (CI = 0.5, rescaled CI = 0.32), presented a paraphyletic Protorosauria due to the intercalation of *Prolacerta* among the archosauriformes. As previously suggested by Dilkes (1998), this intercalation may be indicative that *Prolacerta* is not a protorosaur (Modesto and Sues 2004). Drepanosauridae was also found to be monophyletic, and *Protorosaurus* was the most basal protorosaur.

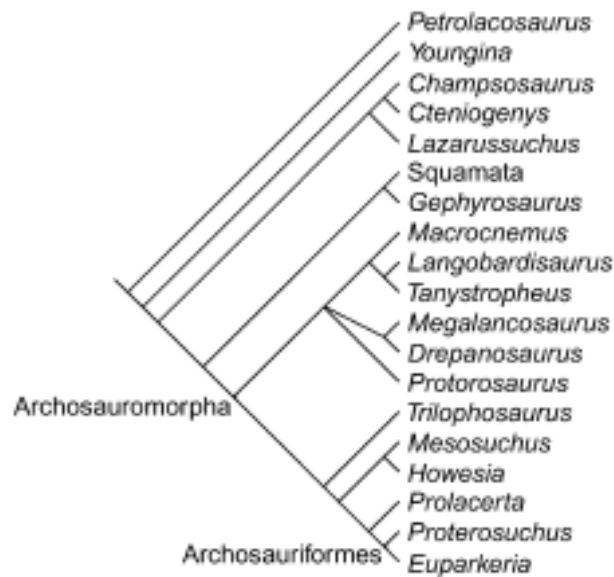


FIGURE 31. The cladistic analysis of Archosauromorpha as presented by Modesto and Sues (2004).

In 2008, Hone and Benton presented a cladistic analysis of Archosauromorpha that showed a monophyletic Protorosauria, assuming that *Prolacerta* is indeed not a protosauroid as suggested by Dilkes (1998) and Modesto and Sues (2004). Within their fifty percent Majority-Rule Consensus Supertree (comprised from 33,937 most parsimonious trees, seen in Figure 32), Tanystropheidae was monophyletic, whereas Drepanosauridae was monophyletic. All of Protorosauria formed a sister clade to *Malutinisuchus*, and the two most basal protosauroids were a polytomy of *Prolacertoides* and *Jesairosaurus*.



FIGURE 32. The cladistic analysis of Archosauromorpha as presented by Hone and Benton (2008).

MATERIALS AND METHODS

Taxa Selection and Character Compilation

A total of thirty-two taxa were researched, consisting of the outgroup taxon *Petrolacosaurus*, twenty-one protorosaurs, and nine representative taxa from other archosauromorph groups. The protorosaurs included in the data matrix were *Boreopricea*, *Cosesaurus*, *Czatkowiella harae*, *Jesairosaurus*, *Kadimakara*, *Langobardisaurus*, *Macrocnemus bassanii*, *Malerisaurus langstoni*, *Malerisaurus robinsonae*, *Prolacerta*, *Prolacertoides*, *Protorosaurus*, the tanystropheids *Amotosaurus*, *Dinocephalosaurus*, *Tanystropheus longobardicus*, *Tanystropheus meridensis*, and *Tanytrachelos ahynis*, and the drepanosaurids *Drepanosaurus*, *Hypuronector*, *Megalancosaurus*, and *Vallesaurus*. Representatives of other archosauromorph groups in the analyses were *Youngina* (Younginiformes), *Trilophosaurus* (Trilophosauria) *Proterosuchus* (Proterosuchia), *Euparkeria* (Euparkeriidae), *Scleromochlus* (Scleromochlidae), *Herrerasaurus* (Dinosauria), *Rhynchosaurus* (Rhynchosauria), *Marasuchus* (Ornithodira), and *Eudimorphodon* (Pterosauria).

Of the total 201 characters that were compiled, 46 were taken from Benton and Allen (1997), 51 were taken from Jalil (1997), 103 were taken from Dilkes (1998), and one was newly created. Over half of the characters (54%) addressed cranial material, while 28% of the characters addressed the appendicular skeleton and 18% of the characters addressed the axial skeleton and miscellaneous structures.

Cladistic Analysis of Protorosauria

With the exception of *Tanytrachelos*, which was directly observed, and *Prolacertoides*, whose data came directly from the coding performed by Benton and Allen (1997) and Jalil (1997), the character states for all taxa were coded based on their published descriptions. Due to the widely variable quantity of data available for the included taxa (shown in Table 12), two cladistic analyses were performed. The first cladistic analysis included all thirty-two taxa regardless of the percentage of complete data available in the matrix. The second analysis included the twenty taxa that had a data completeness of 50% or higher (*Petrolacosaurus*, *Boreopricea*, *Czatkowiella harae*, *Dinocephalosaurus*, *Euparkeria*, *Herrerasaurus*, *Langobardisaurus*, *Macrocnemus bassanii*, *Malerisaurus robinsonae*, *Megalancosaurus*, *Prolacerta*, *Proterosuchus*, *Protorosaurus*, *Rhynchosaurus*, *Scleromochlus*, *Tanystropheus longobardicus*, *Tanytrachelos*, *Trilophosaurus*, *Vallesaurus*, and *Youngina*). Both analyses were performed in the software PAST (Hammer et al. 2001). Characters were equally weighted with the heuristic tree bisection and reconnection (TBR) option and used Fitch optimization, with 1,000 bootstraps.

Genus	# with Data	% Complete
<i>Petrolacosaurus</i>	201	100.0
<i>Amotosaurus</i>	66	32.8
<i>Boreopricea</i>	110	54.7
<i>Cosesaurus</i>	74	36.8
<i>Czatkowiella harae</i>	118	58.7
<i>Dinocephalosaurus</i>	132	65.7
<i>Drepanosaurus</i>	62	30.8
<i>Eudimorphohodon</i>	32	15.9
<i>Euparkeria</i>	186	92.5
<i>Herrerasaurus</i>	174	86.6
<i>Hypuronector</i>	40	19.9
<i>Jesairosaurus</i>	96	47.8
<i>Kadimakara</i>	48	23.9
<i>Langobardisaurus</i>	102	50.7
<i>Macrocnemus bassanii</i>	171	85.1
<i>Malerisaurus langstoni</i>	63	31.3
<i>Malerisaurus robinsonae</i>	106	52.7
<i>Marasuchus</i>	58	28.9
<i>Megalancosaurus</i>	118	58.7
<i>Prolacerta</i>	197	98.0
<i>Prolacertoides</i>	8	4.0
<i>Proterosuchus</i>	189	94.0
<i>Protorosaurus</i>	145	72.1
<i>Rhynchosaurus</i>	190	94.5
<i>Scleromochlus</i>	118	58.7
<i>Tanystropheus longobardicus</i>	190	94.5
<i>Tanystropheus meridensis</i>	88	43.8
<i>Tanytrachelos</i>	111	55.2
<i>Trachelosaurus</i>	25	12.4
<i>Trilophosaurus</i>	177	88.1
<i>Vallesaurus</i>	113	56.2
<i>Youngina</i>	192	95.5

TABLE 12. Data completeness for taxa used in study.

RESULTS

Results of the Analysis Including All Taxa

The analysis of all thirty-two taxa yielded a single most parsimonious tree 665 steps long, with a Consistency Index of 0.3248 and a Retention Index of 0.873 (Figure 33). This tree shows a paraphyletic Protorosauria as a sister group to the more primitive clade containing *Eudimorphodon* and *Scleromochlus* and the more derived clade containing *Rhynchosaurus* and *Trilophosaurus*. This paraphyly is a result of the presence of non-protorosaur members of Archosauromorpha within two clades of Protorosauria. First, the ornithodiran *Marasuchus* serves as the sister taxon to *Malerisaurus robinsonae*. Additionally, *Euparkeria*, *Herrerasaurus*, and *Proterosuchus* collectively serve as a sister clade to the clade containing *Prolacerta* and *Macrocnemus bassani*.

Within Protorosauria, *Boreoprincea* was found as the most basal protrosaur. The family Drepanosauridae was found to be monophyletic, but the family Tanystropheidae forms a paraphyletic family, due to the intercalation of *Prolacerta* within the tanystropheid clade. The genus *Tanystropheus* is monophyletic and serves as the sister clade to *Tanytrachelos*. *Malerisaurus* is a paraphyletic genus, with *Malerisaurus langstoni* as a sister taxon to *Kadimakara* and *Malerisaurus robinsonae* as a sister taxon to *Marasuchus*.

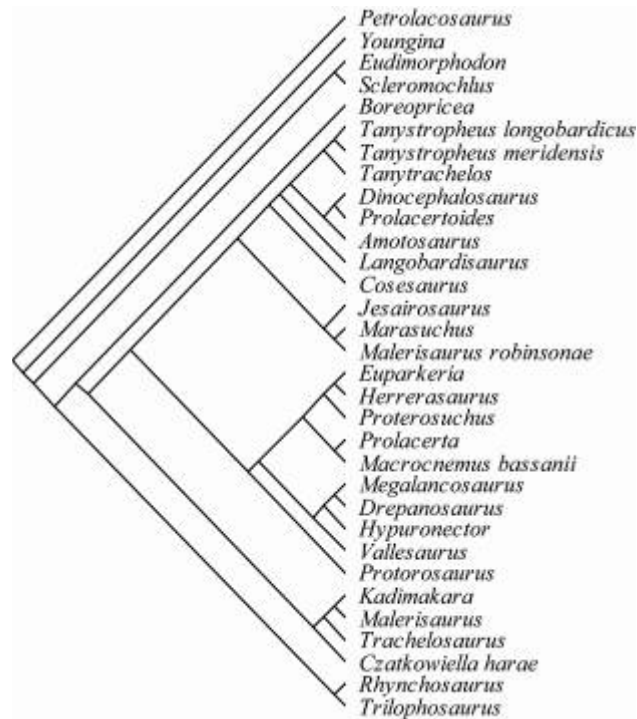


FIGURE 33. Single most parsimonious tree of all thirty-two taxa in the study (CI = 0.3248, RI = 0.873)..

Results of the Analysis Including Only Taxa with 50% or Higher Data Completeness

Analyzing the twenty taxa that had 50% or higher data completeness resulted in a single most parsimonious tree 552 steps long, with a Consistency Index of 0.3822 and a Retention Index of 0.785 (Figure 34). Like the cladogram of all thirty-two taxa, this cladogram also shows a paraphyletic Protorosauria. This paraphyly is caused by the members of the monophyletic Drepanosauridae *Vallesaurus* and *Megalancosaurus* occurring as a sister clade to the *Euparkeria-Proterosuchus-Herrerasaurus-Scleromochlus* clade. Additionally, *Rhynchosaurus* pairs with *Boreopricea* to form a sister clade to nine protorosaurs. However, due to the pairing of the the *Euparkeria-Proterosuchus-Herrerasaurus-Scleromochlus* clade with the two drepanosaurids, as well as the pairing of *Rhynchosaurus* with *Boreopricea*, *Youngina* is found to be the sister taxon to all protorosaurs out of this sample of taxa. Tanystropheidae is monophyletic, and *Protorosaurus* is found to be the most basal protorosaur.

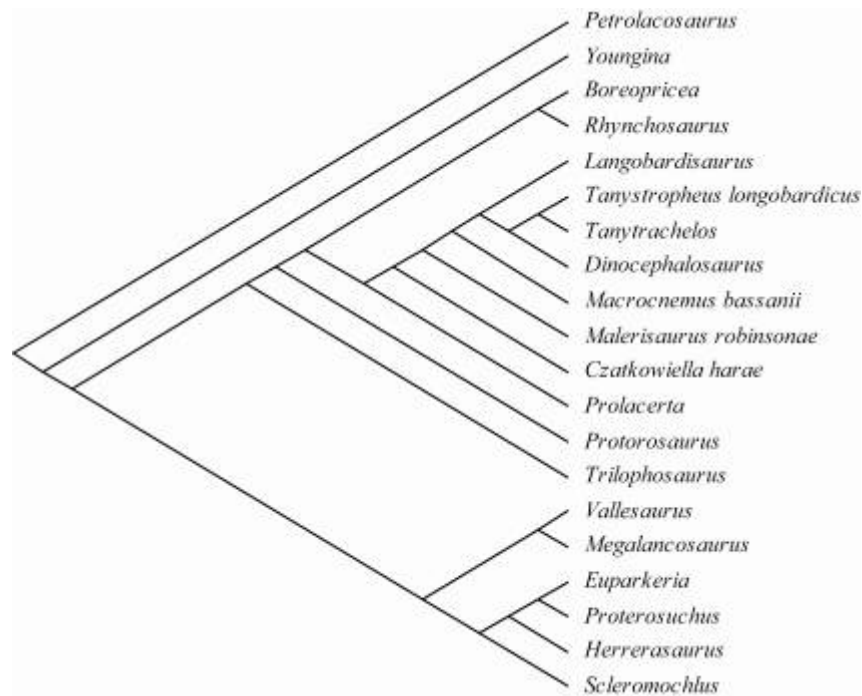


FIGURE 34. Single most parsimonious tree of the twenty taxa in the study with 50% or higher data completeness (CI = 0.3822, RI = 0.785).

DISCUSSION

Consistencies and Inconsistencies between Both Analyses

Although the second analysis consisted of twelve fewer taxa than the first analysis, a few consistencies are present between the results of both. Both analyses present Protorosauria as paraphyletic. The family Drepanosauridae is also paraphyletic in both analyses, with *Vallesaurus* and *Megalancosaurus* occupying a clade separate from *Macrocnemus bassanii*. Furthermore, the family Tanystropheidae forms a sister clade to *Langobardisaurus* in both analyses.

There are, however, several inconsistencies between the results of both analyses. Although both analyses rendered a paraphyletic Protorosauria, the exact structures of their paraphyly differ. In the analysis of all taxa (Figure 33), the paraphyly stems from the presence of the *Euparkeria-Herrerasaurus-Proterosuchus* clade as a sister clade to the *Prolacerta-Macrocnemus bassanii* clade. In contrast, the paraphyly in the analysis of the twenty most complete taxa (Figure 34) is a result of *Boreopricea* as a sister taxon to *Rhynchosaurus* (which together form a sister clade to the protorosaurs), and the drepanosaurid *Vallesaurus-Megalancosaurus* clade forming a sister clade to the *Euparkeria-Proterosuchus-Herrerasaurus-Scleromochlus* clade. Furthermore, the most basal protorosaur differs between the analyses, with *Boreopricea* as the most basal protorosaur in the analysis of all taxa, and *Protorosaurus* as the most basal protorosaur in the analysis of twenty taxa. The family Tanystropheidae is paraphyletic in the analysis of all taxa due to the presence of *Prolacertoides* in the clade. However, when this taxon was removed due to having only 4% of its data complete, Tanystropheidae became monophyletic in the second analysis. The clade of non-protorosaur archosauromorphs also differs in structure between the two analyses; the analysis of all taxa places *Euparkeria* as a sister taxon to *Herrerasaurus*, whereas the analysis of the twenty most complete taxa places *Euparkeria* as a sister taxon to *Proterosuchus*. Other specific details of the two cladograms are inconsistent with each other, such as the location of *Prolacerta*, which is the sister taxon to *Macrocnemus bassanii* in the analysis of all taxa, and is the sister taxon to the *Czatkowiella harae-Malerisaurus robinsonae-Macrocnemus bassanii-Tanystropheidae-Langobardicus* clade in the analysis of the twenty most complete taxa.

These inconsistencies raise the question as to which analysis is more acceptable. The analysis of all taxa has a lower Consistency Index (0.3248) than does the analysis of the twenty most complete taxa (0.3822), but has a higher Retention Index (0.873) than does the second analysis (0.785). The analysis of the twenty most complete taxa has the advantage of a smaller tree length (552 steps) as well as stronger restrictions against including taxa with missing data than does the analysis of all taxa, which has a tree length of 665 steps. The analysis of twenty taxa also has slightly higher bootstrap values at the nodes than does the analysis of all taxa. For these reasons, the cladogram featuring the twenty most complete taxa is most likely the more accurate of the two cladograms.

Comparison of Results to Previous Studies

Like the results of Dilkes (1998), Rieppel et al. (2003), and Modesto and Sues (2004), the results of these two analyses present a paraphyletic Protorosauria. The analysis of all taxa (Figure 33) also presents a paraphyletic Drepanosauridae within Protorosauria (as do Dilkes (1998), Modesto and Sues (2004), and Hone and Benton (2008)), the placement of *Prolacerta* as a sister taxon to the drepanosaurid *Macrocnemus bassanii* challenges the idea proposed by Dilkes (1998), Modesto and Sues (2004), and Hone and Benton (2008) that *Prolacerta* did not belong in Protorosauria. The analysis of taxa with a data completeness of 50% or higher also presents a paraphyletic Drepanosauridae, but places *Prolacerta* within the *Langobardisaurus-Tanystropheidae-Macrocnemus bassanii-Malerisaurus robinsonae-Czatkowiella harae-Prolacerta* clade, which is the sister clade to *Protorosaurus* (the most basal protorosaur in this analysis). This also challenges the idea that *Prolacerta* did not belong to Protorosauria, as the result of Dilkes (1998) and Modesto and Sues (2004) place *Prolacerta* as a sister taxon to the *Proterosuchus-Euparkeria* clade, and Hone and Benton place *Prolacerta* as an outgroup to Archosauria. Although the placement of *Prolacerta* was the main reason for the paraphyletic results of these three studies, the analysis of all taxa within this study was paraphyletic due to the presence of the *Euparkeria-Herrerasaurus-Proterosuchus* clade as a sister clade to *Prolacerta-Macrocnemus bassanii*. This configuration is congruent with the paraphyly presented by Rieppel et al (2003), which presents a *Proterosuchus-Euparkeria* clade as the sister clade to *Prolacerta*. In contrast, the analysis of the twenty most complete taxa was paraphyletic due to the drepanosaurids *Vallesaurus* and *Megalancosaurus* forming a sister clade to the *Euparkeria-Proterosuchus-Herrerasaurus-Scleromochlus* clade.

The presence of *Prolacertoides* in the tanystropheid clade renders Tanystropheidae paraphyletic in the analysis of all taxa, a condition that is not seen in any previous work. However, *Prolacertoides* only had 4% of its data available, and thus its placement within the tanystropheid clade is likely an error due to missing data. Furthermore, the analysis of the twenty most complete taxa present a monophyletic Tanystropheidae, a condition which is supported in the results of Benton and Allen (1997), Jalil (1997), and Hone and Benton (2008) (the other studies featured only *Tanystropheus*). Therefore, it is reasonable to consider Tanystropheidae as a solidly monophyletic family, as is Drepanosauridae. In both analyses, *Langobardisaurus* serves as the sister taxon to Tanystropheidae, as is the case in Dilkes (1998), Rieppel et al. (2003), Modesto and Sues (2004), and Benton and Hone (2008). In contrast, Benton and Allen (1997) and Jalil (1997) present *Cosesaurus* as the sister taxon to *Tanystropheus*. In the analysis of all taxa, *Cosesaurus* acts as a sister taxon to *Langobardisaurus*, indicating the evolutionary proximity between these three groups.

The question of which protorosaur is the most primitive remains yet unresolved. The analysis of all taxa presents *Boreopricea* as the most basal protorosaur, in congruence with Benton and Allen (1997) and Rieppel et al. (2003). However, the analysis of the twenty most complete taxa presents *Protorosaurus* as the most basal protorosaur, in congruence with Jalil (1997), Dilkes (1998), and Modesto and Sues (2004). Hone and Benton (2008) presented a polytomy between *Jesairosaurus* and

Prolacertoides, two taxa that were not included in this study's second analysis due to insufficient data, as the most basal protorosaur clade.

The specific archosauromorphs that form sister clades to Protorosauria differ between the two analyses. In the analysis of all taxa, the *Rhynchosaurus-Trilophosaurus* clade is the sister clade to Protorosauria. This is somewhat in congruence with Benton and Allen (1997), which presents the *Trilophosaurus-Prolacertoides* clade as the sister clade to Protorosauria (this work did not include *Rhynchosaurus* in its analysis). Jalil (1997), who included *Rhynchosaurus* and *Trilophosaurus* in his analysis, presents *Trilophosaurus* as a sister taxon to Protorosauria, and *Rhynchosaurus* as a sister taxon to the *Trilophosaurus*-Protorosauria clade. Rieppel et al. (2003) also included both taxa in their analysis, and defined *Rhynchosaurus* and *Trilophosaurus* as members of the sister group to Protorosauria. In contrast, Dilkes (1998) presented a polytomy between the *Gephyrosaurus*-Squamata clade and the *Champosaurus-Cteniogenys-Lazarussuchus* clade as possible sister groups to Protorosauria. Modesto and Sues (2004) also presented a *Lazarussuchus-Gephyrosaurus* clade as the sister group to Protorosauria. Because these taxa were not included in this analysis, it is impossible to look for congruence between these two studies on this matter. Hone and Benton (2008) proposed that *Mesosuchus* was the sister taxon to Protorosauria, a taxon that was included neither in this study nor in those performed by the other five aforementioned works. The analysis of twenty taxa presented *Youngina* as the sister taxon to Protorosauria, which is a result of the intercalation of four non-protorosaur archosauromorphs within the protorosaurs.

Possibilities for Future Work

The largest impediment to this study was the lack of available data for most of the taxa. With the exception of *Tanytrachelos*, all taxa had to be coded based solely on published descriptions. *Prolacertoides* had to be coded directly from the codings of Benton and Allen (1997) and Jalil (1997) because its sole description was written entirely in Chinese. Ideally, specimens of each taxon would be directly observed for the next analysis of evolutionary relationships between the protorosaurs and basal archosauromorphs. This would most likely increase the data completeness for the included taxa. Addition of other archosauromorphs, such as the Choristoderes, *Lazarussuchus*, *Cteniogenys*, *Stenaulorhynchus*, *Scaphonyx*, *Hyperodapodon*, *Champosaurus*, and *Mesosuchus*, would also be beneficial. This would generate a cladogram that would address the evolutionary relationships between a broader array of taxa, and the result would be more comparable to previous studies, which have included these additional taxa.

LITERATURE CITED

- BARTHOLOMAI, A. 1979. New lizard-like reptiles from the early Triassic of Queensland. *Alcheringa*, 3: 225-234.
- BENTON, M. 1999. *Scleromochlus taylori* and the origin of dinosaurs and pterosaurs. *Philosophical Transactions of the Royal Society of London (B)*, 354: 1423-1446.
- BENTON, M. and J. ALLEN. 1997. *Boreopricea* from the Lower Triassic of Russia, and the relationships of the prolacertiform reptiles. *Palaeontology*, 40, 931-953
- BORSUK-BIALYNICKA, M. and S. E. EVANS. 2009. A long-necked archosauromorph from the Early Triassic of Poland. *Palaeontologia Polonica* 65, 203-234.
- BROILI, F. and E. FISCHER. 1916. *Trachelosaurus fischeri* nov. gen. nov. sp. Ein neuer Saurier aus dem Buntsandstein von Bernburg. *Jarbuch der Königlichen Preussischen Geologischen Landesanstalt*, 37: 359-414.
- BROOM, M. D. 1903. On a new Reptile (*Proterosuchus fergusi*) from the Karoo Beds of Tarkastad, South Africa. *Annals of the South African Museum*, 4: 159-163.
- CHATTERJEE, S. K. 1980. *Malerisaurus*, a new eosuchian reptile from the late Triassic of India. *Philosophical Transactions of the Royal Society of London, Series B*, 291: 163-200.
- CHATTERJEE, S. K. 1986. *Malerisaurus langstoni*, a new diapsid from the Triassic of Texas. *Journal of Vertebrate Paleontology*, 6: 297-312.
- COLBERT, E. H. 1987. The Triassic Reptile *Prolacerta* in Antarctica. *American Museum Novitates*, 2882: 1-19.
- COLBERT, E. H. AND P. E. OLSEN. 2001. A new and unusual aquatic reptile from the Lockatong Formation of New Jersey (Late Triassic, Newark Supergroup). *American Museum Novitates*, 3334: 1-24.
- CRUICKSHANK, A. R. I. 1972. The proterosuchian thecodonts. In JOYSEY, K. A. and T. S. KEMP (Eds.), *Studies in Vertebrate Evolution*. Oliver and Boyd, Edinburgh, 89-119.
- CURRIE, P. J. 1980. The vertebrae of *Youngina* (Reptilia: Eosuchia). *Canadian Journal of Earth Sciences*, 18: 815-818.
- DALLA VECCHIA, F. M. 2003. An *Eudimorphodon* (Diapsida, Pterosauria) specimen from the Norian (Late Triassic) of North-Eastern Italy. *Gortania – Atti. Museo Friul. Di Storia Nat.*, 25: 47-72.

- DILKES, D. W. 1998. The Early Triassic rhynchosaur *Mesosuchus browni* and the interrelationships of basal archosauromorph reptiles. *Philosophical Transactions of the Royal Society of London, Series B*, 353: 501-541.
- ELLENBERGER, P. 1977. Quelques precisions sur l'anatomie et la place systematique tres speciale de *Cosmosaurus aviceps*. *Cuadernos Geología Ibérica*, 4, 169-188.
- EWER, R.F. 1965. The Anatomy of the Thecodont Reptile *Euparkeria capensis* Broom. *Philosophical Transactions of the Royal Society of London, Series B*, 248(751): 379-435.
- FRASER, N. C. and O. RIEPPEL. 2006. A new protorosaur (Diapsida) from the Upper Buntsandstein of the Black Forest, Germany. *Journal of Vertebrate Paleontology* 26: 866–871.
- GOTTMAN-QUESADA, A. and P. M. SANDER. 2009. A redescription of the early archosauromorph *Protorosaurus speneri* MEYER, 1832, and its phylogenetic relationships. *Palaeontographica Abt. A*, 287: 123-220.
- GOW, C. E. 1975. The morphology and relationships of *Youngina capensis* Broom and *Prolacerta broomi* Parrington. *Palaeontologica Africana*, 18: 89-131.
- GOWER, D. J., and E. WEBBER. 1998. The braincase of *Euparkeria*, and the evolutionary relationships of birds and crocodylians. *Biological Review*, 73: 367-341.
- GREGORY, W. K. (1944). Osteology and relationships of *Trilophosaurus*. *University of Texas Contributions to Geology*, 4401, 273–332.
- HAMMER, Ø., HARPER, D.A.T., and P. D. RYAN, 2001. PAST: Paleontological Statistics Software Package for Education and Data Analysis. *Palaeontologia Electronica* 4(1): 9pp. http://palaeo-electronica.org/2001_1/past/issue1_01.htm.
- HECKERT, A. B., LUCAS, S. G., RINEHART, L. F., SPIELMAN, J. A., HUNT, A. P., and R. KAHLE. 2005. Revision of the archosauromorph reptile *Trilophosaurus*, with a description of the first skull of *Trilophosaurus jacobsi*, from the upper Triassic Chinle group, West Texas, USA. *Palaeontology*, 49(3):621-640.
- JALIL, N. E. 1997. A new prolacertiform diapsid from the Triassic of North Africa and the interrelationships of the Prolacertiformes. *Journal of Vertebrate Paleontology*, 17: 506-525.
- JENKINS, F. A. Jr., SHUBIN, N. H., GATESY, S. M., and K. PADIAN. 2001. A diminutive pterosaur (Pterosauria: Eudimorphodontidae) from the Greelandic Triassic. *Bull. Mus. Comp. Zool., Harvard*, 156: 151-170.

- KLEMBARA, J. and J. WELMAN. 2009. The anatomy of the palatoquadrate in the Lower Triassic *Proterosuchus fergusi* (Reptilia, Archosauromorpha) and its morphological transformation within the archosauriform clade. *Acta Zoologica*, 90: 275-284.
- LANE, H. H. 1945. New Mid-Pennsylvanian Reptiles from Kansas. *Transactions of the Kansas Academy of Science*, 47(3):381-390.
- LI, C. 2003. First Record of Protorosaurid Reptile (Order Protorosauria) from the Middle Triassic of China. *Acta Geologica Sinica*, 77(4): 419-423.
- LI, C., RIEPPEL, O., AND M. C. LABARBERA. 2004. A Triassic Aquatic Protorosaur with an Extremely Long Neck. *Science*, 305(5692): 1931.
- MODESTO, S. P., AND H-D SUES. 2004. The skull of the Early Triassic archosauromorph reptile *Prolacerta broomi* and its phylogenetic significance. *Zoological Journal of the Linnean Society*, 140: 335-351.
- NOSOTTI, S. 2007. *Tanystropheus longobardicus* (Reptilia, Protorosauria): reinterpretations of anatomy based on new specimens from the Middle Triassic of Besano (Lombardy, northern Italy). *Memorie della Società Italiana di Scienze Naturali e del Museo Civico di Storia Naturale di Milano*, 35(3): 1-88.
- NOVAS, F. E. 1994. New information on the systematics and postcranial skeleton of *Herrerasaurus ischigualastensis* (Theropoda: Herrerasauridae) from the Ischigualasto Formation (Upper Triassic) of Argentina. *Journal of Vertebrate Paleontology*, 13(4): 400-423.
- OLSON, E.C. 1936. Notes on the skull of *Youngina capensis* Broom. *The Journal of Geology*, 44(4): 523-533.
- PEABODY, F. E. 1952. *Petrolacosaurus kansensis* Lane, a Pennsylvanian reptile from Kansas. *University of Kansas Paleontological Contribution* 10: 1-41.
- PINNA, G. 1984. Osteologia di *Drepanosaurus unguicaudatus*, lepidosauro triassico del sottordine Lacertilia. *Atti della Società italiana di scienze naturali e del Museo civico di storia naturale di Milano*, 24: 7-28.
- REISZ, R. R. 1977. *Petrolacosaurus*, the Oldest Known Diapsid Reptile. *Science*, 196(4294): 1091-1093.
- RENESTO, S. 1994. A new prolacertiform reptile from the Late Triassic of Northern Italy. *Rivista Italiana Paleontologia Stratigrafia*, 100(2): 285-306.

- RENESTO, S. 1994. The shoulder girdle and anterior limb of *Drepanosaurus unguicaudatus* (Reptilia, Neodiapsida) from the upper Triassic (Norian) of Northern Italy. *Zoological Journal of the Linnean Society*, 111: 247–264.
- RENESTO, S. 1994. *Megalancosaurus*, a possibly arboreal archosauromorph (Reptilia) from the Upper Triassic of northern Italy. *Journal of Vertebrate Paleontology* 14 (1): 38-52.
- RENESTO, S. 2000. Bird-like head on a chameleon body: new specimens of the enigmatic diapsid reptile *Megalancosaurus* from the Late Triassic of Northern Italy. *Rivista Italiana di Paleontologia e Stratigrafia*, 106(2): 157-180.
- RENESTO, S. 2005. A new specimen of *Tanystropheus* (Reptilia Protorosauria) from the Middle Triassic of Switzerland and the ecology of the genus. *Rivista Italiana di Paleontologia e Stratigrafia*, 111(3): 377-394.
- RENESTO, S. and M. AVANZINI. 2002. Skin remains in a juvenile *Macrocnemus bassanii* Nopsca (Reptilia, Prolacertiformes) from the Middle Triassic of Northern Italy. *Neues Jahrb. Geol. Paläont., Abhandl.*, 224: 31-48.
- RENESTO, S. and G. BINELLI. 2006. *Vallesaurus cenensis* Wild, 1991, a drepanosaurid (Reptilia, Diapsida) from the Late Triassic of northern Italy. *Rivista Italiana di Paleontologia e Stratigrafia*, 112: 77-94.
- RENESTO, S. AND F. M. DALLA VECCHIA. 2000. The unusual dentition and feeding habits of the prolacertiform reptile *Langobardisaurus* (Late Triassic, Northern Italy). *Journal of Vertebrate Paleontology*, 20(3): 622-627.
- RENESTO, S. and F. M. DALLA VECCHIA. 2005. The skull and lower jaw of the holotype of *Megalancosaurus preonensis* (Diapsida, Drepanosauridae) from the Upper Triassic of Northern Italy. *Rivista Italiana di Paleontologia e Stratigrafia*, 111(2): 247-257.
- RENESTO, S., DALLA VECCHIA, F. M., and D. PETERS. 2002. Morphological evidence for Bipedalism in the Late Triassic Prolacertiform Reptile *Langobardisaurus*. *Senckenbergiana lethaea*, 82(1): 95-106.
- RENESTO, S. AND A. PAGANONI. 1995. A new *Drepanosaurus* (Reptilia, Neodiapsida) from the Upper Triassic of Northern Italy. *Neues Jahrb. Geol. Paläont., Abhandl.*, 197:87-99.
- RIEPPPEL, O. 1989. The hind limb of *Macrocnemus bassani* (Nopsca) (Reptilia, Diapsida): development and functional anatomy. *Journal of Vertebrate Paleontology*, 9: 373-387.

- RIEPPPEL, O., JIANG, D-Y., FRASER, N. C., HAO, W-C., MOTANI, R, SUN, Y.-L., AND Z.-Y. SUN. 2010. *Tanystropheus* cf *T. longobardicus* from the Early Late Triassic of Guizhou Province, Southwestern China. *Journal of Vertebrate Paleontology*, 30(4): 1082-1089.
- RIEPPPEL, O., LI, C., AND N. C. FRASER. 2008. The Skeletal Anatomy of the Triassic Protorosaur *Dinocephalosaurus orientalis* Li, from the Middle Triassic of Guizhou Province, Southern China. *Journal of Vertebrate Paleontology*, 28(1): 95-110.
- SANZ, J. L. and N. LOPEZ-MARTINEZ. 1984. The prolacertid lepidosaurian *Cosesaurus aviceps* Ellenberger & Villalta, a claimed 'protoavian' from the Middle Triassic of Spain. *Géobios* 17: 747-753.
- SERENO, P. C. 1994. The pectoral girdle and forelimb of the basal theropod *Herrerasaurus ischigualastensis*. *Journal of Vertebrate Paleontology*, 13(4): 425-450.
- SERENO, P. C. and A. B. ARCUCCI. 1994. Dinosaurian precursors from the Middle Triassic of Argentina: *Marasuchus lilloensis* gen. nov. *Journal of Vertebrate Paleontology*, 14: 53-73.
- SERENO, P. C. and F. E. NOVAS. 1994. The skull and neck of the basal theropod *Herrerasaurus ischigualastensis*. *Journal of Vertebrate Paleontology*, 13(4): 451-476.
- SMITH, R. M. H., and S. E. EVANS. 1996. New material of *Youngina*: evidence of a juvenile aggregation in Permian diapsid reptiles. *Palaeontology*, 39(2): 289-303.
- WILD, R. 1973. *Tanystropheus longobardicus* (Bassani) (Neue Ergebnisse). In KUHN-SCHNYDER, E. and B. PEYER. Die Triasfauna der Tessiner Kalkalpen XXIII. *Schweizerische paläontologische Abhandlungen*, 95: 1-162.
- WILD, R. 1980. Neue Funde von *Tanystropheus* (Reptilia, Squamata). In KUHN-SCHNYDER, E. and B. PEYER. Die Triasfauna der Tessiner Kalkalpen XXIV. *Schweizerische Paläontologische Abhandlungen*, 102: 1-43.
- YOUNG, C. C. 1973. [*Prolacertoides jimusarensis*]. *Vertebrata Palasiatica*, 2: 46-48.

SYNOPSIS

Several characteristics help to identify specimens of *Tanytrachelos*. *Tanytrachelos* averages about 21 cm long, with thirteen elongate cervical vertebrae (25% total vertebral length), thirteen dorsal vertebrae (21% total vertebral length), two sacral vertebrae (4% total vertebral length), and thirty-one caudal vertebrae (50% vertebral length). Its distinctive characteristics include a large orbit that occupies between 11% and 13% of the lateral skull area, a fused atlas and axis, cervical centra that are subequal in length and correlate to short cervical ribs, procoelous dorsal vertebrae, a homodont dentition, a non-sigmoidal femur, metatarsals I through IV that are subequal in length, and paired curved heterotopic bones in some specimens.

Because the paired heterotopic bones are found in some specimens but not all, they are likely the result of sexual dimorphism and not a taphonomic signal (Casey et al. 2007). Beyond this, their exact function is yet undetermined. Due to differences in size and shape, these paired post-cloacal bones cannot be compared to those of *Tanytropheus* (Rieppel et al. 2010), nor to the hemipenes of extant monitor lizards (Card and Kluge 1995) or the post-cloacal bones of extant geckos and night lizards (Kluge 1982). Because these structures seem to be present within a skin flap of one of the juvenile specimens of *Tanytrachelos* (Figure 25A), it may be that they supported a brood pouch within the animal. Alternatively, they may have been a pair of internal claspers in the male. Although their functional status is unknown, the possible presence of these structures within a juvenile lends support to the idea that *Tanytrachelos* may have been neotenic. Another piece of evidence in favor of neoteny is the consistently large orbit within adult specimens, as proportionally large eyes are characteristic of juvenile animals. On the other hand, neotenic animals generally retain the high growth rates of a juvenile throughout their lifespan, resulting in larger body sizes. This conflicts with the status of *Tanytrachelos* as one of the smallest protorosaurs. If *Tanytrachelos* were truly neotenic, then its small stature may be explained by a dwarfism caused by the constraints of a lake environment, or by relatively short lifespans resulting from early sexual maturity.

Gwyneddosaurus, a small protorosaur found in the Triassic sediments of the Lockatong Formation in Montgomery County, Pennsylvania, bears several qualitative and quantitative similarities to *Tanytrachelos ahynis* that indicate they belong to the same genus. Both taxa possess procoelous vertebrae, fan-shaped scapulae, relatively large, oval coracoids, holocephalous dorsal ribs, and straight femora. Furthermore, they share the same length ranges of femora, fingers, and toes. However, as *Gwyneddosaurus* lacks any diagnostic qualities, it should not replace *Tanytrachelos* as a generic name. Three species of ichnofossil within the genus *Gwyneddichnium* have also been found with *Gwyneddosaurus*, and differ from each other in digit lengths. The pedes of the largest ichnofossil, *Gwyneddichnium majore*, are noticeably larger than the pedes of *Tanytrachelos*, and may be a result of a different type of reptile. However, the two smaller ichnofossils, *Gwyneddichnium elongatum* and *Gwyneddichnium minore*, have pedes that are just slightly larger and smaller respectively than those of *Tanytrachelos*, and are likely a result of *Gwyneddosaurus/Tanytrachelos*. In addition to these ichnofossils, an ichnofossil left by *Tanytrachelos* in what is now the Solite Quarry indicates that *Tanytrachelos* could walk on land or in shallow water. This ichnofossil shows two manus prints, indicating a quadrupedal gait. Although individual phalanges

could not be discerned, minor webbing could be interpreted between the bases of the digits. This webbing was probably used to stabilize the animal in the water. Although such webbing has not been seen on the pedes, the disparity of size between the front and rear limbs, as well as large soft tissue traces seen on the femora of the juvenile (Figure 25A) imply that *Tanytrachelos* propelled itself through the water with its back legs.

Tanytrachelos shares several characteristics in common with its proposed sister taxon *Tanystropheus* that are diagnostic for the family Tanystropheidae. Both taxa have thirteen elongate cervical vertebrae, thirteen dorsal vertebrae, fan-shaped scapulae, the same phalangeal formulas, carpals, and tarsals in the manus and pedes respectively, and the presence of post-cloacal heterotopic bones in some of the specimens. On the other hand, there are several differences between the two taxa that easily differentiate them. The most noticeable difference is the disparity of average size between *Tanytrachelos*, which averages at 21 cm long, and *Tanystropheus*, which averages at 5 m long. The dentitions also differ between taxa, as *Tanytrachelos* has a homodont dentition of conical teeth, whereas *Tanystropheus* has a heterodont dentition that includes tricuspid teeth. Other morphological qualities possessed by *Tanystropheus* that are not possessed by *Tanytrachelos* are amphicoelous dorsal vertebrae, dorsal ribs that are fused to the vertebrae, ten more caudal vertebrae than *Tanytrachelos*, an obturator foramen, sigmoidal femora, unequal metacarpal lengths, and a concave-convex astragalo-calcaneal contact in the tarsus. In spite of these differences, *Tanytrachelos* paired consistently with *Tanystropheus* in the cladistic analysis of all taxa as well as the analysis of the twenty most complete taxa. Tanystropheidae was monophyletic in the analysis with the most complete taxa, and would have been monophyletic in the analysis of all taxa had *Prolacertoides*, which only had 4% data completeness, not been placed in the tanystropheid clade.

Although the two cladistic analyses in this study did not produce identical results, they each yielded a paraphyletic Protorosauria. This result is consistent with the paraphyletic results of Dilkes (1998), Rieppel et al. (2003), and Modesto and Sues (2004), and conflicts with the monophyletic results of Benton and Allen (1997), Jalil (1997), and Hone and Benton (2008). Within Protorosauria, the family Drepanosauridae was monophyletic in the tree of all taxa and the tree of the twenty most complete taxa. A monophyletic Drepanosauridae has been supported by Dilkes (1998), Modesto and Sues (2004), and Hone and Benton (2008), and Rieppel et al. (2003).

The most basal protorosaur differed between the two cladistic results of this study. The analysis of all taxa presented *Boreopricea* as the most basal protorosaur, as also found by Rieppel et al (2003), and by Benton and Allen (1997), who identified *Boreopricea* and *Prolacerta* as the most basal clade in Protorosauria. In contrast, the analysis of the twenty most complete taxa named *Protorosaurus* as the most basal protorosaur, supporting the results of Jalil (1997), Dilkes (1998), and Modesto and Sues (2004).

The sister clades to Protorosauria differed greatly between these two analyses as well as between previously published analyses, as did the specific structure of clades. One way to increase comparability between these results is to perform an analysis that also includes other archosauromorphs. Furthermore, taxa may achieve a higher level of data completeness if they can be coded from direct observation, instead of relying predominantly on published descriptions.

APPENDIX A

LIST OF *TANYTRACHELOS AHYNIS* SPECIMENS EXAMINED

#12	LOT 30.143	LOT 30.235.58	LOT 30.286	LOT 30.299	VMNH1004	VMNH120015
#57	LOT 30.217.52	LOT 30.235.59	LOT 30.294	LOT 30.300	VMNH1006	VMNH120016
#98	LOT 30.226	LOT 30.235.60	LOT 30.297	LOT 30.781	VMNH2572	VMNH120019
04-19	LOT 30.227.247	LOT 30.235.62	LOT 30.314	LOT 30.3115	VMNH2746	VMNH120023
04-21	LOT 30.235.0	LOT 30.235.63	LOT 30.315	VMNH776	VMNH2758	VMNH120042
04-22	LOT 30.235.1	LOT 30.235.64	LOT 30.322	VMNH960	VMNH2826	VMNH120044
04-23	LOT 30.235.3	LOT 30.235.65	LOT 30.357	VMNH961	VMNH2827	VMNH120047
04-24	LOT 30.235.4	LOT 30.235.68	LOT 30.393	VMNH962	VMNH2828	W2-30
04-25	LOT 30.235.5	LOT 30.235.70	LOT 30.394	VMNH963	VMNH2850	WS02-2
04-26	LOT 30.235.6	LOT 30.235.71	LOT 30.397	VMNH965	VMNH2852	WS02-41
04-27	LOT 30.235.8	LOT 30.235.74	LOT 30.398	VMNH966	VMNH2992	WS02-42
04-30	LOT 30.235.9	LOT 30.237	LOT 30.401	VMNH967	VMNH2993	WS02-58
04-31	LOT 30.235.11	LOT 30.239	LOT 30.537	VMNH968	VMNH2997	WS02-64
04-32	LOT 30.235.11-7	LOT 30.240	LOT 30.624	VMNH969	VMNH3059	WS02-71
04-33	LOT 30.235.12	LOT 30.241	LOT 30.637	VMNH972	VMNH3184	WS02-113
04-34	LOT 30.235.13	LOT 30.242	LOT 30.647	VMNH973	VMNH3216	WS02-113
04-35	LOT 30.235.17	LOT 30.243	LOT 30.697.522	VMNH974	VMNH3217	WS02-49
5	LOT 30.235.18	LOT 30.244	LOT 30.715	VMNH975	VMNH3218	WS02-109
8-27X	LOT 30.235.22	LOT 30.245	LOT 30.716	VMNH976	VMNH3219	YPM7482
8-31X	LOT 30.235.23	LOT 30.246	LOT 30.746	VMNH977	VMNH3220	YPM7484
11	LOT 30.235.24	LOT 30.249	LOT 30.749	VMNH978	VMNH3221	YPM7496A
50	LOT 30.235.26	LOT 30.250	LOT 30.751	VMNH979	VMNH3222	YPM7540
101	LOT 30.235.30	LOT 30.251	LOT 30.752	VMNH980	VMNH3223	YPM7541B
466	LOT 30.235.32	LOT 30.255	LOT 30.753	VMNH981	VMNH3224	YPM7621
558	LOT 30.235.33	LOT 30.256	LOT 30.754	VMNH982	VMNH3225	YPM8600
990	LOT 30.235.34	LOT 30.258	LOT 30.755	VMNH983	VMNH3226	16
1005	LOT 30.235.35	LOT 30.259	LOT 30.756	VMNH985	VMNH3227	VMNH984
05805	LOT 30.235.36	LOT 30.266	LOT 30.757	VMNH986	VMNH3228	VMNH120045
7541A	LOT 30.235.37	LOT 30.267	LOT 30.758	VMNH987	VMNH3229	VMNH120046
7622	LOT 30.235.38	LOT 30.268	LOT 30.759	VMNH988	VMNH3230	VMNH120048
7623	LOT 30.235.39	LOT 30.269	LOT 30.760	VMNH989	VMNH3231	VMNH120049
FN17A1&BI	LOT 30.235.47	LOT 30.270	LOT 30.762	VMNH991	VMNH3233	WS02-130
FN17A2&B2	LOT 30.235.48	LOT 30.271	LOT 30.764	VMNH992	VMNH3234	LOT 30.625
FN17A3&B3	LOT 30.235.49	LOT 30.272	LOT 30.765	VMNH993	VMNH3235	VMNH2768
FN17A4&B4	LOT 30.235.50	LOT 30.273	LOT 30.766	VMNH994	VMNH3237	VMNH3243
FN12A2&B2	LOT 30.235.51	LOT 30.274	LOT 30.767	VMNH995	VMNH3238	VMNH3652
FN12A3&B3	LOT 30.235.52	LOT 30.275	LOT 30.769	VMNH998	VMNH3239	VMNH3668
LOT 30.325.19	LOT 30.235.53	LOT 30.276	LOT 30.770	VMNH999	VMNH3240	
LOT 30.235.20	LOT 30.235.54	LOT 30.281	LOT 30.771	VMNH1000	VMNH3241	
LOT 30.235.21	LOT 30.235.55	LOT 30.282	LOT 30.772	VMNH1001	VMNH3242	
LOT 30.235.21.5	LOT 30.235.56	LOT 30.283	LOT 30.773	VMNH1002	VMNH3408	
LOT 30.325.67	LOT 30.235.57	LOT 30.285	LOT 30.780	VMNH1003	VMNH3651	

APPENDIX B

MORPHOMETRIC MEASUREMENTS OF *TANYTRACHELOS* SPECIMEN ELEMENTS

Specimen	Skull Diameter (cm)	Orbit Diameter (cm)	Distance from Orbit to Front of Skull	Distance from Orbit to Back of Skull	Dentary Length (cm)
YPM7496A	1.27	0.44	0.4	0.49	0.89
7622	0.79	0.27	0.18	0.22	
VMNH982	1.52	0.53	0.36	0.43	1.24
VMNH3651	1.08	0.4	0.28	0.51	1.02

TABLE 13. Linear measurements of the skull, orbit, and dentary.

Specimen	Cervical 2	Cervical 3	Cervical 4	Cervical 5	Cervical 6	Cervical 7	Cervical 8	Cervical 9	Cervical 10	Cervical 11	Cervical 12	Cervical 13
YPM7496A	0.51	0.52	0.34	0.34	0.3	0.62	0.44	0.47	0.45	0.45	0.6	0.44
VMNH120016										0.42	0.41	0.4
Lot 30.258	0.58	0.5	0.48	0.47	0.49	0.45	0.5	0.45	0.32	0.44	0.4	0.43
VMNH961					0.21	0.17	0.19	0.2	0.19	0.2	0.16	0.19
Lot 30.764		0.36	0.38	0.33	0.35	0.33	0.37	0.34	0.34	0.31	0.28	0.27
VMNH2993					0.38	0.37	0.38					
VMNH989							0.62	0.57	0.55	0.45	0.37	0.41
VMNH974					0.32	0.34	0.36	0.37	0.37	0.4	0.47	0.42
WS02--41										0.49	0.48	0.4
VMNH988										0.38	0.43	0.42
VMNH120023				0.5	0.47	0.46	0.43	0.5	0.54	0.52	0.21	0.29
VMNH120019			0.42		0.52	0.56	0.44	0.45	0.44	0.45	0.41	0.4
7622	0.57	0.56	0.54	0.34	0.49							
YPM7484	0.34	0.43	0.47	0.4	0.47	0.74						
VMNH982	0.7	0.61	0.53	0.6	0.4	0.42	0.51	0.48	0.56	0.67	0.54	0.53
VMNH2850	0.36	0.41	0.39	0.42	0.44	0.49	0.45	0.49	0.47	0.47	0.44	0.38
VMNH120042						0.3	0.32	0.39	0.45	0.41	0.41	0.39
VMNH3651	0.36	0.4	0.56	0.48	0.5	0.32	0.4	0.5	0.42	0.41	0.38	0.34

TABLE 14. Length measurements of cervical vertebrae, in centimeters.

Specimen	Cervical Rib 5 Average Width	Cervical Rib 6 Average Width	Cervical Rib 7 Average Width	Cervical Rib 8 Average Width	Cervical Rib 9 Average Width	Cervical Rib 10 Average Width	Cervical Rib 11 Average Width	Cervical Rib 12 Average Width	Cervical Rib 13 Average Width
VMNH120015					0.25	0.34	0.41	0.5	0.46
VMNH120019				0.23	0.25	0.26	0.31	0.38	0.33
VMNH120042						0.27	0.34	0.44	0.57
YPM7484	0.29	0.21							
VMNH3651		0.12	0.14	0.19	0.21	0.3	0.43	0.36	

TABLE 15. Averaged width measurements of cervical ribs, in centimeters. (No data is available for cervical vertebrae 1 through 3.)

Specimen	Cervical Rib 5 Average Length	Cervical Rib 6 Average Length	Cervical Rib 7 Average Length	Cervical Rib 8 Average Length	Cervical Rib 9 Average Length	Cervical Rib 10 Average Length	Cervical Rib 11 Average Length	Cervical Rib 12 Average Length	Cervical Rib 13 Average Length
VMNH120015					0.35	0.56	0.4	0.43	
VMNH120019				0.48	0.55	0.55	0.56	0.53	
VMNH120042						0.28	0.38	0.39	0.31
YPM7484	0.56	0.62							
VMNH3651		0.48	0.55	0.63	0.56	0.56	0.49	0.47	

TABLE 16. Averaged length measurements of cervical ribs, in centimeters. (No data is available for cervical vertebrae 1 through 3.)

Specimen	Dorsal 1	Dorsal 2	Dorsal 3	Dorsal 4	Dorsal 5	Dorsal 6	Dorsal 7	Dorsal 8	Dorsal 9	Dorsal 10	Dorsal 11	Dorsal 12	Dorsal 13
YPM7496A	0.51	0.47	0.46	0.55	0.42	0.53			0.36	0.5	0.42	0.43	0.35
VMNH120016	0.38	0.46	0.36	0.27	0.24	0.3	0.44	0.36	0.4	0.45	0.44	0.31	0.36
Lot 30.325 20 04--22	0.37	0.36	0.44	0.43	0.32	0.38	0.26	0.28	0.22	0.28	0.32	0.38	0.38
Lot 30.757	0.53	0.48		0.5	0.47	0.45	0.44	0.37	0.42	0.47	0.39	0.33	
Lot 30.299			0.34	0.35	0.4		0.48	0.42	0.42	0.37	0.37	0.37	0.4
Lot 30.258						0.38	0.35	0.39	0.4	0.41	0.37	0.38	0.41
7623	0.4	0.36	0.44	0.47	0.47	0.43	0.41	0.44	0.45	0.39	0.36	0.46	0.38
Lot 30.217					0.4	0.45	0.39						
VMNH961		0.21			0.28	0.24	0.24	0.28	0.24	0.23	0.28	0.25	0.22
VMNH995		0.37	0.38	0.37	0.4	0.34							
VMNH120015	0.37	0.3	0.36	0.33							0.33	0.38	0.39
VMNH974	0.42	0.34	0.4	0.38	0.39	0.34	0.38	0.35	0.35	0.38	0.39	0.35	0.38
VMNH988	0.33	0.33	0.34	0.31	0.31	0.33	0.33	0.32	0.33	0.34	0.38	0.37	0.33
VMNH120023	0.39	0.4	0.38	0.39	0.38								
7622	0.44	0.4	0.43	0.4	0.38	0.42	0.42	0.37	0.38	0.39	0.36	0.34	0.39
VMNH977								0.23	0.25	0.24	0.25	0.25	0.24
VMNH2850	0.42	0.4	0.36	0.41	0.37	0.35	0.37	0.34					
120042	0.48	0.41	0.43										
VMNH3651	0.34	0.35	0.45	0.36	0.44	0.43	0.37	0.29	0.3	0.35	0.3	0.36	0.31

TABLE 17. Length measurements of dorsal vertebrae, in centimeters.

Specimen	Left or Right	Sacral Vertebra 1 Length (cm)	Sacral 1 Rib Length Average (cm)	Sacral Vertebra 2 Length (cm)	Sacral 2 Rib Length Average (cm)	Ilium Length (cm)	Ischium Length (cm)
YPM7496A		0.35	0.46	0.34	0.47		
VMNH120016		0.3	0.47	0.3	0.55		
04--22		0.34	0.49	0.29	0.55		
ot 30.235 19		0.59		0.48			
04--19		0.35		0.34			
04--21				0.31	0.56		
04--32			0.53	0.33	0.53		
VMNH961		0.27		0.25			
VMNH120015		0.41	0.47	0.46	0.47		
VMNH988		0.31		0.33			
WS02--2		0.56		0.5			
7622		0.4		0.37			
YPM8600				0.26	0.5		
WS-02-109					0.52		
VMNH977		0.36		0.31	0.44		
YPM7484		0.36	0.64	0.37	0.67		
04-22		0.3	0.48	0.27	0.56		
VMNH3651		0.44					
VMNH120044				0.62	0.67		
YPM7621	left						1.16
	right					0.9	1.23

TABLE 18. Linear measurements of sacral vertebrae and individual hip bones.

Specimen	Caudal 1	Caudal 2	Caudal 3	Caudal 4	Caudal 5	Caudal 6	Caudal 7	Caudal 8	Caudal 9	Caudal 10	Caudal 11	Caudal 12	Caudal 13	Caudal 14	Caudal 15	Caudal 16	Caudal 17
YPM7496A	0.51	0.6	0.39	0.35													
VMNH120016	0.34	0.44	0.36	0.47	0.45	0.64	0.38	0.55									
04--22	0.48	0.33															
Lot 30.235-19	0.45	0.49	0.53	0.53	0.59	0.72	0.66		0.46								
04--19		0.45	0.43	0.47	0.46												
04--21	0.29	0.31															
Lot 30.267						0.37	0.26	0.39	0.43	0.51	0.44	0.45	0.48	0.46	0.46	0.46	0.48
04--32	0.34	0.39															
VMNH961	0.26	0.24	0.3	0.26	0.25	0.27											
04--23		0.38	0.41	0.44													
VMNH120015	0.38	0.33	0.43	0.45													
Lot 30.764	0.38	0.39	0.31	0.29	0.33	0.32	0.41										
VMNH988	0.47	0.45	0.48	0.45	0.36	0.42											
VMNH776	0.32																
Lot 30.297	0.39	0.36	0.36														
8--31X	0.43	0.39	0.37														
Lot 30.767	0.46	0.45	0.47	0.47	0.52												
WS02--2	0.49	0.71															
7622	0.37	0.41	0.38	0.38	0.38												
YPM8600	0.28	0.25	0.29														
VMNH2826	0.41	0.35	0.45														
VMNH2827	0.41	0.4	0.38	0.4	0.38	0.36	0.37	0.36	0.33	0.35	0.37	0.34	0.37	0.38	0.38	0.36	0.22
WS-02-109		0.35															
VMNH977	0.23	0.25	0.23	0.24													
YPM7484B			0.45	0.42	0.36												
04--22	0.38	0.37	0.31														
VMNH120044	0.67																
YPM7621	0.53	0.59	0.45	0.55	0.53												

TABLE 19. Length measurements of caudal vertebrae 1 through 17, in centimeters.

Specimen	Caudal 18	Caudal 19	Caudal 20	Caudal 21	Caudal 22	Caudal 23	Caudal 24	Caudal 25	Caudal 26	Caudal 27	Caudal 28	Caudal 29	Caudal 30	Caudal 31
Lot 30.267	0.47	0.52	0.57	0.56	0.57	0.54	0.45	0.49	0.47	0.38	0.44	0.41	0.4	0.4
VMNH2827	0.32	0.36												

TABLE 20. Length measurements of caudal vertebrae 18 through 31, in centimeters.

Specimen	Caudal 1 Tranverse Process Length Average	Caudal 2 Tranverse Process Length Average	Caudal 3 Tranverse Process Length Average	Caudal 4 Tranverse Process Length Average	Caudal 5 Tranverse Process Length Average	Caudal 6 Tranverse Process Length Average	Caudal 7 Tranverse Process Length Average
YPM7496A	0.58	0.46					
VMNH120016	0.28	0.49	0.4	0.6	0.37	0.32	0.27
04--22	0.42	0.64					
04--32	0.53	0.55					
04--23		0.46	0.49	0.46			
VMNH120015	0.46		0.46	0.42			
VMNH776	0.45	0.51					
Lot 30.297	0.46	0.46	0.43				
8--31X	0.64	0.67					
YPM8600	0.38	0.44	0.48				
VMNH2826	0.47	0.31					
WS-02-109	0.54	0.5					
VMNH3059	0.8	0.78	0.8	0.58	0.58	0.42	
YPM7484A	0.72	0.74	0.79				
YPM7484B	0.74	0.72	0.73	0.33			
04--22	0.53	0.63	0.58				
VMNH120044	0.63						
YPM7621	0.64	0.7	0.5	0.6	0.66		

TABLE 21. Averaged length measurements of the caudal transverse processes, in centimeters.

Specimen	Left or Right	Humerus Length (cm)	Proximal Humerus Width (cm)	Distal Humerus Width (cm)	Humerus Aspect Ratio	Ulna Length(cm)	Radius Length (cm)
YPM7496A	left	2.29	0.53	0.49	0.22270742	0.93	0.81
	right	1.74	0.33	0.44	0.22126437		
VMNH120016	left	2.13	0.26	0.39	0.15258216		0.87
	right	2.47	0.33	0.38	0.1437247		
Lot 30.299	left	2.04	0.3	0.29	0.14460784	0.94	0.85
Lot 30.267	left	2.02	0.42	0.2	0.15346535	0.94	0.86
	right	1.97	0.38	0.14	0.1319797	1.02	0.93
558	left	2.36	0.31	0.26	0.12076271	1.01	0.88
#57	left						
7623	left	2.3	0.36	0.36	0.15652174		
	right	2.29	0.25	0.35	0.13100437		
04--23	left		0.29			0.73	0.68
	right			0.25		0.71	0.67
WS02--41	left			0.41			
VMNH983	left	1.81	0.17	0.22	0.10773481	1.01	0.87
VMNH2992	left					1.19	1.09
VMNH120023	left	1.74	0.2	0.17	0.10632184		
Lot 30.315	left						0.79
VMNH3239	left					1.16	1.21
Lot 30.235-5	left	1.99	0.46	0.5	0.24120603		
7622	left	2.46	0.33	0.4	0.14837398	0.87	0.79
	right		0.4	0.35		1.08	1.07
VMNH3217	left	2.14	0.28	0.29	0.13317757	0.82	0.71
YPM7484	left	2.33				0.83	
	right	2.41				0.82	
VMNH982	left	2.92	0.5	0.37	0.1489726		
VMNH3651	left	1.99	0.24	0.22	0.11557789	0.91	0.82
	right	1.69	0.35	0.27	0.18343195	0.93	0.8
VMNH2828	right					0.73	
466	right	2.22	0.21	0.32	0.11936937		
VMNH961	right	2.11	0.23	0.19	0.09952607		
VMNH995	right	2.44	0.16	0.2	0.07377049		
VMNH120015	right	2.32	0.3	0.38	0.14655172	0.95	0.95
VMNH120043	left		0.2				
	right	1.6	0.17	0.21	0.11875	0.81	0.77
Lot 30.755	right					0.71	
VMNH3243	right	2.28	0.48	0.43	0.1995614		
	left	2.3	0.44	0.39	0.18043478		

TABLE 22. Linear measurements and aspect ratio of the forelimb long bones.

Specimen	Left or Right	Metacarpal I	Metacarpal II	Metacarpal III	Metacarpal IV	Metacarpal V
YPM7496A	left	0.4	0.25	0.22		
Lot 30.267	left	0.42	0.46	0.47		
04-23	left		1.09	1.16		
VMNH2828	right	0.13	0.25	0.26		
Lot 30.315	right	0.47	0.61	0.59	0.6	0.52
VMNH3651	right	0.19	0.18	0.24	0.24	

TABLE 23. Length measurements of individual metacarpals, in centimeters.

Specimen	Left or Right	Digit I		Digit II			Digit III			
		Phalanx 1	Phalanx 2	Phalanx 1	Phalanx 2	Phalanx 3	Phalanx 1	Phalanx 2	Phalanx 3	Phalanx 4
YPM7496A	left	0.2	0.08	0.19	0.15	0.12	0.11	0.12	0.08	
Lot 30.315	right	0.16	0.09	0.38	0.3	0.12	0.41	0.27	0.22	0.15
YPM7621	right						0.31	0.23		

TABLE 24. Length measurements of individual phalanges of manus digits I through III, in centimeters.

Specimen	Left or Right	Digit IV				Digit V		
		Phalanx 1	Phalanx 2	Phalanx 3	Phalanx 4	Phalanx 1	Phalanx 2	Phalanx 3
Lot 30.315	right	0.33	0.22	0.18	0.15	0.24	0.18	0.12

TABLE 25. Length measurements of individual phalanges of manus digits IV and V, in centimeters.

Specimen	Left or Right	Femur Length (cm)	Femur Proximal Width (cm)	Femur Distal Width (cm)	Femur Aspect Ratio	Tibia Length (cm)	Fibula Length (cm)
YPM7496A	left	2.76	0.46	0.36	0.1485507	2.22	
VMNH120016	left	2.81	0.4	0.21	0.1085409		
	right	2.81				1.74	1.65
VMNH3184	left	2.7	0.49	0.44	0.1722222		
04-19	left		0.31				
	right	2.33	0.27	0.21	0.1030043	1.77	1.63
466	left			0.4			
04-32	left		0.3				
7623	left	2.92	0.47	0.31		1.78	1.74
04-23	left	2.83	0.34	0.26	0.1060071	1.54	1.34
	right		0.34				
VMNH120015	left	2.81	0.35	0.24	0.1049822	1.88	1.79
	right	2.88	0.38	0.25	0.109375		
VMNH988	left	2.92	0.23	0.18	0.0702055	2.11	1.98
	right	2.93	0.33	0.29	0.105802	2.38	1.96
VMNH776	left	2.89				2.15	1.96
#98	left			0.41			
WS02-58	left					1.11	1.05
WS02-113	left					2.1	2.17
Lot 30.322	left					2.05	1.89
VMNH3233	left					1.42	1.34
VMNH3239	left	2.59				1.84	1.75
Lot 30.235	left	2.67				0.4	0.17
Lot 30.235-12	left	2.88	0.22	0.32	0.09375	1.49	
Lot 30.235-70	left	2.3	0.36	0.23	0.1282609	1.62	1.53
	right	2.27	0.33	0.22	0.1211454	1.62	

TABLE 26. Linear measurements and aspect ratio of the hind limb long bones.

TABLE 26 (cont'd)

7622	left		0.39				
	right		0.37				
VMNH2852	left	1.68	0.29	0.21	0.1488095	1.43	1.35
VMNH2827	left	1.62	0.32	0.21	0.1635802	1.6	1.29
	right					1.59	1.33
02-109	left	2.92	0.64		0.2191781	1.74	1.64
VMNH977	left	2	0.23	0.27	0.125	1.27	1.18
	right	1.88	0.29	0.14	0.1143617	1.51	1.45
VMNH3059	left	3.44	0.53	0.3	0.1206395	2.29	2.43
	right	3.18	0.61	0.43	0.163522	2.54	2.8
VMNH962	left		0.43	0.37		2.08	2.02
YPM7540	left			0.21		1.73	1.59
04-22	left	3.09	0.33	0.26	0.0954693	1.99	1.74
YPM7621	left	2.9	0.5	0.26	0.1310345	2.33	2.32
	right	3	0.53	0.26	0.1316667		
VMNH3651	left	2.49	0.36	0.25	0.12249		
04-21	right	2.68	0.34	0.25	0.1100746		
Lot 30.267	right	2.08	0.48	0.41	0.2139423		
101	right	2.62	0.12	0.21	0.0629771		
VMNH995	right	2.85	0.33	0.32	0.1140351		
VMNH974	right	2.65	0.39	0.36	0.1415094		
VMNH984	right	2.4	0.48	0.22	0.1458333	1.47	1.46
Lot30.755	right			0.19		1.54	1.65
Lot 30.767	right	2.55	0.39	0.22	0.1196078	1.61	1.39
WS02-2	right	2.75	0.55	0.27	0.1490909		
VMNH2826	right	3.02	0.3	0.36	0.1092715	1.83	1.72
YPM7621	right	3	0.53	0.26	0.1316667		
VMNH120049	left	2.69	0.47	0.32	0.1468401	2.41	2.28
	right	3.38	0.32	0.19	0.0754438	2.06	2.01
VMNH120047						1.96	1.88
VMNH2850	right	2.49	0.4	0.22	0.124498		

Specimen	Left or Right	Metatarsal I	Metatarsal II	Metatarsal III	Metatarsal IV	Metatarsal V
VMNH120016	left	1.04	1.32	1.35	1.17	0.28
	right	0.94	1.04	0.93	1.02	0.22
Lot 30.245	left	0.79	1.05	1	0.99	0.29
WS02-58	left					0.21
YPM8600	left	0.83	1.1	1.17	0.83	
VMNH2826	left	1.13	1.36	1.3	0.87	
VMNH2827	left	0.81	0.85	0.95	1.05	0.21
	right	0.8	0.84	0.84	0.74	0.33
VMNH962	left	1.07	1.23			
YPM7540	left	0.6	0.76	1.02	1.11	0.23
YPM7621	left	1.57	1.54	1.6	1.23	0.31
04-19	right	0.88	0.94	1.03	0.86	0.55

TABLE 27. Length measurements of individual metatarsals, in centimeters.

Specimen	Left or Right	Digit I		Digit II			Digit III			
		Phalanx 1	Phalanx 2	Phalanx 1	Phalanx 2	Phalanx 3	Phalanx 1	Phalanx 2	Phalanx 3	Phalanx 4
YPM8600	left	0.32		0.35	0.2		0.43	0.31		
VMNH2827	left						0.25			
	right			0.38	0.23		0.44	0.17	0.07	0.06
YPM7540	left	0.29		0.18	0.18		0.5	0.24	0.24	0.12

TABLE 28. Length measurements of individual phalanges of pes digits I through III, in centimeters.

Specimen	Left or Right	Digit IV				Digit V		
		Phalanx 1	Phalanx 2	Phalanx 3	Phalanx 4	Phalanx 1	Phalanx 2	Phalanx 3
YPM7540	left	0.43	0.25	0.2	0.08	0.93	0.23	0.2
VMNH2827	right	0.36	0.28			0.59	0.29	
YPM7621	left					1.14		

TABLE 29. Length measurements of individual phalanges of pes digits IV and V, in centimeters.

Specimen	Left			Right		
	Medial Heterotopic Bone Length (cm)	Distal Heterotopic Bone Length (cm)	Angle from Median (degrees)	Medial Heterotopic Bone Length (cm)	Distal Heterotopic Bone Length (cm)	Angle from Median (degrees)
VMNH120016	0.64	1.4	104.3	1.04	1.42	109.4
9		2.2	114.2		2.33	128.4
04-19			101.4	1.09	1.84	101.7
04-23	1.57	1.87	82.3	1.42		110.5
Lot 30.235-70		1.74	107.2			
YPM7621	1.29	1.66		1.11	1.42	

TABLE 30. Length and angle measurements of individual heterotopic bones.

Specimen	A	B	C	D	E	F	G	H	I	J	K	L	M	N	O	P	Q	R	S	T	U	V
7451A	0.58																					
Lot 30.235-67	0.61	0.5	0.51																			
8-27x	0.31	0.34																				
Lot 30.300	0.57	0.48	0.53	0.52																		
Lot 30.272	0.57																					
Lot 30.251	0.39	0.32	0.31	0.31	0.28	0.28	0.3	0.25	0.26	0.28	0.27	0.28	0.35	0.34	0.3	0.34	0.32	0.28	0.37	0.58	0.28	0.26
FN17A3B3	0.59																					
FN17A2B2	0.56	0.53	0.56																			
VMNH3408	0.29	0.3	0.31	0.32	0.47	0.37	0.38	0.41														
VMNH975	0.42	0.4	0.39	0.39	0.39	0.35																
VMNH1000	0.47	0.45	0.48	0.5																		
Lot 30.277-247	0.3	0.3	0.29	0.29	0.3	0.3	0.33	0.29	0.25	0.29	0.36	0.35										
VMNH3227	0.5	0.42																				
Lot 30.269	0.47	0.51	0.57	0.43	0.53	0.51	0.48	0.48	0.38													
Lot 30.286	0.39																					
Lot 30.749	0.33	0.35	0.38	0.34	0.37	0.34	0.37															
Lot 30.537	0.44																					
Lot 30.274	0.32	0.38	0.37	0.36																		
Lot 30.647	0.46	0.39	0.44	0.43	0.41	0.45																
VMNH1002	0.47																					
Lot 30.281	0.45	0.46																				
Lot 30.758	0.44	0.38																				
Lot 30.746	0.5	0.39	0.35	0.38																		
Lot 30.770	0.33	0.37																				
Lot 30.766	0.4	0.38	0.35	0.35	0.34	0.46	0.42	0.34	0.31													
Lot 30.773	0.3	0.28	0.33																			
Lot 30.780	0.36	0.36	0.34	0.32																		
Lot 30.781	0.45	0.46	0.44	0.42	0.43	0.48	0.45	0.43	0.49	0.47	0.43	0.44	0.43	0.47	0.42	0.45	0.47	0.48	0.42			
VMNH991	0.39	0.38																				
Lot 30.772	0.37																					
VMNH3235	0.43	0.4	0.4	0.42	0.44	0.38	0.4															
VMNH3224	0.42	0.51	0.42	0.45																		
Lot 30.357	0.47	0.49																				

TABLE 31. Length measurements of vertebrae of unknown type and articulation. Here each vertebra is labeled arbitrarily with a letter.

TABLE 31 (cont'd)

VMNH3241	0.76	0.68	0.66	0.71	0.58	0.53	0.59														
VMNH993	0.3	0.32																			
Lot 30.240	0.61	0.64	0.65	0.54																	
W2-30	0.37	0.29	0.3																		
VMNH981	0.46																				
VMNH979	0.34	0.3																			
VMNH976	0.4	0.42																			
VMNH992	0.35																				
VMNH998	0.46	0.47	0.41	0.47	0.44	0.45	0.42	0.49													
VMNH3218	0.45	0.4	0.63	0.58	0.53	0.59	0.59	0.41	0.47	0.4	0.46	0.42	0.45	0.44	0.44	0.46					
Lot 30.393	0.67	0.62	0.52	0.48	0.53	0.48															
VMNH776	0.58	0.36	0.34	0.5	0.45	0.52	0.48	0.35													
VMNH3229	0.42	0.36	0.41	0.4																	
VMNH3216	0.51	0.47	0.44	0.47																	
Lot 30.765	0.41	0.37	0.36																		
Lot 30.401	0.2	0.23	0.26	0.24	0.18	0.22	0.28	0.31	0.31												
WS02-71	0.55																				
Lot 30.266	0.5	0.51	0.5	0.55	0.57	0.44	0.48	0.4	0.38												
Lot 30.755	0.45	0.58	0.33	0.38	0.43	0.4	0.42	0.37													
Lot 30.322	0.33	0.43	0.32	0.41																	
VMNH2758	0.53	0.53	0.6	0.5	0.55	0.44	0.47	0.49	0.49	0.48	0.39										
Lot 30.255	0.46																				
Lot 30.315	0.5	0.47	0.53	0.45	0.5	0.53	0.45	0.42	0.3	0.38	0.48										
Lot 30.394	0.4	0.33	0.39	0.3	0.38	0.33	0.27	0.27	0.31	0.26											
YPM7541B	0.41																				
VMNH3233	0.37	0.42																			
Lot 30.753	0.37	0.34	0.51	0.54	0.45																
VMNH3240	0.7	0.65	0.71	0.47																	
VMNH3220	0.33	0.44	0.46																		
VMNH1001	0.68	0.45	0.46	0.41																	
Lot 30.769	0.53	0.5	0.44	0.42	0.4																
VMNH3221	0.51	0.6																			
VMNH3231	0.48																				
Lot 30.235-4	0.49	0.47	0.46																		

TABLE 31 (cont'd)

Lot 30.235-5	0.34	0.37	0.4																		
Lot 30.235-6	0.49	0.42	0.44																		
Lot 30.235-9	0.55																				
Lot 30.235-11	0.44																				
Lot 30.235-59	0.5	0.4																			
Lot 30.235-A/B	0.3	0.27	0.35																		
Lot 30.235-13A3	0.36	0.37	0.4	0.4	0.32	0.59	0.54	0.56	0.57	0.41											
Lot 30.235-22	0.5	0.51	0.52	0.4	0.47	0.49	0.4	0.47	0.5	0.47	0.47	0.43	0.39	0.4	0.4						
Lot 30.235-30	0.44	0.38	0.31	0.42																	
Lot 30.235-32	0.57	0.55	0.47	0.48	0.42	0.42	0.38	0.41	0.39	0.39	0.3	0.45	0.42								
Lot 30.235-36	0.46	0.53	0.42																		
Lot 30.235-33	0.54																				
Lot 30.235-34	0.47	0.5	0.38	0.37	0.39	0.4	0.39	0.41	0.43	0.35											
Lot 30.235-35	0.42	0.45	0.65	0.62	0.65	0.63															
Lot 30.235-37	0.37	0.34	0.35	0.32	0.34	0.36	0.37	0.31													
Lot 30.235-39	0.35																				
Lot 30.235-47	0.59																				
Lot 30.235-52	0.43																				
Lot 30.235-55	0.38																				
Lot 30.235-60	0.38	0.35	0.34	0.32	0.4																

Specimen	Cervical Vertebra A	Cervical Vertebra B	Cervical Vertebra C	Cervical Vertebra D	Cervical Vertebra E
VMNH2828	0.54				
04-23	0.35	0.39	0.36	0.3	0.27
YPM7541B	0.44	0.5			

TABLE 32. Length measurements of cervical vertebrae of unknown articulation. Here each vertebra is labeled arbitrarily with a letter.

Specimen	Dorsal Vertebra A	Dorsal Vertebra B	Dorsal Vertebra C	Dorsal Vertebra D	Dorsal Vertebra E	Dorsal Vertebra F
Lot 30.251	0.75	0.7	0.64	0.62	0.5	
VMNH973	0.45	0.41	0.35			
Lot 30.759	0.33	0.3	0.27	0.26	0.3	0.27

TABLE 33. Length measurements of dorsal vertebrae of unknown articulation. Here each vertebra is labeled arbitrarily with a letter.

Specimen	Caudal Vertebra A	Caudal Vertebra B	Caudal Vertebra C	Caudal Vertebra D	Caudal Vertebra E	Caudal Vertebra F	Caudal Vertebra G	Caudal Vertebra H	Caudal Vertebra I	Caudal Vertebra J	Caudal Vertebra K	Caudal Vertebra L	Caudal Vertebra M	Caudal Vertebra N
VMNH2828	0.51	0.5	0.44	0.45	0.44	0.43								
Lot 30.235-20	0.6	0.63	0.58	0.58	0.56	0.59	0.55							
LOT 30.143	0.56													
Lot 30.277-247	0.41													
04-35	0.26	0.27	0.25	0.33										
30.715	0.33													
Lot 30.245	0.41	0.42												
ws-0249	0.57	0.54	0.5	0.5	0.54	0.58								
Lot 30.624	0.42	0.47	0.38	0.47	0.45	0.47	0.48	0.43	0.41	0.5	0.38	0.36	0.37	0.37
VMNH986	0.34	0.39	0.33	0.38	0.37	0.31	0.33	0.38	0.32					
04-25	0.39	0.33												
X5	0.42	0.47	0.63											
VMNH965	0.59	0.55	0.56	0.6	0.61	0.59	0.61	0.59	0.53	0.57	0.51			
WS02-113	0.61													
Lot 30.767	0.39	0.33	0.29	0.28	0.3	0.31	0.26							
VMNH3238	0.49	0.48	0.47	0.49	0.53									
VMNH3228	0.48													
Lot 30.235-8	0.54	0.56												

TABLE 34. Length measurements of caudal vertebrae of unknown articulation. Here each vertebra is labeled arbitrarily with a letter.

Specimen	Caudal A Rib Length Average	Caudal B Rib Length Average	Caudal C Rib Length Average	Caudal D Rib Length Average	Caudal E Rib Length Average
04-27	0.47				
Lot 30.277-247	0.34				
04-35	0.54	0.59	0.64	0.69	
30.715	0.58				
Lot 30.245	0.51	0.51			
WS-0249		0.59	0.61	0.62	0.55
X5	0.7	0.54	0.66		
WS02-113	0.77				
VMNH3238	0.9	0.75	0.79	0.7	0.57
VMNH3228	0.83	0.82			
Lot 30.235-8	0.6	0.51			

TABLE 35. Averaged length measurements of ribs on caudal vertebrae of unknown articulation. Here each rib average is assigned a letter that corresponds to the letter of that specimen's vertebra in Table 34.

Specimen	Humerus or Femur Length	Humerus or Femur End 1 Width	Humerus or Femur End 2 Width	Humerus or Femur Aspect Ratio	Forearm or Foreleg Bone Length	Unknown Long Bone Length	Scapula
Lot 30.235-21	1.77	0.3	0.37	0.1892655	0.7		
	2.5	0.3	0.23	0.106			
Lot 30.235-20					1.08		
Lot 30.143					0.89		
FN17A3B3	2.28	0.48	0.32	0.1754386			
FN17A2B2					0.86		
VMNH975	2.54	0.34	0.26	0.1181102			
	2.53	0.31	0.45	0.1501976			
Lot 30.270					0.38		
Lot 30.759	2.61	0.32	0.29	0.1168582			
Lot 30.245	2.32	0.18	0.33	0.1099138		1.26	
	2.74	0.3	0.42	0.1313869		1.67	
VMNH3235	2.17	0.2	0.34	0.124424		0.65	
						1.93	
						1.64	
VMNH999	1.88	0.31	0.36	0.1781915			
FN17A4&17B4	2.89	0.37	0.34	0.1228374		1.18	
Lot 30.624	2.06	0.22	0.2	0.1019417			
8-31X	2.21	0.29	0.39	0.1538462			
WS02--113	2.09	0.22	0.37	0.1411483			
Lot 30.755	2.14	0.28	0.38	0.1542056			
VMNH1001	2.66					2.07	
	2.47						
Lot 30.756	2.55	0.28	0.29	0.1117647			
04-22	2.54	0.41	0.37	0.1535433			
Lot 30.235-3	2.43	0.49	0.3	0.1625514		1.19	

TABLE 36. Length measurements of appendicular long bones of unknown articulation. Here each long bone is arbitrarily labeled with a letter.

TABLE 36 (cont'd)

Lot 30.235-5	1.98	0.23	0.3	0.1338384	1.03	1.03	
Lot 30.235-9	2.45	0.35	0.47	0.1673469		1.08	
Lot 30.235-A/B	1.99	0.43	0.41	0.2110553			
Lot 30.235-50	1.77	0.21	0.32	0.1497175			
Lot 30.235-53	1.73	0.24	0.26	0.1445087			
Lot 30.235-54	1.98	0.35	0.26	0.1540404			
Lot 30.235-55	2.1	0.36	0.35	0.1690476		1.08	
Lot 30.235-56					1.24		
Lot 30.235-57	1.88	0.44	0.44	0.2340426	0.84		
Lot 30.249						1.23	
Lot 30.237						0.46	
Lot 30.256						1.84	
Lot 30.259						2.02	
VMNH1000						2.04	
VMNH3227						1.29	
VMNH3226						1.59	
VMNH3223						1.16	
Lot 30.246						0.97	
Lot 30.282						2.82	
Lot 30.314						0.85	
Lot 30.294						1.58	
Lot 30.647						2.06	
VMNH3219						1.4	
Lot 30.716						1.41	
Lot 30.398						0.76	
						2.52	
FN17A1&B1						1.35	
						1.38	
VMNH978						0.65	
VMNH979						1.62	
WS02--41						0.9	
Lot 30.266							0.93
VMNH3222						1.05	
Lot 30.315						1.8	
						1.33	
Lot 30.753						1.83	
VMNH3234						1.34	
						1.02	
Lot 30.235-4						1.14	
Lot 30.235-8						1.23	
Lot 30.235-71						1.75	
Lot 30.235-34						1.22	
Lot 30.235-47						1.48	
Lot 30.235-58						0.66	

APPENDIX C

CHARACTERS USED IN THE CLADISTIC ANALYSIS

NOTE: Characters 1 through 46 are from Benton and Allen (1997), characters 47 through 96 are from Jalil (1997), characters 97 through 201 are from Dilkes (1998), and the remaining character is novel and has been created for this publication's analysis. Characters from different publications have been combined and/or modified where appropriate.

1. Dorsomedial process of premaxilla: extends between middle of narial openings (0); reduced to anterior portion of narial openings (1).
2. Relative length of nasals and frontals: nasals shorter than frontals (0); nasals longer than frontals (1)
3. Fronto-parietal suture: interdigitating (0); straight (1).
4. Pineal Foramen: present and large (0); small or absent (1).
5. Lacrimal contact with nasal: present (0); absent (1).
6. Lacrimal extent: element runs forward from orbit (0); restricted to orbital rim in lateral view (1).
7. Postfrontal dimensions: substantial tripartite element (0); short element lacking clear processes (1).
8. Posterior processes of postorbital: does not extend beyond the back of lower temporal fenestra (0); extends back beyond the posterior margin of the lower temporal fenestra (1).
9. Ventral ramus of squamosal: present extending below quadrate head (0); reduced and cotyle formed for quadrate head (1).
10. Posterior process of jugal: present (0); reduced and spur-like (1); absent (2).
11. Quadratojugal shape (complete lower temporal bar): low with anterior process (0); tall with reduced anterior process (1).
12. Quadratojugal: present (0); absent (1).
13. Supratemporal: present (0); absent (1).
14. Relative positions of posterior terminations of tooth rows: posterior dentary teeth lie level with or behind posterior maxillary teeth (0); posterior dentary teeth lie anterior to posterior maxillary teeth (1).
15. Numbers of premaxillary teeth on each side: seven or fewer (0); more than seven (1).
16. Pterygoid flange teeth: present (0); absent (1).
17. Numbers of cervical vertebrae: seven or fewer (0); eight or nine (1); ten or eleven (2); twelve or more (3).
18. Averaged relative length of mid and posterior (second half) cervical and dorsal vertebral centra: cervical centra subequal in length to dorsals' (0); cervical centra longer than dorsals' (1).
19. Cervical neural spine shape: short (parallel to centrum) and tall (0); long and low (1).
20. Ovoid spine-table on top of neural spine: absent (0); present (1).
21. Cervical ribs: short and stout (0); long and slender (1).
22. Neural spines of dorsal vertebrae: short and slender (0); tall and rectangular (1).
23. Trunk intercentra: present (0); absent (1).
24. Attachment of ribs to posterior dorsal vertebrae: not fused (0); fused (1).
25. Scapula size: larger than coracoid (0); subequal in size to coracoid (1).

26. Entepicondylar groove or foramen in humerus: present (0); absent (1).
27. Radius length relative to humerus: radius 80%-90% length of humerus (0); radius 40%-65% length of humerus (1).
28. Intermedium in carpus: present (0); absent (1).
29. Centralia in manus: present (0); absent (1).
30. First distal carpal: present (0); absent or fused (1).
31. Relative length of metacarpals III and IV: metacarpal III shorter than IV (0); metacarpal III equal in length to or longer than IV (1).
32. Relative lengths of metacarpals I and V: shorter than metacarpals II and IV (0); similar in length to metacarpals II and IV (1).
33. Ilium length relative to ischium: ilium is longer (0); ilium is equal or shorter (1).
34. Preacetabular buttress on ilium: absent or insignificant (0); well-developed (1).
35. Thyroid foramen in pelvis: absent (0); present (1).
36. Pubis shape: broad (0); narrow and waisted (1).
37. Femur shape: sigmoidal (0); straight (1).
38. Length of tibia relative to length of femur: tibia shorter than or subequal to femur (0); tibia longer than femur (1).
39. Foramen in ankle between astragalus and calcaneum: present (0); absent (1).
40. Lateral calcaneal tuber: absent (0); present (1).
41. Pes centrale: present (0); absent (1).
42. First distal tarsal: present (0); absent (1).
43. Second distal tarsal: present (0); absent (1).
44. Relative lengths of metatarsals IV and V: metatarsal IV less than 300% length metatarsal V (0); metatarsal IV more than 300% length of metatarsal V (1).
45. Metatarsal V shape: L-shaped (0); symmetrical and very short (1).
46. Postcloacal (heterotopic) bones: absent (0); present (1).
47. Prefrontal-nasal suture: oriented anteroposteriorly parallel to internasal suture (0); anterolaterally directed (1).
48. Tabular: present (0); absent (1).
49. Postparietal: large (0); small (1); absent (2).
50. Ventral flange of squamosal narrow or confined to dorsal half of lower temporal fenestra: unconfined (0); confined (1)
51. Quadrate: not emarginated (0); or emarginated (1).
52. Stapedial foramen: present (0); absent (1).
53. Paroccipital process-suspensorium contact: weak (0); strong (1).
54. Retroarticular process development: poorly developed (0); well development (1).
55. Cleithrum: present (0); absent (1).
56. Lateral centrale of manus: present (0); small or absent (1).
57. Fifth distal tarsal: present (0); absent (1).
58. Metatarsal V shape: straight (0); hooked (1).
59. Lower temporal arcade: complete (0); incomplete (1).
60. Lacrimal: size is 50% or larger than the size of nasals (0); size is less than 50% that of the nasals (1).
61. Prominent lateral conch on quadrate: absent (0); present (1).
62. Lateral exposure of angular: large (~50% area of lower jaw) (0); restricted (1).
63. Retroarticular process entirely formed by articular: no (0); yes (1).

64. Anterior five dorsal ribs holocephalous: no (0); yes (1).
65. Intervertebral articulation formed by zygosphenes-zygantrum: no (0); yes (1).
66. Ectepicondylar foramen: absent (0); present (1).
67. Fourth distal tarsal has dorsal process fitting into recess on astragalocalcaneum: no (0); yes (1).
68. Premaxilla has well-developed posterodorsal process: no (0); yes (1).
69. External naris elongated anteroposteriorly and close to midline: no (0); yes (1).
70. Quadratojugal L-shaped and/or situated behind upper temporal fenestra: no (0); yes (1).
71. Posterior process of jugal extending posteriorly nearly to the back of skull: no (0); yes (1).
72. Vertebrae of adult: notochordal (0); non-notochordal (1).
73. Cervical ribs dicephalous: no (0); yes (1).
74. Transverse processes of trunk vertebrae development: poorly developed (0); well developed (1).
75. Medial centrale in carpus: present (0); absent (1).
76. Concavo-convex astragalo-calcaneal articulation: no (0); yes (1).
77. Cervical ribs with anterior process: no (0); yes (1).
78. Skull low and narrow with short and narrow postorbital region: no (0); yes (1).
79. Quadratojugal (if present) reduced and situated behind lower temporal fenestra: no (0); yes (1).
80. Tapering cervical ribs oriented posteriorly parallel to neck axis: no (0); yes (1).
81. Scapula high and narrow: no (0); yes (1).
82. Low sublunate scapula: no (0); yes (1).
83. Ilium with reduced contribution in acetabulum: no (0); yes (1).
84. Nasal tapering anteromedially: no (0); yes (1).
85. Number of ossified tarsals: more than five (0); five or fewer (1).
86. Pedal centrale: present (0); absent (1).
87. Ventral flange of squamosal: not reduced (0); reduced (1).
88. Perforating foramen in ankle: present (0); absent (1).
89. Teeth recurved and laterally compressed: no (0); yes (1).
90. Long and narrow snout: no (0); yes (1).
91. Post-temporal fenestra: large (0); small or absent (1).
92. Occipital condyle anterior to craniomandibular joint: no (0); yes (1).
93. Parasphenoid-basisphenoid in side wall of braincase: no (0); yes (1).
94. Pila antotica: absent (0); present (1).
95. Crista prootica: absent (0); present (1).
96. First phalanx of digit V of pes as long as metacarpals I-IV: no (0); yes (1).
97. Dimensions of skull: midline length greater than maximum width (0); midline length less than maximum width (1).
98. Relative length of snout: 550% of total skull length (0); 550% of total skull length (1).
99. Upper temporal fenestra: oval in outline and not elongated caudally (0); elongated caudally with inner surface of parietal and squamosal facing dorsally (1).
100. Lower temporal fenestra: present and closed ventrally (0); present and open ventrally (1); absent (2).
101. Antorbital fenestra: absent (0); present (1).
102. Shape of premaxilla: horizontal ventral margin (0); down-turned ventral margin (1).

103. Premaxilla and prefrontal: no contact (0); contact present (1).
104. Shape of maxillary ramus of premaxilla: contributes only to ventral border of external naris (0); extends as a posterodorsal process to form caudal border of external naris (1).
105. External nares: separate (0); single, medial naris (1).
106. External nares shape: rounded (0); elongate (1).
107. Shape of cranial margin of nasal at midline: strongly convex with anterior process (0); transverse with little convexity (1).
108. Septomaxilla: present (0); absent (1).
109. Maxilla: horizontal ventral margin (0); convex ventral margin (1).
110. Form of suture between premaxilla and maxilla above dentigerous margin: simple vertical or diagonal contact (0); notch present in maxilla (1).
111. Ratio of lengths of frontals to parietals: >1.0 (0); ≤ 1.0 (1).
112. Shape of dorsal surface of frontal next to sutures with postfrontal and parietal: flat to slightly concave (0); longitudinal depression with deep pits is present (1).
113. Shape of dorsal surface of postfrontal: flat or slightly concave towards raised orbital rim (0); depression present with deep pits (1).
114. Postorbital and parietal contact: present (0); absent (1).
115. Ratio of lengths of anteroventral and posterodorsal processes of postorbital: >1.0 (0); <1.0 (1).
116. Postfrontal: excluded from upper temporal fenestra (0); entering upper temporal fenestra (1).
117. Median contact of parietals: suture present (0); parietals fused with loss of suture (1).
118. Parietal table: broad (0); constricted without sagittal crest (1); sagittal crest present (2).
119. Parapineal foramen: present (0); absent (1).
120. Shape of median border of parietal: level with skull table (0); drawn downwards to form ventrolateral flange (1).
121. Subtemporal process of jugal: robust with height 450% of length (0); slender with height 550% of length (1).
122. Lateral surface of jugal above maxilla: continuous (0); lateral shelf present (1).
123. Anteroventral process of squamosal: broad ventrally with distal width that is approximately equal to dorsoventral height (0); narrow ventrally with distal width less than dorsoventral height (1); absent (2).
124. Quadrate: covered laterally (0); exposed laterally (1).
125. Contact between vomer and maxilla: absent (0); present (1).
126. Contact between ectopterygoid and jugal: restricted with area of contact approximately equal to or less than contact between ectopterygoid and pterygoid (0); ectopterygoid expanded caudally (1).
127. Contact between ectopterygoid and maxilla: absent (0); or present (1).
128. Elements contributing to lateral border of suborbital fenestra: ectopterygoid, palatine and maxilla (0); ectopterygoid and palatine contact to exclude maxilla (1).
129. Shape of ectopterygoid along suture with pterygoid: transversely broad (0); posteroventrally elongate and does not reach lateral corner of transverse flange (1); posteroventrally elongate and reaches corner of transverse flange (2).
130. Orientation of basipterygoid processes: anterolateral (0); lateral (1).
131. Parasphenoid teeth: present (0); absent (1).

132. Foramen for entrance of internal carotid arteries: lateral wall of braincase (0); ventral surface of parasphenoid (1).
133. Club-shaped ventral ramus of opisthotic: absent (0); present (1).
134. Anterior inferior process of prootic: absent (0); present (1).
135. Abducens foramina: in dorsum sella (0); between prootic and dorsum sella (1).
136. Laterosphenoid: absent (0); present (1).
137. Paroccipital process: ends freely (0); reaches suspensorium (1)
138. Supraoccipital: plate-like (0); pillar-like (1).
139. Tooth implantation: subthecodont (0); ankylothecodont (1); pleurodont (2).
140. Caniniform teeth: present (0); absent (1).
141. Serrated teeth: absent (0); present (1).
142. Maxillary tooth plate: absent (0); present (1).
143. Number of tooth rows on maxilla: single row (0); multiple rows (1).
144. Number of grooves on maxilla: none (0); one (1); two (2).
145. Location of maxillary teeth: only on occlusal surface (0); on occlusal and lingual surfaces (1).
146. Number of tooth rows on dentary: one (0); two (1); more than two (2).
147. Jaw occlusion: Single-sided overlap (0); flat occlusion (1); blade and groove (2).
148. Vomerine teeth: present (0); absent (1).
149. Palatine teeth: present (0); absent (1).
150. Teeth on palatine ramus of pterygoid: present in two fields (0); present in one field (1); present in three fields (2); absent (3).
151. Teeth on transverse flange of pterygoid: single row (0); multiple rows (1); absent (2).
152. Depth of lower jaw measured at maximum height of adductor fossa relative to length of jaw from tip to articular: <25% (0); >25% (1).
153. Jaw symphysis: formed largely or wholly by dentary (0); formed only by splenial (1).
154. Divergence of dentaries cranial to symphysis: absent (0); present (1).
155. Dentary-coronoid-surangular profile: horizontal to convex (0); concave caudal to coronoid (1).
156. Uprturned retroarticular process: absent (0); present (1).
157. Lateral mandibular fenestra: absent (0); present (1)
158. Neural arches of mid-dorsals: shallowly excavated (0); deeply excavated (1).
159. Second sacral rib: not bifurcate (0); bifurcate with caudal process pointed bluntly (1); bifurcate with caudal process truncated sharply (2).
160. Proximal caudal neural spine height: moderately tall with height/length >1.0 and <2.0 (0); low with height/length <1.0 (1), tall with height/length >2.0 and <3.0 (2); very tall with height/length >3.0 (3).
161. Ratio of lengths of caudal transverse processes and centra: ≤1.0 (0); >1.0 (1).
162. Proximal caudal ribs: recurved (0); project laterally (1).
163. Distal width of haemal spine: equivalent to proximal width (0); tapering (1); wider than proximal width (2).
164. Gastralia: absent (0); present (1).
165. Coracoid process: small (0); large (1).
166. Clavicular shape: broad proximally (0); narrow proximally (1).
167. Interclavicle proximal shape: broad diamond (0); gracile anchor (1).

168. Cranial margin of interclavicle: smoothly convex (0); notch present between clavicles (1).
169. Caudal stem of interclavicle: little change in width along entire length (0); expansion present (1).
170. Acetabulum: elongate (0); circular (1).
171. Dorsal margin of ilium: posterior process only (0); large posterior process and smaller anterior process (1); equally developed anterior and posterior processes (2); large anterior projection (3).
172. Processus lateralis: present (0); absent (1).
173. Anterior apron of pubis: absent (0); present (1).
174. Femoral humeral ratio of lengths: 1:1 (0); femur > humerus (1).
175. Femoral distal surfaces: unequal (0); equal (1).
176. Relative proportions of femur: distal width/total length ≤ 0.3 (0); distal width/total length > 0.3 (1).
177. Number of proximal tarsals in a transverse row: two consisting of astragalus and calcaneum (0); three consisting of astragalus, calcaneum and centrale (1).
178. Centrale: present and does not contact tibia (0); present and contacts tibia (1).
179. Centrale: present and contacts distal tarsal 4 (0); present and does not contact distal tarsal 4 (1).
180. Fifth distal tarsal: present (0); absent (1).
181. Ratio of lengths of metatarsals I and IV: ≥ 0.4 (0); < 0.4 and ≥ 0.3 (1); < 0.3 (2).
182. Ratio of lengths of digits 3 to 4: ≤ 0.8 (0); > 0.8 and < 0.9 (1); ≥ 0.9 (2).
183. Prefrontals: separate along midline (0); meet along midline (1).
184. Pterygoids: join cranially (0); remain separate (1).
185. Symphysis: small (0); extended caudally (1).
186. First caudal: separate from sacrum (0); incorporated in to sacrum (1).
187. Caudal zygapophysis: inclined (0); nearly or fully vertical (1).
188. Basicranial joint: metakinetic (0); fused (1).
189. Neurocentral sutures: closed in adult (0); open in adult (1).
190. Sacral and caudal ribs: fused to centra (0); unfused (1).
191. Odontoid prominence on atlas pleurocentrum: absent (0); present (1).
192. Cranial margin of cervical neural arch: straight (0); notched to form overhang (1).
193. Shape of astragalus: L-shaped with broad base (0); elongate (1).
194. Crown of marginal teeth: single point (0); tricuspid (1).
195. Lumbar region: not differentiated (0); ribs of last few presacrals project laterally and are not expanded (1); ribs of last few presacrals fused or lost, project laterally and are not expanded distally (2).
196. Distal ends of caudal neural spines: not expanded (0); expanded (1).
197. Distal ends of first five to six dorsal neural spines: not expanded (0); expanded (1).
198. Curvature of haemal spines: no curvature (0); cranial curvature present (1).
199. Suture between ectopterygoid and pterygoid: simple overlap of ectopterygoid and pterygoid (0); complex overlap between ectopterygoid and pterygoid (1).
200. Pubic apron on ilium: absent (0); present (1).
201. Scapula and coracoid: fused together (0); not fused together (1).

APPENDIX D

MATRIX OF CHARACTER STATES USED IN THE CLADISTIC ANALYSES

	1	2	3	4	5	6	7
<i>Petrolacosaurus</i>	0	0	0	0	0	0	0
<i>Amotosaurus</i>	?	?	?	?	?	?	?
<i>Boreopricea</i>	?	1	1	?	0	0	0
<i>Cosesaurus</i>	?	?	?	?	?	?	?
<i>Czatkowiella harae</i>	1	1	0	1	0	0	1
<i>Dinocephalosaurus</i>	0	1	1	1	1	0	1
<i>Drepanosaurus</i>	?	?	?	?	?	?	?
<i>Eudimorphohodon</i>	?	?	?	?	?	?	?
<i>Euparkeria</i>	0	1	0	1	1	1	0
<i>Herrerasaurus</i>	0	1	0	1	0	0	?
<i>Hypuonector</i>	?	?	?	?	?	?	?
<i>Jesairosaurus</i>	?	?	0	?	?	?	1
<i>Kadimakara</i>	?	1	0	0	0	0	0
<i>Langobardisaurus</i>	0	0	?	1	0	0	1
<i>Macrocnemus bassanii</i>	0	0	0	0	1	0	0
<i>Malerisaurus langstoni</i>	?	?	?	0	?	?	?
<i>Malerisaurus robinsonae</i>	0	0	0	1	0	1	1
<i>Marasuchus</i>	?	?	?	?	?	?	?
<i>Megalancosaurus</i>	0	0	0	?	?	0	?
<i>Prolacerta</i>	1	1	0	0	0	0	0
<i>Prolacertoides</i>	?	1	?	?	0	0	?
<i>Proterosuchus</i>	0	1	0	1	0	0	1
<i>Protorosaurus</i>	0	1	?	0	0	0	0
<i>Rhynchosaurus</i>	0	0	0	0	1	0	0
<i>Scleromochlus</i>	0	1	0	1	0	?	?
<i>Tanystropheus longobardicus</i>	1	0	0	0	1	1	1
<i>Tanystropheus meridensis</i>	1	1	0	0	1	1	1
<i>Tanytrachelos</i>	0	1	0	1	0	1	1
<i>Trachelosaurus</i>	?	?	?	?	?	?	?
<i>Trilophosaurus</i>	0	0	0	1	?	?	0
<i>Vallesaurus</i>	0	1	0	1	0	1	0
<i>Youngina</i>	0	1	0	0	0	0	0

TABLE 37. Matrix of the character states used in the cladistic analysis of Protorosauria and selected archosauromorphs. Characters 1 through 46 are from Benton and Allen (1997), characters 47 through 97 are from Jalil (1997), characters 98 through 200 are from Dilkes (1998), and character 201 is novel.

TABLE 37 (cont'd)

	8	9	10	11	12	13	14	15	16	17	18
<i>Petrolacosaurus</i>	0	0	0	0	0	0	0	0	0	0	0
<i>Amotosaurus</i>	?	?	2	?	?	?	?	?	0	1	?
<i>Boreopricea</i>	0	1	0	1	0	0	1	?	?	1	0
<i>Cosesaurus</i>	?	1	0	1	0	?	0	1	?	1	1
<i>Czatkowiella harae</i>	0	0	0	?	0	0	?	0	1	?	1
<i>Dinocephalosaurus</i>	0	1	2	?	1	1	0	0	1	3	1
<i>Drepanosaurus</i>	?	?	?	?	?	?	?	?	?	?	?
<i>Eudimorphohodon</i>	?	?	0	?	?	?	?	0	?	0	?
<i>Euparkeria</i>	0	1	0	1	1	1	0	0	0	?	0
<i>Herrerasaurus</i>	1	1	0	0	0	1	1	0	1	?	0
<i>Hypuronector</i>	?	?	?	?	?	?	?	?	?	?	?
<i>Jesairosaurus</i>	0	0	1	?	1	0	?	?	?	1	?
<i>Kadimakara</i>	0	1	0	1	0	0	1	1	1	?	?
<i>Langobardisaurus</i>	0	?	?	?	?	?	1	0	?	1	1
<i>Macrocnemus bassanii</i>	0	0	1	1	0	0	0	1	0	1	1
<i>Malerisaurus langstoni</i>	?	?	0	?	?	?	?	?	?	1	1
<i>Malerisaurus robinsonae</i>	0	0	0	0	0	1	0	0	0	1	1
<i>Marasuchus</i>	?	?	?	?	?	?	?	?	?	1	?
<i>Megalancosaurus</i>	?	0	1	?	?	?	0	0	?	1	1
<i>Prolacerta</i>	0	0	1	1	0	0	1	1	0	1	1
<i>Prolacertoides</i>	?	?	?	?	?	?	?	?	1	?	?
<i>Proterosuchus</i>	0	0	0	1	0	0	1	0	0	1	0
<i>Protorosaurus</i>	0	1	?	?	?	1	0	0	0	0	1
<i>Rhynchosaurus</i>	0	0	0	0	0	0	0	0	0	0	0
<i>Scleromochlus</i>	0	1	0	?	?	1	?	0	?	1	0
<i>Tanystropheus longobardicus</i>	0	1	0	?	1	0	0	0	0	3	1
<i>Tanystropheus meridensis</i>	0	1	0	?	1	0	0	0	0	?	?
<i>Tanytrachelos</i>	1	1	0	?	?	?	0	0	?	3	1
<i>Trachelosaurus</i>	?	?	0	1	1	1	1	1	1	2	1
<i>Trilophosaurus</i>	0	0	0	?	0	?	0	0	1	0	0
<i>Vallesaurus</i>	0	?	?	?	?	1	0	?	?	1	?
<i>Youngina</i>	1	0	0	0	0	0	1	0	0	0	0

TABLE 37 (cont'd)

	19	20	21	22	23	24	25	26	27	28	29
<i>Petrolacosaurus</i>	0	0	0	0	0	0	0	0	0	0	0
<i>Amotosaurus</i>	1	0	1	1	1	?	1	?	?	?	?
<i>Boreopricea</i>	1	?	?	1	?	0	0	0	0	?	?
<i>Cosesaurus</i>	1	?	1	1	1	0	1	?	0	?	?
<i>Czatkowiella harae</i>	1	1	1	0	1	0	?	0	?	?	?
<i>Dinocephalosaurus</i>	1	0	1	1	1	0	?	1	1	0	0
<i>Drepanosaurus</i>	?	?	?	1	1	?	0	?	1	?	?
<i>Eudimorphohodon</i>	?	?	?	?	1	?	0	1	0	?	?
<i>Euparkeria</i>	0	1	1	1	0	?	0	1	?	?	?
<i>Herrerasaurus</i>	0	1	?	1	0	?	0	1	0	1	0
<i>Hypuronector</i>	?	?	?	0	1	1	1	?	1	?	?
<i>Jesairosaurus</i>	1	?	?	1	1	1	0	0	?	?	?
<i>Kadimakara</i>	?	?	?	?	?	?	?	?	?	?	?
<i>Langobardisaurus</i>	1	?	0	0	0	0	1	1	1	0	0
<i>Macrocnemus bassanii</i>	1	1	1	1	1	1	0	1	0	0	0
<i>Malerisaurus langstoni</i>	1	?	?	1	1	0	0	0	0	?	?
<i>Malerisaurus robinsonae</i>	1	1	?	1	1	0	0	0	0	?	?
<i>Marasuchus</i>	0	0	?	1	1	?	0	?	0	?	?
<i>Megalancosaurus</i>	1	0	?	1	?	1	0	1	1	0	0
<i>Prolacerta</i>	1	1	1	1	0	0	0	0	0	0	0
<i>Prolacertoides</i>	?	?	?	?	?	?	?	?	?	?	?
<i>Proterosuchus</i>	0	1	1	1	?	1	0	?	0	?	?
<i>Protorosaurus</i>	1	0	1	1	0	0	0	0	0	0	0
<i>Rhynchosaurus</i>	0	0	0	0	1	0	0	0	0	0	0
<i>Scleromochlus</i>	1	0	0	1	1	?	1	?	0	?	?
<i>Tanystropheus longobardicus</i>	1	1	1	0	1	1	1	0	1	1	1
<i>Tanystropheus meridensis</i>	1	?	1	?	1	?	?	?	?	?	?
<i>Tanytrachelos</i>	1	0	0	1	1	0	1	1	1	1	1
<i>Trachelosaurus</i>	1	1	1	1	1	0	?	?	?	?	?
<i>Trilophosaurus</i>	0	0	0	1	0	0	0	0	1	0	0
<i>Vallesaurus</i>	0	0	?	1	1	1	?	1	?	0	?
<i>Youngina</i>	0	0	0	0	0	0	0	0	0	0	0

TABLE 37 (cont'd)

	30	31	32	33	34	35	36	37	38	39	40
<i>Petrolacosaurus</i>	0	0	0	0	0	0	0	0	0	0	0
<i>Amotosaurus</i>	?	?	?	1	1	0	1	?	?	0	?
<i>Boreopricea</i>	?	1	0	?	?	?	?	0	0	1	1
<i>Cosesaurus</i>	?	1	0	0	?	?	0	0	0	1	0
<i>Czatkowiella harae</i>	?	?	?	?	1	?	?	?	?	?	?
<i>Dinocephalosaurus</i>	1	1	0	?	?	1	0	0	0	0	0
<i>Drepanosaurus</i>	?	1	1	1	0	1	1	1	0	0	1
<i>Eudimorphohodon</i>	?	1	1	?	?	?	?	0	1	?	?
<i>Euparkeria</i>	?	1	0	1	0	1	1	0	0	1	0
<i>Herrerasaurus</i>	0	?	?	1	1	1	1	0	0	?	0
<i>Hypuonector</i>	?	1	0	0	1	?	0	1	0	?	?
<i>Jesairosaurus</i>	?	?	?	?	1	?	0	1	?	?	?
<i>Kadimakara</i>	?	?	?	?	?	?	?	?	?	?	?
<i>Langobardisaurus</i>	0	1	0	?	?	1	?	0	0	1	1
<i>Macrocnemus bassanii</i>	0	0	0	0	1	1	1	0	1	0	0
<i>Malerisaurus langstoni</i>	?	?	?	0	1	0	0	0	0	?	?
<i>Malerisaurus robinsonae</i>	?	?	?	0	1	0	0	0	0	1	1
<i>Marasuchus</i>	?	?	?	1	1	1	1	0	1	1	0
<i>Megalancosaurus</i>	0	1	1	0	1	1	0	1	0	0	1
<i>Prolacerta</i>	0	0	0	0	1	0	0	0	1	0	1
<i>Prolacertoides</i>	?	?	?	?	?	?	?	?	?	?	?
<i>Proterosuchus</i>	?	0	?	1	1	1	1	1	0	0	1
<i>Protorosaurus</i>	0	1	0	?	0	0	0	0	0	0	1
<i>Rhynchosaurus</i>	1	1	0	1	0	0	0	1	0	0	0
<i>Scleromochlus</i>	?	1	1	1	0	?	1	0	1	?	?
<i>Tanystropheus longobardicus</i>	1	1	0	1	0	1	1	0	0	0	0
<i>Tanystropheus meridensis</i>	?	?	?	?	?	?	?	?	?	?	?
<i>Tanytrachelos</i>	1	1	0	1	0	0	1	1	0	0	?
<i>Trachelosaurus</i>	?	?	?	?	1	?	?	0	?	?	?
<i>Trilophosaurus</i>	0	0	0	0	1	0	0	0	0	0	1
<i>Vallesaurus</i>	?	1	0	?	?	1	0	1	0	?	?
<i>Youngina</i>	0	0	0	1	1	0	0	0	0	0	0

TABLE 37 (cont'd)

	41	42	43	44	45	46	47	48	49	50	51
<i>Petrolacosaurus</i>	0	0	0	0	0	0	0	0	0	0	0
<i>Amotosaurus</i>	1	1	0	1	1	?	?	?	?	?	?
<i>Boreopricea</i>	0	?	?	0	0	?	1	?	?	1	1
<i>Cosesaurus</i>	0	1	1	1	1	?	?	?	?	1	?
<i>Czatkowiella harae</i>	?	?	?	?	?	?	?	?	?	?	?
<i>Dinocephalosaurus</i>	1	1	1	0	1	0	?	?	?	?	?
<i>Drepanosaurus</i>	0	0	0	0	1	0	?	?	?	?	?
<i>Eudimorphohodon</i>	?	?	?	?	?	0	?	?	?	?	?
<i>Euparkeria</i>	1	1	1	0	0	0	0	1	2	1	0
<i>Herrerasaurus</i>	1	1	1	0	1	0	0	1	2	0	0
<i>Hypuonector</i>	?	?	?	?	?	?	?	?	?	?	?
<i>Jesairosaurus</i>	?	?	?	?	?	?	?	1	2	1	1
<i>Kadimakara</i>	?	?	?	?	?	?	?	?	?	?	?
<i>Langobardisaurus</i>	0	?	?	1	1	0	?	?	?	?	?
<i>Macrocnemus bassanii</i>	0	0	1	1	0	0	?	1	1	1	1
<i>Malerisaurus langstoni</i>	?	?	?	?	?	?	?	?	?	?	0
<i>Malerisaurus robinsonae</i>	1	1	1	0	0	?	?	?	?	?	?
<i>Marasuchus</i>	1	1	1	0	1	0	?	?	?	?	?
<i>Megalancosaurus</i>	0	0	0	0	1	0	?	?	?	0	0
<i>Prolacerta</i>	0	0	0	0	0	0	1	1	2	1	1
<i>Prolacertoides</i>	?	?	?	?	?	?	1	?	?	?	?
<i>Proterosuchus</i>	1	0	0	1	0	0	0	1	2	1	0
<i>Protorosaurus</i>	0	0	0	1	0	0	1	1	2	1	1
<i>Rhynchosaurus</i>	0	0	0	0	0	0	1	1	2	1	1
<i>Scleromochlus</i>	1	0	0	1	0	0	0	?	2	1	?
<i>Tanystropheus longobardicus</i>	1	1	1	1	1	1	1	1	1	1	1
<i>Tanystropheus meridensis</i>	?	?	?	?	?	?	?	1	?	?	1
<i>Tanytrachelos</i>	1	1	1	1	1	1	?	?	?	1	0
<i>Trachelosaurus</i>	?	?	?	?	?	?	?	?	?	?	?
<i>Trilophosaurus</i>	0	0	0	0	0	0	?	?	?	?	0
<i>Vallesaurus</i>	?	0	0	0	1	0	1	1	?	?	?
<i>Youngina</i>	0	0	0	0	0	0	0	0	0	0	0

TABLE 37 (cont'd)

	52	53	54	55	56	57	58	59	60	61	62
<i>Petrolacosaurus</i>	0	0	0	0	0	0	0	0	0	0	0
<i>Amotosaurus</i>	?	?	?	1	?	1	1	?	?	?	?
<i>Boreoprincea</i>	?	?	?	1	?	1	1	1	1	1	0
<i>Cosesaurus</i>	?	?	1	1	?	1	1	?	?	?	?
<i>Czatkowiella harae</i>	?	?	?	?	?	?	?	1	1	0	1
<i>Dinocephalosaurus</i>	?	?	?	?	1	1	0	1	1	0	1
<i>Drepanosaurus</i>	?	?	?	1	?	0	0	?	?	?	?
<i>Eudimorphohodon</i>	?	?	?	1	?	?	?	?	1	?	?
<i>Euparkeria</i>	?	?	1	1	?	1	1	0	1	0	0
<i>Herrerasaurus</i>	1	?	0	1	1	1	0	0	1	0	0
<i>Hypuonector</i>	?	?	?	1	?	?	?	?	?	?	1
<i>Jesairosaurus</i>	?	1	1	1	?	?	?	1	?	?	0
<i>Kadimakara</i>	?	?	?	?	?	?	?	?	?	?	?
<i>Langobardisaurus</i>	?	?	?	?	0	1	1	?	?	?	1
<i>Macrocnemus bassanii</i>	?	?	1	1	?	1	1	1	1	?	0
<i>Malerisaurus langstoni</i>	?	?	?	?	?	?	?	1	?	0	1
<i>Malerisaurus robinsonae</i>	?	?	?	?	?	?	?	1	?	?	0
<i>Marasuchus</i>	?	?	?	1	?	1	0	?	?	?	?
<i>Megalancosaurus</i>	?	?	1	1	0	1	0	?	1	0	1
<i>Prolacerta</i>	1	1	1	1	1	1	1	1	1	0	0
<i>Prolacertoides</i>	?	?	?	?	?	?	?	?	?	?	?
<i>Proterosuchus</i>	1	?	1	1	?	1	1	0	0	0	0
<i>Protorosaurus</i>	1	?	1	?	0	1	1	1	1	0	1
<i>Rhynchosaurus</i>	?	1	1	1	?	1	1	1	1	0	0
<i>Scleromochlus</i>	?	?	1	?	?	1	0	0	?	?	1
<i>Tanystropheus longobardicus</i>	1	1	1	1	1	1	1	1	1	0	1
<i>Tanystropheus meridensis</i>	?	?	1	?	?	?	?	1	1	0	1
<i>Tanytrachelos</i>	?	?	?	1	1	1	1	1	1	?	1
<i>Trachelosaurus</i>	?	?	?	?	?	?	?	?	?	?	?
<i>Trilophosaurus</i>	?	?	?	1	0	1	1	1	?	0	0
<i>Vallesaurus</i>	?	?	0	1	?	1	0	?	1	?	0
<i>Youngina</i>	0	0	0	0	0	0	0	0	0	0	?

TABLE 37 (cont'd)

	63	64	65	66	67	68	69	70	71	72	73
<i>Petrolacosaurus</i>	0	0	0	0	0	0	0	0	0	0	0
<i>Amotosaurus</i>	?	1	?	?	0	?	?	?	0	?	?
<i>Boreopricea</i>	0	?	0	1	0	?	?	0	1	1	1
<i>Cosesaurus</i>	?	?	?	0	?	1	?	?	?	?	?
<i>Czatkowiella harae</i>	0	0	0	0	?	0	0	0	0	1	1
<i>Dinocephalosaurus</i>	0	1	?	0	0	1	1	?	0	1	1
<i>Drepanosaurus</i>	?	1	?	?	0	?	?	?	?	1	?
<i>Eudimorphohodon</i>	?	?	?	?	?	?	?	?	?	1	?
<i>Euparkeria</i>	1	0	0	1	0	0	0	1	0	1	1
<i>Herrerasaurus</i>	1	?	0	1	0	0	0	1	0	1	?
<i>Hypuonector</i>	?	1	?	?	?	?	?	?	?	0	0
<i>Jesairosaurus</i>	?	?	0	1	?	1	?	0	0	0	?
<i>Kadimakara</i>	?	?	?	?	?	?	?	?	?	?	?
<i>Langobardisaurus</i>	?	1	0	0	1	1	1	?	?	1	1
<i>Macrocnemus bassanii</i>	?	0	0	0	0	1	1	?	0	1	1
<i>Malerisaurus langstoni</i>	?	?	0	1	?	?	?	0	0	1	1
<i>Malerisaurus robinsonae</i>	?	?	0	0	?	?	?	0	0	1	1
<i>Marasuchus</i>	?	?	0	?	0	?	?	?	?	?	?
<i>Megalancosaurus</i>	?	0	0	?	0	0	1	0	0	1	?
<i>Prolacerta</i>	0	0	0	0	0	1	1	1	0	1	1
<i>Prolacertoides</i>	?	?	?	?	?	1	?	?	?	?	?
<i>Proterosuchus</i>	1	1	0	?	0	1	1	1	1	1	0
<i>Protorosaurus</i>	1	0	0	?	0	0	1	?	0	1	1
<i>Rhynchosaurus</i>	0	0	0	0	0	0	1	0	1	1	1
<i>Scleromochlus</i>	0	?	?	?	?	0	0	?	1	?	?
<i>Tanystropheus longobardicus</i>	0	1	0	0	0	1	1	0	0	1	1
<i>Tanystropheus meridensis</i>	0	1	?	?	?	1	1	0	0	?	?
<i>Tanytrachelos</i>	?	1	?	0	0	?	?	?	0	1	0
<i>Trachelosaurus</i>	?	?	0	?	?	?	?	?	?	1	?
<i>Trilophosaurus</i>	0	0	0	0	0	1	0	0	0	1	1
<i>Vallesaurus</i>	0	1	0	0	?	1	1	?	0	1	?
<i>Youngina</i>	?	1	0	?	0	0	0	0	0	0	0

TABLE 37 (cont'd)

	74	75	76	77	78	79	80	81	82	83	84
<i>Petrolacosaurus</i>	0	0	0	0	0	0	0	0	0	0	0
<i>Amotosaurus</i>	?	?	0	0	?	?	1	0	1	0	?
<i>Boreopricea</i>	1	?	1	0	0	0	0	0	0	?	0
<i>Cosesaurus</i>	?	?	?	1	1	?	1	?	1	1	?
<i>Czatkowiella harae</i>	0	?	?	1	0	1	1	?	?	0	1
<i>Dinocephalosaurus</i>	0	0	0	1	0	0	1	0	?	0	1
<i>Drepanosaurus</i>	1	1	0	?	?	?	?	0	?	0	?
<i>Eudimorphohodon</i>	1	?	?	?	?	?	?	1	0	?	?
<i>Euparkeria</i>	0	?	0	0	0	1	1	0	0	0	1
<i>Herrerasaurus</i>	0	0	1	?	1	1	0	1	0	0	1
<i>Hypuonector</i>	?	?	?	?	?	?	?	1	0	0	?
<i>Jesairosaurus</i>	1	?	?	?	1	?	1	1	0	0	?
<i>Kadimakara</i>	?	?	?	?	?	1	?	?	?	?	?
<i>Langobardisaurus</i>	1	?	1	1	0	?	1	?	1	0	0
<i>Macrocnemus bassanii</i>	1	1	0	1	1	1	1	0	1	1	1
<i>Malerisaurus langstoni</i>	1	?	?	?	?	0	?	1	0	0	?
<i>Malerisaurus robinsonae</i>	1	?	?	?	?	?	?	1	0	1	?
<i>Marasuchus</i>	1	?	0	?	?	?	?	1	0	0	?
<i>Megalancosaurus</i>	0	0	?	?	1	?	?	1	0	?	0
<i>Prolacerta</i>	1	?	1	1	1	1	1	0	0	0	0
<i>Prolacertoides</i>	?	?	?	?	?	?	?	?	?	?	1
<i>Proterosuchus</i>	1	?	0	0	1	1	1	1	0	0	1
<i>Protorosaurus</i>	1	0	0	1	1	?	1	1	0	0	0
<i>Rhynchosaurus</i>	1	?	1	0	0	1	0	0	0	0	0
<i>Scleromochlus</i>	1	?	0	0	0	?	?	0	0	0	0
<i>Tanystropheus longobardicus</i>	1	1	1	1	1	?	1	0	1	0	1
<i>Tanystropheus meridensis</i>	?	?	?	?	0	?	?	?	?	?	1
<i>Tanytrachelos</i>	1	1	0	1	1	?	1	0	1	0	?
<i>Trachelosaurus</i>	1	?	?	1	?	?	1	?	?	?	?
<i>Trilophosaurus</i>	1	0	1	1	0	0	1	1	0	0	?
<i>Vallesaurus</i>	0	?	0	0	0	?	0	1	0	?	0
<i>Youngina</i>	0	0	0	0	0	0	0	0	0	0	0

TABLE 37 (cont'd)

	85	86	87	88	89	90	91	92	93	94	95
<i>Petrolacosaurus</i>	0	0	0	0	0	0	0	0	0	0	0
<i>Amotosaurus</i>	1	1	?	0	0	?	?	?	?	?	?
<i>Boreopricea</i>	0	0	1	1	0	1	?	1	1	?	?
<i>Cosesaurus</i>	1	1	1	1	?	1	?	?	?	?	?
<i>Czatkowiella harae</i>	?	?	0	?	0	0	?	?	1	0	1
<i>Dinocephalosaurus</i>	1	1	0	?	0	1	0	0	?	?	?
<i>Drepanosaurus</i>	0	1	?	0	?	?	?	?	?	?	?
<i>Eudimorphohodon</i>	?	?	?	?	0	?	?	?	?	?	?
<i>Euparkeria</i>	1	1	0	1	1	0	0	1	1	1	1
<i>Herrerasaurus</i>	1	1	0	?	0	1	0	1	1	0	0
<i>Hypuronector</i>	?	?	?	?	?	?	?	?	?	?	?
<i>Jesairosaurus</i>	?	?	0	?	1	1	?	1	?	?	?
<i>Kadimakara</i>	?	?	1	?	1	?	?	?	?	?	?
<i>Langobardisaurus</i>	1	0	?	0	0	1	?	1	?	?	?
<i>Macrocnemus bassanii</i>	0	0	0	0	1	1	1	?	?	?	?
<i>Malerisaurus langstoni</i>	?	?	?	?	?	1	?	?	?	?	?
<i>Malerisaurus robinsonae</i>	?	?	?	?	?	1	?	1	?	?	?
<i>Marasuchus</i>	1	1	?	1	?	?	?	?	?	?	?
<i>Megalancosaurus</i>	0	0	?	0	1	1	0	?	?	?	?
<i>Prolacerta</i>	0	0	1	0	1	1	1	1	1	1	1
<i>Prolacertoides</i>	?	?	?	?	?	?	?	?	?	?	?
<i>Proterosuchus</i>	0	1	0	0	1	1	0	1	1	0	0
<i>Protorosaurus</i>	0	0	0	0	0	0	0	1	?	?	?
<i>Rhynchosaurus</i>	0	0	1	0	0	0	0	1	1	0	0
<i>Scleromochlus</i>	?	1	?	?	?	1	0	0	?	0	0
<i>Tanystropheus longobardicus</i>	1	1	1	0	0	1	0	1	?	?	1
<i>Tanystropheus meridensis</i>	?	?	?	?	0	1	0	?	?	?	?
<i>Tanytrachelos</i>	1	1	1	0	1	1	?	?	?	?	?
<i>Trachelosaurus</i>	?	?	?	?	?	?	?	?	?	?	?
<i>Trilophosaurus</i>	0	0	1	0	0	0	0	0	1	1	1
<i>Vallesaurus</i>	0	?	?	1	0	0	0	?	?	?	?
<i>Youngina</i>	0	0	0	0	0	1	?	0	0	0	0

TABLE 37 (cont'd)

	96	97	98	99	100	101	102	103	104	105	106
<i>Petrolacosaurus</i>	0	0	0	0	0	0	0	0	0	0	0
<i>Amotosaurus</i>	?	1	1	?	?	?	?	?	0	1	1
<i>Boreopricea</i>	0	0	?	?	1	?	?	?	?	0	?
<i>Cosesaurus</i>	0	1	0	?	?	?	?	?	?	?	?
<i>Czatkowiella harae</i>	?	0	0	0	1	0	0	0	0	0	0
<i>Dinocephalosaurus</i>	0	0	1	0	1	0	0	0	0	0	1
<i>Drepanosaurus</i>	?	?	?	?	?	?	?	?	?	?	?
<i>Eudimorphohodon</i>	?	?	?	?	?	?	?	?	?	?	?
<i>Euparkeria</i>	0	0	1	0	0	1	0	0	1	0	0
<i>Herrerasaurus</i>	0	0	1	0	0	1	1	0	1	0	0
<i>Hypuonector</i>	?	?	?	?	?	?	?	?	?	?	?
<i>Jesairosaurus</i>	?	0	1	0	1	0	0	?	?	?	?
<i>Kadimakara</i>	?	?	?	0	1	0	?	?	?	?	?
<i>Langobardisaurus</i>	1	?	?	0	?	?	0	?	?	?	?
<i>Macrocnemus bassanii</i>	0	0	1	?	1	0	0	0	1	?	1
<i>Malerisaurus langstoni</i>	?	?	?	?	?	?	?	?	?	?	?
<i>Malerisaurus robinsonae</i>	?	0	1	?	?	?	0	?	1	0	1
<i>Marasuchus</i>	0	?	?	?	?	?	?	?	?	?	?
<i>Megalancosaurus</i>	1	0	1	?	?	?	0	?	1	0	1
<i>Prolacerta</i>	1	0	1	0	1	0	0	0	1	0	1
<i>Prolacertoides</i>	?	?	?	?	?	?	?	?	?	?	?
<i>Proterosuchus</i>	0	0	1	0	0	1	1	0	1	0	1
<i>Protorosaurus</i>	0	0	1	0	1	0	0	?	1	0	?
<i>Rhynchosaurus</i>	0	0	0	0	?	0	1	1	1	1	1
<i>Scleromochlus</i>	0	0	0	1	0	1	0	0	1	0	0
<i>Tanystropheus longobardicus</i>	1	0	1	0	1	0	0	0	1	0	1
<i>Tanystropheus meridensis</i>	?	0	1	?	1	0	0	0	0	0	1
<i>Tanytrachelos</i>	1	?	0	?	?	0	?	?	?	?	?
<i>Trachelosaurus</i>	?	?	?	?	?	?	?	?	?	?	?
<i>Trilophosaurus</i>	0	0	0	1	?	0	0	0	1	0	1
<i>Vallesaurus</i>	0	?	0	?	?	0	?	0	1	0	1
<i>Youngina</i>	?	0	0	0	0	0	0	0	0	0	0

TABLE 37 (cont'd)

	107	108	109	110	111	112	113	114	115	116	117
<i>Petrolacosaurus</i>	0	0	0	0	0	0	0	0	0	0	0
<i>Amotosaurus</i>	?	?	1	?	?	?	?	?	?	?	?
<i>Boreopricea</i>	1	?	1	0	0	0	0	0	0	0	0
<i>Cosesaurus</i>	?	?	?	?	?	?	?	?	?	?	?
<i>Czatkowiella harae</i>	?	?	0	0	?	0	0	0	?	?	0
<i>Dinocephalosaurus</i>	0	?	1	0	0	0	0	?	?	1	1
<i>Drepanosaurus</i>	?	?	?	?	?	?	?	?	?	?	?
<i>Eudimorphohodon</i>	?	?	?	?	?	?	?	?	?	?	?
<i>Euparkeria</i>	0	1	0	1	0	0	0	0	0	0	0
<i>Herrerasaurus</i>	1	1	1	0	0	0	0	1	1	?	0
<i>Hypuonector</i>	?	?	?	?	?	?	?	?	?	?	?
<i>Jesairosaurus</i>	?	?	0	0	?	0	0	0	0	1	1
<i>Kadimakara</i>	1	?	0	?	1	?	?	1	0	0	0
<i>Langobardisaurus</i>	?	?	0	?	?	?	?	?	?	?	?
<i>Macrocnemus bassanii</i>	0	?	0	0	0	0	0	0	0	1	0
<i>Malerisaurus langstoni</i>	?	?	?	?	?	?	?	1	?	?	0
<i>Malerisaurus robinsonae</i>	?	?	0	1	0	0	?	?	?	?	1
<i>Marasuchus</i>	?	?	?	?	?	?	?	?	?	?	?
<i>Megalancosaurus</i>	?	?	0	?	?	?	?	?	?	?	?
<i>Prolacerta</i>	0	?	0	1	0	0	0	0	0	0	0
<i>Prolacertoides</i>	?	?	?	?	?	?	?	?	?	?	?
<i>Proterosuchus</i>	0	1	0	1	0	0	0	0	0	0	0
<i>Protorosaurus</i>	?	?	0	?	0	?	?	?	0	?	1
<i>Rhynchosaurus</i>	1	1	1	0	1	?	?	0	1	0	1
<i>Scleromochlus</i>	1	1	0	0	1	0	?	0	?	?	0
<i>Tanystropheus longobardicus</i>	0	?	0	0	0	0	0	2	0	1	1
<i>Tanystropheus meridensis</i>	1	?	0	1	0	0	0	1	?	1	0
<i>Tanytrachelos</i>	0	?	0	0	?	?	?	0	?	?	?
<i>Trachelosaurus</i>	?	?	?	?	?	?	?	?	?	?	?
<i>Trilophosaurus</i>	0	1	0	0	0	0	0	0	?	1	0
<i>Vallesaurus</i>	?	?	0	0	0	1	1	0	0	?	0
<i>Youngina</i>	0	?	0	0	0	0	0	1	0	0	0

TABLE 37 (cont'd)

	118	119	120	121	122	123	124	125	126	127	128
<i>Petrolacosaurus</i>	0	0	0	0	0	0	0	0	0	0	0
<i>Amotosaurus</i>	?	?	?	0	0	?	?	?	?	?	?
<i>Boreopricea</i>	0	?	0	0	0	?	1	?	?	?	?
<i>Cosesaurus</i>	?	?	?	?	?	?	1	?	?	?	?
<i>Czatkowiella harae</i>	1	1	0	1	0	?	1	1	0	?	0
<i>Dinocephalosaurus</i>	0	0	1	?	0	?	1	?	?	?	?
<i>Drepanosaurus</i>	?	?	?	?	?	?	?	?	?	?	?
<i>Eudimorphohodon</i>	?	?	?	?	?	?	?	?	?	?	?
<i>Euparkeria</i>	0	1	1	1	0	2	1	1	1	0	0
<i>Herrerasaurus</i>	0	1	1	1	0	0	1	0	0	0	1
<i>Hypuonector</i>	?	?	?	?	?	?	?	?	?	?	?
<i>Jesairosaurus</i>	0	?	?	0	0	1	1	?	?	?	?
<i>Kadimakara</i>	0	0	0	1	0	0	?	?	?	?	?
<i>Langobardisaurus</i>	?	?	?	?	?	?	?	?	?	?	?
<i>Macrocnemus bassanii</i>	1	1	1	1	0	2	1	?	?	?	?
<i>Malerisaurus langstoni</i>	0	0	?	1	1	?	1	?	?	?	?
<i>Malerisaurus robinsonae</i>	0	?	0	?	?	?	?	0	?	?	?
<i>Marasuchus</i>	?	?	?	?	?	?	?	?	?	?	?
<i>Megalancosaurus</i>	?	?	?	?	?	?	?	?	?	?	?
<i>Prolacerta</i>	0	0	1	1	0	2	1	0	?	1	0
<i>Prolacertoides</i>	?	?	?	?	?	?	?	?	?	?	?
<i>Proterosuchus</i>	0	1	1	1	0	2	1	1	1	1	0
<i>Protorosaurus</i>	2	1	1	0	0	2	?	?	?	?	?
<i>Rhynchosaurus</i>	2	1	1	1	1	2	1	?	0	1	1
<i>Scleromochlus</i>	0	?	?	0	0	?	?	0	?	?	?
<i>Tanystropheus longobardicus</i>	2	0	1	1	0	2	1	0	0	1	0
<i>Tanystropheus meridensis</i>	?	0	1	1	0	2	1	0	0	1	0
<i>Tanytrachelos</i>	?	1	?	?	?	?	1	?	?	?	?
<i>Trachelosaurus</i>	?	?	?	?	?	?	?	?	?	?	?
<i>Trilophosaurus</i>	2	1	1	1	0	?	1	0	0	?	0
<i>Vallesaurus</i>	0	1	?	1	0	?	?	?	?	?	?
<i>Youngina</i>	0	0	1	1	0	1	1	0	0	0	0

TABLE 37 (cont'd)

	129	130	131	132	133	134	135	136	137	138	139
<i>Petrolacosaurus</i>	0	0	0	0	0	0	0	0	0	0	0
<i>Amotosaurus</i>	?	?	?	?	?	?	?	?	?	?	0
<i>Boreopricea</i>	?	?	?	?	?	?	?	?	1	?	0
<i>Cosesaurus</i>	?	?	?	?	?	?	?	?	?	?	?
<i>Czatkowiella harae</i>	?	0	1	1	0	1	1	0	?	0	0
<i>Dinocephalosaurus</i>	?	?	1	?	?	?	?	?	?	?	?
<i>Drepanosaurus</i>	?	?	?	?	?	?	?	?	?	?	?
<i>Eudimorphohodon</i>	?	?	?	?	?	?	?	?	?	?	?
<i>Euparkeria</i>	1	1	1	0	1	1	1	1	1	0	0
<i>Herrerasaurus</i>	1	?	1	?	?	?	?	1	0	?	?
<i>Hypuonector</i>	?	?	?	?	?	?	?	?	?	?	?
<i>Jesairosaurus</i>	?	?	1	?	?	?	?	?	?	0	0
<i>Kadimakara</i>	?	?	?	?	?	?	?	?	0	?	1
<i>Langobardisaurus</i>	?	?	?	?	?	?	?	?	?	?	0
<i>Macrocnemus bassanii</i>	?	1	?	?	?	?	?	0	?	?	0
<i>Malerisaurus langstoni</i>	0	?	?	0	?	?	?	?	?	?	?
<i>Malerisaurus robinsonae</i>	?	?	?	?	?	?	?	?	?	?	0
<i>Marasuchus</i>	?	1	?	?	?	?	?	?	?	?	?
<i>Megalancosaurus</i>	?	?	?	?	?	?	?	?	?	?	0
<i>Prolacerta</i>	1	0	1	1	1	1	1	0	1	0	0
<i>Prolacertoides</i>	?	?	?	?	?	?	?	?	?	?	?
<i>Proterosuchus</i>	1	1	1	1	1	1	1	1	1	0	0
<i>Protorosaurus</i>	?	?	?	?	?	?	?	?	?	0	0
<i>Rhynchosaurus</i>	2	0	1	1	0	1	1	0	1	1	1
<i>Scleromochlus</i>	0	?	?	?	?	?	?	?	?	?	0
<i>Tanystropheus longobardicus</i>	2	1	1	0	?	0	?	0	1	0	0
<i>Tanystropheus meridensis</i>	2	?	?	?	?	?	?	0	?	0	0
<i>Tanytrachelos</i>	?	?	?	?	?	?	?	?	?	?	2
<i>Trachelosaurus</i>	?	?	?	?	?	?	?	?	?	?	?
<i>Trilophosaurus</i>	?	0	1	1	?	1	?	0	1	0	1
<i>Vallesaurus</i>	?	?	?	?	?	?	?	?	?	?	?
<i>Youngina</i>	0	0	1	0	1	0	1	0	1	0	0

TABLE 37 (cont'd)

	140	141	142	143	144	145	146	147	148	149	150
<i>Petrolacosaurus</i>	0	0	0	0	0	0	0	0	0	0	0
<i>Amotosaurus</i>	1	0	0	0	?	0	0	?	0	0	?
<i>Boreopricea</i>	1	0	0	0	?	0	0	0	?	0	?
<i>Cosesaurus</i>	1	0	?	0	?	0	0	1	?	?	?
<i>Czatkowiella harae</i>	1	0	0	0	0	0	0	0	0	0	?
<i>Dinocephalosaurus</i>	1	0	0	0	?	0	0	0	0	0	3
<i>Drepanosaurus</i>	?	?	?	?	?	?	?	?	?	?	?
<i>Eudimorphohodon</i>	1	0	0	0	0	0	0	?	?	?	?
<i>Euparkeria</i>	1	1	0	0	0	0	0	0	0	0	0
<i>Herrerasaurus</i>	0	1	0	0	0	0	0	1	1	1	3
<i>Hypuronector</i>	1	0	?	?	?	?	?	?	?	?	?
<i>Jesairosaurus</i>	1	0	?	0	?	0	0	0	?	0	0
<i>Kadimakara</i>	1	0	0	0	2	?	?	?	?	?	?
<i>Langobardisaurus</i>	?	0	0	0	0	0	0	0	?	?	?
<i>Macrocnemus bassanii</i>	1	0	0	0	0	0	0	0	0	0	2
<i>Malerisaurus langstoni</i>	?	?	?	?	?	?	?	?	?	?	?
<i>Malerisaurus robinsonae</i>	1	0	0	0	0	0	0	0	0	0	0
<i>Marasuchus</i>	?	?	?	?	?	?	?	?	?	?	?
<i>Megalancosaurus</i>	1	0	0	0	0	0	0	0	?	?	?
<i>Prolacerta</i>	1	0	0	0	0	0	0	0	0	0	2
<i>Prolacertoides</i>	?	?	?	?	?	?	?	?	?	?	?
<i>Proterosuchus</i>	1	1	0	0	0	0	0	0	0	0	2
<i>Protorosaurus</i>	1	0	0	0	0	0	0	0	0	0	?
<i>Rhynchosaurus</i>	1	0	1	1	2	1	2	2	1	1	3
<i>Scleromochlus</i>	?	?	1	0	0	0	0	?	?	?	?
<i>Tanystropheus longobardicus</i>	1	0	0	0	0	0	0	0	0	1	3
<i>Tanystropheus meridensis</i>	1	0	0	0	0	0	0	0	0	?	?
<i>Tanytrachelos</i>	1	0	?	0	?	0	0	1	?	?	?
<i>Trachelosaurus</i>	?	?	?	?	?	?	?	?	?	?	?
<i>Trilophosaurus</i>	1	0	0	0	0	0	0	0	1	1	3
<i>Vallesaurus</i>	0	0	?	?	?	?	0	?	?	?	?
<i>Youngina</i>	1	0	0	0	0	0	0	0	0	0	0

TABLE 37 (cont'd)

	151	152	153	154	155	156	157	158	159	160	161
<i>Petrolacosaurus</i>	0	0	0	0	0	0	0	0	0	0	0
<i>Amotosaurus</i>	?	?	?	?	?	?	?	?	2	?	?
<i>Boreopricea</i>	?	0	0	0	?	?	0	?	?	1	0
<i>Cosesaurus</i>	?	?	?	?	?	1	?	?	0	?	1
<i>Czatkowiella harae</i>	2	0	0	0	0	?	1	0	?	?	?
<i>Dinocephalosaurus</i>	2	0	0	0	?	0	0	?	?	0	?
<i>Drepanosaurus</i>	?	?	?	?	?	?	?	?	0	3	0
<i>Eudimorphohodon</i>	?	?	?	?	?	?	?	?	?	?	?
<i>Euparkeria</i>	2	0	0	0	0	1	1	1	2	2	1
<i>Herrerasaurus</i>	2	0	0	0	0	1	1	1	0	0	0
<i>Hypuonector</i>	?	?	?	?	?	?	?	?	?	3	0
<i>Jesairosaurus</i>	1	0	0	?	0	0	0	?	0	0	?
<i>Kadimakara</i>	?	0	0	0	?	?	0	?	?	?	?
<i>Langobardisaurus</i>	?	?	?	0	?	?	?	?	1	0	1
<i>Macrocnemus bassanii</i>	2	0	0	0	1	0	0	?	1	0	1
<i>Malerisaurus langstoni</i>	?	?	?	?	?	?	0	?	0	?	?
<i>Malerisaurus robinsonae</i>	1	?	?	?	?	?	0	?	0	1	?
<i>Marasuchus</i>	?	?	?	?	?	?	?	?	0	1	0
<i>Megalancosaurus</i>	?	0	?	0	0	?	0	1	0	3	?
<i>Prolacerta</i>	0	0	0	0	1	1	0	1	2	2	1
<i>Prolacertoides</i>	?	?	?	?	?	?	?	?	?	?	?
<i>Proterosuchus</i>	0	0	0	0	0	1	1	1	1	2	1
<i>Protorosaurus</i>	?	0	0	0	0	?	0	?	0	2	?
<i>Rhynchosaurus</i>	2	0	1	1	1	?	0	?	0	3	0
<i>Scleromochlus</i>	?	0	0	0	0	1	1	?	0	0	0
<i>Tanystropheus longobardicus</i>	2	0	0	0	1	0	0	0	0	0	1
<i>Tanystropheus meridensis</i>	?	0	0	0	?	0	0	?	?	?	?
<i>Tanytrachelos</i>	?	?	0	?	?	?	0	?	0	?	1
<i>Trachelosaurus</i>	?	?	?	?	?	?	?	?	?	?	?
<i>Trilophosaurus</i>	2	0	0	0	1	0	0	1	0	1	?
<i>Vallesaurus</i>	?	?	?	?	?	0	0	?	?	3	1
<i>Youngina</i>	0	0	0	0	0	0	0	0	0	0	0

TABLE 37 (cont'd)

	162	163	164	165	166	167	168	169	170	171	172
<i>Petrolacosaurus</i>	0	0	0	0	0	0	0	0	0	0	0
<i>Amotosaurus</i>	?	?	0	?	?	?	?	?	?	0	?
<i>Boreopricea</i>	?	?	?	?	?	?	?	?	?	?	?
<i>Cosesaurus</i>	1	?	1	?	?	?	?	?	?	?	?
<i>Czatkowiella harae</i>	1	?	?	?	?	?	?	?	?	1	?
<i>Dinocephalosaurus</i>	?	?	1	?	?	?	?	?	?	1	1
<i>Drepanosaurus</i>	1	0	0	?	?	?	?	?	1	1	3
<i>Eudimorphohodon</i>	?	?	0	?	?	?	?	?	?	?	?
<i>Euparkeria</i>	1	1	1	0	1	1	?	0	1	1	1
<i>Herrerasaurus</i>	0	1	1	0	?	?	?	?	1	0	1
<i>Hypuonector</i>	1	1	0	?	1	?	?	?	?	3	?
<i>Jesairosaurus</i>	0	?	1	?	0	1	?	0	?	2	?
<i>Kadimakara</i>	?	?	?	?	?	?	?	?	?	?	?
<i>Langobardisaurus</i>	1	?	1	0	1	?	?	?	1	?	1
<i>Macrocnemus bassanii</i>	1	1	1	0	1	0	1	0	1	1	0
<i>Malerisaurus langstoni</i>	1	?	?	0	0	1	1	0	0	?	?
<i>Malerisaurus robinsonae</i>	?	?	0	1	?	?	?	?	0	1	?
<i>Marasuchus</i>	0	?	0	?	?	?	?	?	1	3	1
<i>Megalancosaurus</i>	?	2	0	0	?	?	?	?	1	3	1
<i>Prolacerta</i>	1	2	1	0	1	0	1	0	1	1	0
<i>Prolacertoides</i>	?	?	?	?	?	?	?	?	?	?	?
<i>Proterosuchus</i>	1	2	1	0	1	1	1	0	1	1	0
<i>Protorosaurus</i>	?	2	1	?	?	?	?	?	1	?	?
<i>Rhynchosaurus</i>	1	0	1	0	?	1	0	1	1	1	0
<i>Scleromochlus</i>	1	?	0	?	?	?	?	?	0	1	?
<i>Tanystropheus longobardicus</i>	1	0	1	0	0	0	?	0	1	1	0
<i>Tanystropheus meridensis</i>	?	?	?	?	?	?	?	?	?	?	?
<i>Tanytrachelos</i>	?	1	1	0	?	?	?	?	0	2	?
<i>Trachelosaurus</i>	?	?	?	?	?	?	?	?	1	1	?
<i>Trilophosaurus</i>	1	0	1	0	1	0	?	1	1	1	1
<i>Vallesaurus</i>	0	0	0	?	1	?	?	?	?	3	?
<i>Youngina</i>	1	0	0	0	1	0	0	0	1	1	0

TABLE 37 (cont'd)

	173	174	175	176	177	178	179	180	181	182	183
<i>Petrolacosaurus</i>	0	0	0	0	0	0	0	0	0	0	0
<i>Amotosaurus</i>	0	?	?	?	0	?	?	1	0	?	?
<i>Boreopricea</i>	?	1	1	0	0	?	?	1	?	?	0
<i>Cosesaurus</i>	?	1	0	0	0	0	0	1	0	1	?
<i>Czatkowiella harae</i>	?	?	?	?	?	?	?	?	?	?	0
<i>Dinocephalosaurus</i>	?	0	1	0	0	?	?	1	0	?	0
<i>Drepanosaurus</i>	1	0	1	1	0	0	0	0	0	2	?
<i>Eudimorphohodon</i>	?	1	?	?	?	?	?	0	0	?	?
<i>Euparkeria</i>	1	1	1	0	0	?	?	1	0	?	0
<i>Herrerasaurus</i>	0	1	1	0	0	?	?	1	2	2	0
<i>Hypuronector</i>	?	0	1	1	?	?	?	?	?	?	?
<i>Jesairosaurus</i>	?	0	?	?	?	?	?	?	?	?	0
<i>Kadimakara</i>	?	?	?	?	?	?	?	?	?	?	0
<i>Langobardisaurus</i>	0	1	1	0	0	1	0	1	0	1	?
<i>Macrocnemus bassanii</i>	0	1	1	0	0	1	0	1	0	1	0
<i>Malerisaurus langstoni</i>	?	1	1	0	?	?	?	?	?	?	?
<i>Malerisaurus robinsonae</i>	0	1	1	0	0	?	?	1	1	1	?
<i>Marasuchus</i>	0	1	1	0	0	?	?	1	0	?	?
<i>Megalancosaurus</i>	0	1	1	0	0	0	0	1	0	2	?
<i>Prolacerta</i>	1	1	1	0	0	1	0	?	0	1	0
<i>Prolacertoides</i>	?	?	?	?	?	?	?	?	?	?	0
<i>Proterosuchus</i>	0	1	1	0	0	1	0	1	1	?	0
<i>Protorosaurus</i>	?	1	1	0	0	0	0	1	0	0	?
<i>Rhynchosaurus</i>	0	1	?	0	1	1	1	1	1	1	0
<i>Scleromochlus</i>	1	1	0	?	0	?	?	?	0	?	0
<i>Tanystropheus longobardicus</i>	0	1	0	0	0	?	?	1	0	2	0
<i>Tanystropheus meridensis</i>	?	?	?	?	?	?	?	?	?	?	0
<i>Tanytrachelos</i>	0	1	0	0	0	?	?	1	0	0	?
<i>Trachelosaurus</i>	?	?	?	?	?	?	?	?	?	?	?
<i>Trilophosaurus</i>	0	1	1	0	0	0	0	1	0	0	0
<i>Vallesaurus</i>	0	1	0	0	1	1	1	1	0	2	0
<i>Youngina</i>	0	1	1	0	0	0	0	0	?	?	0

TABLE 37 (cont'd)

	184	185	186	187	188	189	190	191	192	193	194
<i>Petrolacosaurus</i>	0	0	0	0	0	0	0	0	0	0	0
<i>Amotosaurus</i>	0	?	0	?	?	0	0	?	1	1	0
<i>Boreopricea</i>	?	0	?	0	?	?	?	?	0	?	0
<i>Cosesaurus</i>	?	?	0	?	?	?	?	?	?	?	0
<i>Czatkowiella harae</i>	0	0	0	0	0	0	0	0	1	?	0
<i>Dinocephalosaurus</i>	?	0	?	?	?	?	1	?	?	?	0
<i>Drepanosaurus</i>	?	?	0	1	?	0	?	?	?	?	?
<i>Eudimorphohodon</i>	?	?	?	?	?	?	1	?	?	?	1
<i>Euparkeria</i>	1	0	0	?	0	0	0	0	0	0	0
<i>Herrerasaurus</i>	0	0	0	0	0	0	0	0	0	1	0
<i>Hypuonector</i>	?	?	0	1	?	0	0	?	?	?	?
<i>Jesairosaurus</i>	0	0	0	?	?	?	0	?	?	?	0
<i>Kadimakara</i>	?	1	?	?	?	?	?	?	?	?	0
<i>Langobardisaurus</i>	?	0	0	?	?	0	0	?	1	1	1
<i>Macrocnemus bassanii</i>	?	0	0	0	0	0	0	?	1	1	0
<i>Malerisaurus langstoni</i>	?	?	0	0	?	0	0	?	?	?	?
<i>Malerisaurus robinsonae</i>	?	?	0	?	?	0	0	0	1	0	0
<i>Marasuchus</i>	?	?	0	?	?	?	0	?	0	?	?
<i>Megalancosaurus</i>	?	0	?	1	?	0	0	?	1	0	0
<i>Prolacerta</i>	1	0	0	0	0	0	0	0	1	0	0
<i>Prolacertoides</i>	?	?	?	?	?	?	?	?	?	?	?
<i>Proterosuchus</i>	1	0	0	0	0	0	0	?	0	0	0
<i>Protorosaurus</i>	?	0	0	0	?	0	0	?	0	1	0
<i>Rhynchosaurus</i>	0	0	0	1	0	0	0	0	0	0	0
<i>Scleromochlus</i>	0	0	0	?	?	?	0	?	0	0	?
<i>Tanystropheus longobardicus</i>	0	0	0	0	0	0	0	?	1	1	1
<i>Tanystropheus meridensis</i>	0	0	?	?	?	?	?	?	1	?	1
<i>Tanytrachelos</i>	?	?	0	?	?	?	0	?	?	1	0
<i>Trachelosaurus</i>	?	?	?	?	?	?	?	?	?	?	?
<i>Trilophosaurus</i>	?	0	0	0	0	0	0	0	0	0	0
<i>Vallesaurus</i>	?	0	0	0	?	0	0	?	1	0	0
<i>Youngina</i>	0	0	0	0	0	0	0	?	0	0	0

TABLE 37 (cont'd)

	195	196	197	198	199	200	201	% Data Complete
<i>Petrolacosaurus</i>	0	0	0	0	0	0	0	100.0
<i>Amotosaurus</i>	?	?	?	?	?	?	?	32.8
<i>Boreoprincea</i>	?	?	?	?	?	?	0	54.7
<i>Cosesaurus</i>	0	0	?	?	?	?	0	36.8
<i>Czatkowiella harae</i>	1	0	1	?	?	0	?	58.7
<i>Dinocephalosaurus</i>	?	0	?	?	?	?	1	65.7
<i>Drepanosaurus</i>	0	1	1	1	?	0	1	30.8
<i>Eudimorphohodon</i>	?	?	?	?	?	?	?	15.9
<i>Euparkeria</i>	0	0	0	0	1	0	1	92.5
<i>Herrerasaurus</i>	0	0	0	?	0	0	0	86.6
<i>Hypuronector</i>	0	0	?	0	?	?	0	19.9
<i>Jesairosaurus</i>	0	?	0	?	?	?	0	47.8
<i>Kadimakara</i>	?	?	?	?	?	?	?	23.9
<i>Langobardisaurus</i>	2	0	0	0	?	?	?	50.7
<i>Macrocnemus bassanii</i>	1	0	0	0	?	0	1	85.1
<i>Malerisaurus langstoni</i>	0	0	0	?	?	0	1	31.3
<i>Malerisaurus robinsonae</i>	?	0	0	?	?	0	0	52.7
<i>Marasuchus</i>	?	0	0	?	?	0	1	28.9
<i>Megalancosaurus</i>	0	1	1	1	?	?	1	58.7
<i>Prolacerta</i>	0	0	0	0	1	0	0	98.0
<i>Prolacertoides</i>	?	?	?	?	?	?	?	4.0
<i>Proterosuchus</i>	1	0	0	0	1	0	1	94.0
<i>Protorosaurus</i>	?	0	0	0	?	0	0	72.1
<i>Rhynchosaurus</i>	0	0	0	0	0	0	0	94.5
<i>Scleromochlus</i>	1	0	0	?	?	0	1	58.7
<i>Tanystropheus longobardicus</i>	2	0	0	0	0	0	1	94.5
<i>Tanystropheus meridensis</i>	?	?	?	?	0	?	?	43.8
<i>Tanytrachelos</i>	1	?	?	?	?	1	1	55.2
<i>Trachelosaurus</i>	?	?	?	?	?	?	0	12.4
<i>Trilophosaurus</i>	1	0	0	0	?	0	1	88.1
<i>Vallesaurus</i>	0	0	0	?	?	0	1	56.2
<i>Youngina</i>	0	0	0	0	0	0	0	95.5